University of Lisbon

Faculty of Medicine

Microbiota: Understanding its Role in the Host-*Plasmodium* affair

Debanjan Mukherjee

Supervisor: Professor Maria Manuel Mota

Thesis specially prepared to obtain the Ph.D. degree in Biomedical Sciences with speciality in Microbiology

2022

University of Lisbon

Faculty of Medicine

Microbiota: Understanding its Role in the Host-*Plasmodium* affair

Debanjan Mukherjee

Supervisor: Professor Maria Manuel Mota

Thesis specially prepared to obtain the Ph.D. degree in Biomedical Sciences with speciality in Microbiology

Panel
President: Doutor Mário Nuno Ramos de Almeida Ramirez, Professor Associado com Agregação e Membro do Conselho Científico da Faculdade de Medicina da Universidade de Lisboa
Members
-Doctor Yasmine Belkaid, Distinguished Investigator do National Institute of Allergy and Infectious Diseases (USA)
-Doutora Margarida Sofia da Silva Santos S-araiva, Investigadora Principal do Instituto de Investigação e Inovação em Saúde da Universidade do Porto
-Doutor Luís Manuel Valla Teixeira, Investigador Principal do Instituto Gulbenkian de Ciência da Fundação Calouste Gulbenkian
-Doutor Bruno Miguel de Carvalho e Silva Santos, Professor Catedrático da Faculdade de Medicina da Universidade de Lisboa
-Doutora Maria Manuel Dias da Mota, Professora Associada Convidada com Agregação da Faculdade de Medicina da Universidade de Lisboa (Orientadora)

Bolsa PD/BD/105836/2014 da Fundação para a Ciência e Tecnologia (FCT)

2022

A impressão desta tese foi aprovada pelo Conselho Científico da Faculdade de Medicina de Lisboa em reunião de 20 de outubro de 2020.

As opiniões expressas nesta publicação são da exclusiva responsabilidade do seu autor.

The experimental work herein described was performed at Intituto de Medicina Molecular João Lobo Antunes – Faculdade de Medicina da Universidade de Lisboa, except when otherwise stated, under the supervision of Dr. Maria Manuel Mota.

TABLE OF CONTENTS

ACKNOWLEDGMENTS 1

SUMMARY 3

SUMÁRIO 4

LIST OF ABBREVIATIONS 7

INTRODUCTION

The Human Microbiota 9

Concept of microbiota, dysbiosis and its role in health and disease(s) 10

Microbiota and its role in colonization resistance against pathogens 23

Plasmodium infection, Malaria and Microbiota 30

References 33

AIMS OF THE THESIS 49

RESULTS

Chapter 1: Phenotype 52

Introduction 53

Methods 57

Results 63

Discussion 71

References 73

Chapter 2: Mechanism (Parasite factors) 78

Introduction 79

Methods 80

Results 86

Discussion 94

References 95

Chapter 3: Mechanism (Host factors) 99

Introduction 100

Methods 101

Results 106

Discussion 116

References 119

Chapter 4: Relevance 122

Introduction 123

Methods 124

Results 127

Discussion 130

References 132

CONCLUSIONS AND FUTURE PERSPECTIVES

Conclusions 134

Future Perspectives 137

References 145

Acknowlegements

***If I have seen further it is by standing on the shoulders of Giants.* — Isaac Newton**

I would like to express my gratitude to several people who have supported me during the time of my PhD project.

Firstly, I would like to acknowledge my supervisor, Maria Mota for all her guidance and critical supervision of all my work and writing, as well as for showing me how to think beyond the obvious. I am grateful to Maria for welcoming me in her lab, for giving me the freedom to pursue my project, while being critical and constructive, which highly contributed to my scientific education. She has been instrumental in making me evolve not only as a person but as a scientist during my PhD. Thank you Maria for all the knowledge you shared with me.

I wish to acknowledge all the co-author in the manuscript for the collaborations

My gratitude to Angelo Chora, a great colleague and mentor, for teaching me everything since I arrived, for helping me design and perform most of the experiments and for the scientific discussions that greatly contributed to the quality (and magnitude) of this work. Thank you for the companionship and support.

I thank Marc Veldhoen, Mario Ramirez, Isabel Gordo and Bruno-Silva Santos for all the scientific and technical discussions that were key to pursuing these projects and keeping me on the right track. Most of all, thank you for your infinite knowledge and for your support.

I acknowledge Birte Blankenhaus, Karrine Serre, Riacrdo Ramiro for assisting me in my experiments.

To my lab colleagues, that soon became friends, as they transformed this PhD journey into an exciting and fascinating adventure. Thank you!

I want to thank the LisbonBioMed program for accepting me as a PhD student and to FCT for the fellowship (PD/BD/105836/2014).

And I owe a lot to Helena Brigas, for being there silently always beside me and providing me so much love and support. This would not be possible without you.

Finally, I would like to acknowledge my family, because this journey started because of their believe in me and their constant motivation from all the way back home in India. This PhD is dedicated to my mother, my father and my brother for their unconditioned love and support that they offered me forever.

Summary

The interplay between host and microbiota may define health or disease. Alterations in microbiota composition (mostly in the gut but also in other tissues) commonly referred to as ‘dysbiosis’ have been associated with a wide variety of disorders. However, the role the microbiota may play in malaria infections remains elusive. Here we show that host-*Plasmodium* combinations leading to death due to malaria-associated acute respiratory distress syndrome (MA-ARDS) are associated with lung microbiota dysbiosis in mice. We further show that while host lung microbial dysbiosis contributes to MA-ARDS-induced death in mice, it has no impact on experimental cerebral malaria (eCM), a distinct malaria syndrome. Changes in lung microbiota result from parasite sequestration in the lungs and depend on IL-10 production by T cells. Notably, bacterial clearance using linezolid, an antibiotic used in the clinical setting to control lung-associated bacterial infections, prevented MA-ARDS (without affecting parasite load) but not eCM. These data show that *Plasmodium* infections can induce changes in host lung microbiota, which in turn promote malaria-associated severe disease and death. Thus, we propose that the host’s anti-inflammatory response to limit tissue damage can result in loss of microbial control and constitute a pathological self-amplifying cycle that must be considered when intervening against respiratory life-threatening complications.

SUMÁRIO

A Síndrome da Dificuldade Respiratória Aguda (do inglês, Acute Respiratory Distress Syndrome, ARDS) consiste num padrão de manifestações de hipoxia severa e alteração dos mecanismos do sistema respiratório devido a danos alveolares difusos. Esta síndrome está presente em aproximadamente 10% de todos os doentes em unidades de cuidados intensivos e está associada a uma mortalidade alta - 30% - 40% como indicado na maioria dos. A ARDS tem uma etiologia heterogénea, com causas variadas que envolvem tanto eventos pulmonares como extra-pulmonares. No entanto, a maioria dos casos de ARDS podem ser atribuídos a apenas algumas causas, estando as infeções locais (nos pulmões) ou sistémicas causadas por diversos agentes patogénicos entre as mais comuns.

A malária continua a ser um dos maiores flagelos da humanidade – com mais de 200 milhões de novas infeções e 400 mil mortes a ocorrer todos os anos (World Health Organization, 2021). As razões pelas quais algumas pessoas desenvolvem malária severa enquanto que outras nãocontinuam parcialmente por esclarecer. Estão documentados como fatores críticos associados à probabilidade de desenvolver uma patologia de malária severa, tanto fatores genéticos do hospedeiro, que na maioria afetam as características dos glóbulos vermelhos, como fatores intrínsecos do parasita, tais como polimorfismos nos genes *var* de *Plasmodium falciparum*, que influenciam a sequestração, i.e., a aderência dos glóbulos vermelhos infetados ao endotélio vascular. A Malária severa pode, no entanto, manifestar-se de modo diverso, numa variedade de fenótipos clínicos bem descritos, que podem ser preditivos de morte, e que podem ocorrer independentemente ou em conjunto. Estes incluem a anemia severa, o coma

(malária cerebral), a falha renal e a dificuldade respiratória. Pouco se sabe sobre as razões que levam um indivíduo infetado a desenvolver uma patologia ou a outra, não parecendo no entanto ser devido ao acaso pois as diferentes manifestações têm associações claras com fatores tais como, a idade do hospedeiro e a intensidade de transmissão da malária da área de habitação. A ARDS é única entre as manifestações de malária severa pois é a forma mais severa de todas as complicações respiratórias associadas com a malária e resulta em taxas de mortalidade elevadas mesmo face a procedimentos terapêuticos adequados. Está estimado que pelo menos 5% dos doentes com malária ligeira e 20-30% de doentes com malária grave ou severa que necessitam de admissão a unidades de cuidados intensivos podem desenvolver ARDS associada à malária (do inglês, malaria-associated ARDS, MA-ARDS) o que ocorre normalmente após o início do tratamento anti-malárico.

A influência da microbiota na homeóstase centralizou atenção nos últimos anos com o reconhecimento do seu papel critico nos efeitos sistémicos no meta-organismo. De facto, um desvio no repertorio microbiano do intestino, comummente denominado disbiose intestinal, tem sido associado epidemiologicamente – e em alguns casos casualmente – com uma grande variedade de distúrbios. É relevante notar que a colonização microbiana ocorre em todas as superfícies corporais que estão expostas ao ambiente externo, o que inclui também o trato broncopulmunar. Tradicionalmente os pulmões saudáveis eram considerados estéreis pois não era possível, com recurso a técnicas microbiológicas de rotina, cultivar bactérias das vias respiratórias inferiores. No entanto, atualmente, o recurso a métodos moleculares para a quantificação e sequenciação de DNA bacteriano revelou a presença de comunidades microbianas que

contêm uma complexa diversidade bacteriana em amostras colhidas das vias respiratórias inferiores. Tal como no caso da associação entre as comunidades microbianas que colonizam outros órgãos (ex. o intestino) e patologias específicas, foi demonstrado que as alterações na composição desta comunidade microbiana – disbiose da microbiota pulmonar – estão associadas com a exacerbação de vários distúrbios pulmonares, que incluem a doença pulmonar obstrutiva crónica (do inglês, chronic obstructive pulmonary disease, COPD), a asma e a fibrose quistica e também o cancro pulmonar.

Nesta dissertação, mostra-se que alterações da microbiota que coloniza o pulmão do hospedeiro é determinante da mortalidade num contexto de MA-ARDS. A sequestração de parasitas *Plasmodium* causa uma ativação imunológica persistente e em última análise resulta na produção da citocina anti-inflamatória IL-10 no sentido de reduzir a imunopatologia. No entanto, a produção de IL-10 pelas células T facilita o crescimento da microbiota local, o que por seu lado contribui para a disbiose e resulta em MA-ARDS. Os dados apresentados mostram também que o tratamento com antibióticos ou o bloqueio dos mediadores das alterações da microbiota, sendo eles imunológicos celulares ou moleculares, é suficiente para prevenir a ARDS.

List of abbreviations

AD - Atopic Dermatitis

AMP - Anti-Microbial Peptide

BALT - bronchus-associated lymphoid tissue

COPD - Chronic Obstructive Pulmonary Disorder

CFTR - Cystic Fibrosis Transmembrane Regulator

DAMP - Damage Associated Molecular Pattern

eCM – Experimental Cerebral Malaria

GF – Germ-Free

GWAS - Genome Wide Association Studies

HLA - Human Leukocyte Antigen

IEL - Intra Epithelial Lymphocytes

IBD - Inflammatory Bowel Disease

LPS - lipopolysaccharide

MA-ARDS- Malaria associated Acute Respiratory Distress syndrome

SCFA - Short Chain Fatty Acid

SFB - segmentous-filamentous bacteria

SPF – Specific Pathogen Free

“I learned very early the difference between knowing the name of something and knowing something.” — ***Richard P. Feynman***

Introduction

The Human Microbiota

The seminal observations by Robert Koch, awarded the Nobel Prize in Physiology and Medicine in 1905, relating to the identification of the microbial agents responsible for infectious diseases such as anthrax, cholera and tuberculosis led to the formalization of the Koch's Postulates, where a causative link is established between a given microorganism and a specific disease. Undoubtedly, his - and others' - work established the grounds of modern microbiology and contributed, in a critical manner, for saving millions of lives. It also cemented a concept, prevailing until very recently, where microorganisms are regarded exclusively as pathogenic agents. Notwithstanding, Elie Metchnikoff, Koch's contemporary, proposed in his "*The prolongation of Life: Optimistic Studies*" that certain microorganisms would have a beneficial effect in prolonging life. The advent of metagenomic sequencing, together with the development of sophisticated culturomic techniques, has provide compelling evidence that strengthen this notion. Indeed, commensal polymicrobial communities are now considered critical for the development and function of the tissues they inhabit. They exert significant effects in metabolism and physiology[1] and, thus, regulate the balance between health and disease. These microbial communities - mostly constituted by bacteria, but also by viruses, fungi, and protozoa - that reside within the host organism are collectively referred to as the "microbiota" and are considered a virtual organ.

The main body sites inhabited by trillions of symbiotic microorganisms are the skin[2], nose[3], oral cavity[4], vagina[5], stomach[6], respiratory tract[7,8], and intestine[9]. Taxonomic analyses have revealed that the major phyla dominating these compartments are *Firmicutes*, *Bacteroidetes*, *Proteobacteria*, *Actinobacteria*, *Fusobacteria*, and

Cyanobacteria[2–9]. However, the relative abundance and load of these phyla differs significantly between these different compartments[1] and vary (at least gut microbiome) among different geographic locations and lifestyles[10].

Concept of microbiota, dysbiosis and its role in health and disease(s)

The notion that microbes can promote human health is not a recent concept and was originally proposed by the seminal work of Döderlein (1892) and his understanding of the role of lactobacilli as gatekeepers of the vaginal ecosystem as well as the observation of Metchnikoff associating prolonged life with fermented milk products. Recent sequencing efforts of the human meta-genome have changed our understanding of the microbiome and how variations in these populations can contribute to disease states. Maintenance of tissue homeostasis is absolutely critical for host survival. This fundamental process is dependent on complex and coordinated evens of innate and adaptive responses that selects and calibrates responses against self, food, commensals and pathogens in the most appropriate manner. In order to achieve these successfully, specialized populations of cells have to integrate local cues such as defined metabolites, cytokines, or hormones allowing the induction of responses in a way that preserve the physiological and functional requirements of each tissue in a distinct manner. As such, the regulatory pathways that are involved in the maintenance of a homeostatic relationship with the microbiota are likely to be tissue specific. . It is becoming apparent that the microbiota of the gut, and possibly from other symbiont-colonized tissues like skin and the lung, plays a fundamental role in maintaining homeostasis, namely by modulating the induction, training and function of the host immune system[11,12]. Thus it is important to discuss how alterations in the composition of the microbiota can lead to a variety of disorders that are tissue specific.

Dysbiosis

The most well defined characteristics of a healthy microbial community are diversity, stability and resistance, and resilience[13], which maintains the richness of the ecosystem and a stable state. It is of utmost importance that the host microbiota is able to cope up with the external perturbation and return to the pre-perturbation state. Data from large human cohort studies suggest that multiple stable states of the microbial ecosystem can colonize a healthy host which does not show any overt signs of diseases[14–16]. The most common definition of dysbiosis is a compositional and functional alteration in the stable microbiota, which is driven by a set of environmental and host-related factors. This shift in the microbiota configuration can have different functional manifestations depending on the extent of the triggering agent[17]. There can be different ways to characterize a dysbiosis state:

Bloom of pathobionts: Pathobionts are those commensals that have the potential to have an impact on the pathology of the disease[18]. Such commensals are generally present in very low abundances and proliferate when there is a perturbation in the ecosystem. For example in the intestinal ecosystem, a well-documented example of this is the outgrowth of the bacterial family *Enterobacteriaceae,* which is frequently observed in enteric infection and inflammation[19]. Importantly, this blooming of *Enterobacteriaceae*, has been consistently observed in patients with IBD[20] and also in mouse models of IBD[21]. However, it is still unclear whether this is the cause or consequence of the inflammation-induced changes in the gut ecosystem. This is also true for other mucosal barrier sites such as the lung and the skin. It has been demonstrated in a mouse model of COPD, inflammation caused by LPS (Lipopolysaccharide) exposure and tissue damage caused

an alteration in the composition of the airway microbiome, increasing the abundance of the genera *Pseudomonas* and *Lactobacillus*[22], as reported in human COPD lungs[23]. In the skin blooming of one of the commensals *S. aureus* has also been implicated in the pathogenesis of chronic diseases such as atopic dermatitis, and more recently in systemic lupus erythematosus with renal and skin involvement[24]. Although more than 30% of healthy individuals are colonized asymptomatically by *S. aureus*[25,26], it can cause a wide spectrum of infections. In patients with atopic dermatitis, *S. aureus* isolates grow as biofilms on the skin and produce proteases that degrade host Anti-Microbial-Peptides (AMPs- These are also called host defense peptides that are like broad-spectrum antibiotics and can kill a diverse array of bacterial species), such as cathelicidin LL-37[27].

Loss of commensals: On the contrary to blooming of pathobionts, another cause of dybiosis is a reduction in the normally residing members of the microbiota at steady state. This reduction can be attributed to either bacterial killing or a decrease in bacterial proliferation[28]. This loss in certain members of the microbiota is critical since restoration with those given bacteria or the metabolites they produce has the potential to revert dysbiosis-associated phenotypes. For example, in the diet-induced model[29] of the autism spectrum disorder it has been shown that reconstitution of gut microbiota with *Lactobacillus reuteri* can have beneficial effects. Moreover using another model of autism spectrum disorder called the maternally transmitted model[30] it has been shown that reconstituting the gut microbiota with *Bacteroides fragilis* reduced disease severity significantly. The reconstitution of the gut commensal bacteria has also been demonstrated to be effective against enteric infection. This was shown in the case of

Clostridium difficile induced inflammation, which was ameliorated by colonization with *Clostridium scindens*[31].

Loss of diversity: A commonly concurrent feature of dysbiosis is the loss of diversity within the microbial ecosystem. It is well established now that the microbial richness increases in the early years of life[16], and can be influenced by diet[32] and also influences metabolic health[33]. On the contrary, loss of diversity due to dysbiosis has been associated with a plethora of diseases like, IBD[34], AIDS[35], Type 1 diabetes[36] and many other conditions[37]. This has been also implicated in pulmonary disorders where loss of diversity of the lung microbiota has been linked to pathogenesis of COPD.

The concept that dysbiosis of the microbiota composition in different tissues can be associated with the manifestation, diagnosis and treatment of specific diseases makes it important to understand the mechanisms of origin and perpetuation of such a dysbiotic state.

Factors contributing to dysbiosis

With more and more research in the field of microbiome, several factors have been documented to be involved in establishing dysbiosis. These include the host age, circadian disruption, maternal high fat diet, pregnancy and physical trauma. Some of the most critical and causal ones are discussed below.

Host genetics: Host genetics have been shown to be important in shaping the composition of the gut microbiota[38]. One the best studied examples was a study involving twins where they reported abundances of multiple bacterial taxa being influenced by host genetics[39]. One such occurrence was the abundance of Bifidobacterium genus with the human gene that encodes lactase. Additionally, genome wide association (GWAS)

studies have shown that the locus encoding the vitamin D receptor and other human loci involved in immune and metabolic functions have an impact on the control of microbiota composition through host genetics[40–42]. In mice, genetic studies have also lined host genetics in the colonization of certain specific bacterial taxa[43]. Future studies need to be done to see the relative contribution of host genetics versus diet in shaping the host microbiota composition. Recent studies have also highlighted the importance of studying the respiratory microbiome and its role with potential genetic risk factors identified by genome-wide association studies in pulmonary disorders. For example in one of the pulmonary disorder Cystic Fibrosis, there are more than 2,000 known mutations of the gene encoding CF transmembrane conductance regulator (*CFTR*)[27] (The cystic fibrosis transmembrane conductance regulator (CFTR) protein helps to maintain the balance of salt and water on many surfaces in the body, such as the surface of the lung. When the protein is not working correctly, chloride -- a component of salt -- becomes trapped in cells. Without the proper movement of chloride, water cannot hydrate the cellular surface. This leads the mucus covering the cells to become thick and sticky, causing many of the symptoms associated with cystic fibrosis[27]). Interestingly, reverting CFTR function with ivacaftor modified the airway microbiome and for the better. For idiopathic pulmonary fibrosis (IPF), the most-common mutation in the gene encoding Mucin 5B (*Muc5B*) was found to be associated with the total levels (burden) of bacteria present[27].

Familial transmittance: The main causes of early succession of intestinal colonization after birth is determined by the maternal microbiota[44] and by the mode of delivery[45]. Thus, the shaping of individual microbiomes is dependent on its transmission across generations. However, studies in both germ-free mice and human neonates have

demonstrated that maternal factors are not sufficient to explain an individual's microbiota assembly[44,46]. Another additional important factor seems to be environmental transmission. This seems true because households feature characteristic microbiome signatures, and the microbiomes of members of a particular household are more similar to one another than to the microbiomes of members of other households[47].

Inflammation and infection: The fact that enteric infections can cause dysbiosis was shown in rodent models of Citrobacter rodentium[48] and Salmonella enterica subsp. enterica serovar Typhimurium[49] infection. These studies demonstrated that the inflammation due the infection led to dysbiosis and compromised the microbiota's ability to provide colonization resistance against these invading pathogens. Moreover, inflammation induced by administering dextran sodium sulphate (DSS) to rodents or mice that are genetically deficient in the anti-inflammatory gene IL-10 (IL-10 KO mice) have similar changes in the gut microbiota composition and are prone to infections by enteric pathogens[48,49]. Importantly, inflammation-associated changes in the microbiota such as blooming of certain members of the famlily *Enterobacteriacae* have been shown to promote colorectal cancer[50] and sepsis[51]. Thus inflammation is one of the critical downstream events leading to alterations in the microbiota composition that in turn facilitates certain diseases. This is due the fact that the inflammatory response against infection alters the homeostasis of that tissue and shapes the habitat, and consequently, influences the colonization of certain microbes. Another example is post-influenza bacterial pneumonia, where the viral infection resets the host's immunity to an immunocompromised state, thus predisposing them to bacterial infections[27]. Although numerous studies have shown that this secondary infection could be due to a new

exposure to a bacterial pathogen, such as *Streptococcus* or *Klebsiella*[27] it is quite rationale to postulate that the pathobionts already resident in the airways could also bloom in this altered habitat and present as a secondary infection. Indeed one study in humans supports this concept. In this prospective study an experimental rhinovirus infection was given to healthy individuals or those with COPD. Samples from people with COPD had a low abundance of *Haemophilus influenza* in their respiratory microbiota, and following infection with Rhinovirus, the *H. influenza* levels bloomed[27].

Diet and Xenobiotics: Diet is a very important factor that can have both short-term[52] and long-term[15] impact on the composition of the microbiota. Studies in mice have shown that low-fibre diet reduces the microbial diversity across consecutive generations[53]. On the same grounds, mice fed on a high fat diet also have a marked impact by reducing the diversity of the microbiota composition[54]. In addition to the nutritional content of the food, dietary xenobiotics have been also shown to have a critical impact on the gut microbiota composition. This has been clearly shown in the case of antibiotics[54]. Diet- and dietary xenobiotics-induce dybiosis can strongly impact the pathogenesis of many diseases both in mice[55] and humans[56]. For example, it has shown that antibiotic treatment causes changes in gut microbiota composition that promotes *Clostridium difficile* infection[57]. Importantly, it has been shown in humans that antibiotic usage drives the incidence of IBD[58]. Additional, it been been reported that antibiotic usage can alter both gut and lung microbiota composition and increase the incidence of asthma[59].

Gut microbiota

The human gastrointestinal (GI) tract represents one of the largest interfaces between the host, environmental factors and antigens in the human body. The collection of bacteria, archaea and eukarya colonising the GI tract is collectively termed the 'gut microbiota' and has co-evolved with the host over thousands of years to form an intricate and mutually beneficial relationship[60,61]. Although, in adulthood, the composition of the gut microbiota is relatively stable, it is still subject to perturbation by environmental factors. Indeed, establishment of dysbiosis – an imbalance between the different commensal communities that constitute a particular microbiota - has been shown both epidemiologically – and sometimes causally – to predispose individuals to a wide variety of disorders[62,63], ranging from chronic inflammatory diseases like multiple sclerosis to metabolic disorders like diabetes and obesity and even cancer[64–68].

Over the last few years numerous associations have been made between gut microbiota dysbiosis and a plethora of immune-mediated diseases.

Inflammatory Bowel Disease (IBD): IBD is a disorder characterized by severe intestinal inflammation of the mucosa and also extra-intestinal organs The microbiota colonizing the gut has been shown to be central in the pathogenesis of IBD. One of the features generally associated with IBD is decrease in microbial diversity[20,69]. Several studies have attempted to identify a single bacterium for the cause of IBD which includes pathogens like *Escherichia coli*, *C. difficile* and *Fusobacterium nucleatum*[70]. However, due to variations and inconsistent observations regarding microbiota compositions in the individuals with IBD, till date it has been difficult to understand the causal effects of single bacterial special in the pathophysiology of IBD.

Coeliac disease: This is an autoimmune intestinal disease that is initiated by an immune response to peptides found in dietary gluten. Importantly, the pathogenesis of this disease is accompanied by alterations in both the duodenal and fecal microbiota[70]. The onset of coeliac disease is believed to be due to the induction of a gluten-specific inflammatory TH1 and TH17 cell response together with targeted killing of intestinal epithelial cells by T cells[71]. However, as in the case of IBD no consistent microbial signature has yet been observed in patients with coeliac disease[72]. Several studies have suggested that the composition and function of the intestinal microbiota may be a contributing factor to the development of coeliac disease, however future studies needs to be performed to elucidate the exact mechanisms by which these alterations could drive disease susceptibility. One of the indications is that the levels of short-chain fatty acids (SCFAs) are modified in patients with coeliac disease, and thus it is speculated that through these alterations the microbiota could mediate oral tolerance[72].

Rheumatoid arthritis: This is a systemic inflammatory disease which has been shown to cause joint destruction. The role of the host microbiota in the pathophysiology of RA has been clearly demonstrated using Germ-free mice which are protected from the development of experimental arthritis[73]. Moreover in humans, there has been association with the presence of *Prevotella copri* and new-onset rheumatoid arthritis[74]. Recently, metagenome-wide association study also highlighted the prevalence of *Lactobacillus salivarius* as a marker of rheumatoid arthritis[75]. The intestinal community in patients with rheumatoid arthritis are characterized by deregulation of several metagenomic functions, including metal ion metabolism, redox functions and arginine metabolism that might explain the pathogenesis of RA[75].

Type 1Diabetes (T1D): This is also an autoimmune disease that is triggered by the destruction of insulin-producing cells in the pancreas by T cells. It has been estimated that approximately two-thirds of all patients with T1D have HLA risk alleles[76] (The **human leukocyte antigen** (**HLA**) system is a complex of genes encoding the major histocompatibility complex (MHC) proteins in humans. These cell-surface proteins are responsible for the regulation of the immune system). However, less than 10% of all individuals carrying these alleles do show signs and symptoms of this disease, which suggests an important contribution of non-genetic factors in determining the proportion of individuals that ultimately develop this type of autoimmunity[76]. In a mouse model of T1D, the microbiota has been implicated as an important contributor to disease pathogenesis[77]. A recent study in humans concluded that intestinal community alterations, including loss of bacterial diversity, occur after the sero-conversion of patients with T1D but precede the onset of diabetes symptoms[78], which raises the possibility that the microbiota causally contributes to the onset of autoimmunity.

Asthma: It is well established now that during infancy early life microbial colonization of mucosal surfaces has important long lasting implications, especially with the onset of diseases in later life. For example, in case of allergy and asthma, it has been shown that Germ-free conditions and early-life antibiotic exposure are associated with increased susceptibility to these diseases[79]. It has been demonstrated in animal models of asthma that neonatal colonization trains and educates the immune system. For instance, when mice are treated with Vancomycin the frequency of intestinal regulatory T (Treg) cells is reduced and IgE levels are concomitantly elevated[80]. In an additional study, lung inflammation was elevated when mice were treated with antibiotics which was also

correlated with increased IgE titres and circulating basophil numbers. The main postulates from these studies were that in the absence of a stable microbiota, B cells preferentially undergo isotype switching to IgE rather than IgA that promote allergic inflammation[81]. However, in the presence of the microbiota, through B cell-intrinsic MYD88 signalling, serum IgE levels are reduced and there is an increase in basophil abundance[82].

Cancer: Cementing the perception of the cardinal role of the immune system-microbiota axis for peripheral immune responsiveness, the impact of intestinal microbiota in regulating cancer incidence and progression and in cancer therapy outcome has been highlighted in many recent studies. This led to the identification of specific commensal bacterial species that exhibit immune-stimulatory potential and favour anticancer immune-surveillance[83–85]. For example, 2 independent studies reported that *Akkermansia municiphilia* was overrepresented among patients that responded well to immunotherapy compared to non-responders[86 87] .

Skin microbiota

The skin surface and follicles are physically and chemically distinct from the microbe-rich barrier site: the small and large intestines. The skin has been demonstrated to be a lipid rich environment that is quite distinct from other parts of the body[88]. Among these vast resources of lipids, some such as sapienic acid, can have antimicrobial activities[89]. Interestingly there are other lipids in the skin such as triglycerides that can be metabolized by microbes[90] into free fatty acids and di- and monoglycerides which have been shown to be bioactive against other microbes or stimulatory to host cells.

The chemistry of a skin niche is one of the main drivers of its microbiome composition, but unknown microbial and host factors contribute to important species- and strain-level differences in composition. Recent studies have revealed that alterations in the skin microbiota composition can predispose to certain disorders.

Atopic dermatitis (AD): This is an immune-mediated inflammatory skin disorder and associations have been made between some *Staphylococcus* spp., and in particular, *S. aureus*[91]. Studies in both mice and humans have shown a correlation between overabundant colonization of *S. aureus* correlates with worsening AD[91]. Dysbiosis with relative increase in abundance of *Staphylococcus* spp. and *Corynebacterium* spp. was also observed in a genetically engineered murine model of AD[91]. Importantly, administration of antibiotics to mice deficient in epidermal ADAM17 (Adam17$^{\Delta Sox9}$) prevented eczematous lesion development. This also resulted a decrease in in skin-infiltrating T-cell numbers and increased diversity of the skin microbiome[91]. This study clearly demonstrated that alterations and increase of *S. aureus* contribute to AD-like lesions and could be responsible for acute atopic flares in humans[91].

Psoriasis: This is another chronic inflammatory skin disease that involves a dysregulated interaction among immune cells, keratinocytes and microbiota of the skin. Analyses of microbiota composition in psoriatic patients compared to healthy controls revealed an increased abundance of the genus *Streptococcus* and a relative decrease in abundance of the genus *Propionibacterium*, while presenting inconsistent findings on the abundance of *Staphylococcus*[91].

Lung microbiota

Microbial colonization occurs at all body surfaces that are exposed to the external environment including the bronchopulmonary tract. Indeed, healthy lungs were traditionally considered sterile, mainly due to the inability to culture bacteria from lower airway samples using routine microbiological approaches. A shift towards molecular methods for the quantification and sequencing of bacterial DNA revealed the presence of microbial communities containing a complex diversity of bacteria in the lower respiratory tract[92]. *Proteobacteria*, *Firmicutes* and *Bacteroidetes* are the most prevalent phyla in the human respiratory tract, as determined from bronchoalveolar lavage samples of healthy adults[93,94].

Lung microbiota dysbiosis and diseases

Akin to discoveries in intestinal research, it has been shown that changes in this local microbial community (dysbiosis of the lung microbiota) are associated with the exacerbation of several pulmonary disorders, including chronic obstructive pulmonary disease (COPD), asthma and cystic fibrosis[95,96] as well as lung cancer[97].

Asthma: The first studies that characterised the airway microbiome in asthmatic patients reported an increased abundance of *Proteobacteria*, whereas the *Bacteroidetes* phylum was under-represented compared to healthy control[98,99].

Chronic Obstructive Pulmonary Disorder (COPD): COPD is another lung disease characterised by a largely irreversible chronic obstruction of airflow that interferes with normal breathing. The gradual course of the disease is characterised by intermittent

exacerbations[100]. It has been shown that in the lungs of COPD patients *Moraxella*, *Haemophilus* and *Actinobacteria* are over-represented[100]. In COPD patients with severe impairment of lung function and during exacerbations, it has been observed that there is a reduction of microbial diversity which was particularly associated with dominance of *Pseudomonas* spp[22,101,102]. Importantly, higher abundance of *Moraxella* was found in COPD patients with a more neutrophilic exacerbation phenotype[22].

The influence of the host microbiota on functional aspects of intestinal and systemic immunity is not restricted to immune mediated diseases. The microbiota also has an important role in elimination of pathogens. For example, different studies have shown that mice completely devoid of a microbiota (Germ-Free mice) are more prone to infectious agents like *Shigella flexneri, Bacillus anthracis* and *Leismania*[103], suggesting that depletion of the gut microbiota can dampen intestinal immune response thus increased infections by enteric pathogens like *Citrobacter rodentium* and *Campylobacter jejuni*[104].

Microbiota and its role in colonization resistance against pathogens

The host microbiota has evolved ways to provide colonization resistance against pathogens, which can be either direct or indirect. The direct ways by which the microbiota provides resistance is by direct killing of invading competitors and competition for resources.

Direct killing

Different studies have suggested that the bacteria can produce bacteriocidal compounds called bacteriocins that can directly kill or cause growth suppression of related bacterial species[105]. These compounds are found throughout nature and are mostly small

polypeptide molecules. Most of the compounds have been isolated from the gut of humans and animals, lactic acid bacteria in fermented foods and from common probiotics like *Bifidobacteria*[105]. So it is quite rationale to believe that these compounds can be produced for competition within the gut microenvironment. Indeed, it has been shown in mice that strains of *Escherichia coli* (*E. coli*) that can make bacteriocins have a better and improved long-term persistence as compared to non-producers[106]. However, when these mice are pre-treated with streptomycin, an antibiotic that disrupts the normal gut community structure like *E. coli*, bacteriocin-producing *Enterococcus faecalis* (*E. faecalis*) were demonstrated to be able to colonize the mice much efficiently, in this case without antibiotic pre-treatment. Relevantly, this bacteriocin-positive strain was able to inhibit the colonization of a different *E. faecalis*, an opportunistic pathogen, vancomycin-resistant *Enterococcus* (VRE)[107]. Furthermore, *Lactobacillus* strain, which is a human derived probiotic when administered to mice were shown to protect them from *Listeria monocytogenes* infection, and this was dependent on the Lactobacillus bacteriocin[108]. Another human probiotic *E. coli* Nissle 1917 has been associated to compete with and protect mice from *Salmonella enterica* subsp. *Typhimurium* (*S*. Typhimurium) using bacteriocins[109].

Apart from bacteriocins, there are other antibacterial factors that are also important in the homeostasis of the gut ecosystem. Bacteriophages (viruses that infect bacteria) have been shown to have a critical impact on a population by lysing infected cells, and can also alter the bacterial fitness by transferring genetic information. Recent advances in sequencing technology have revealed abundant bacteriophages in the human gut, which have been mostly uncharacterized. These have been demonstrated to be present as both

viral particles and prophages (bacteriophage DNA that is integrated into a bacterial genome)[110–114]. Evidences have now revealed that inflammation may trigger that activation of prophages[115] and relevantly viral community may be different in people with inflammatory bowel disease[114]. In mouse model, it was also evident that *E. faecalis* that could produce bacteriophage had a competitive advantage against a related strain[116].

Another system employed specially by some gram-negative bacteria is the type VI secretion system (T6SS) which is a protein translocation complex. This system is used by bacteria to export effector proteins into other bacterial or eukaryotic cells. A recent study identified a novel family of T6SS proteins in members of the Bacteroidetes phylum[117], which is a major phylum inhabiting the mammalian guts. Several studies have highlighted the importance of the T6SS and its associated effectors and immunity in the competition between *Bacteroides* species inhabiting the mouse gut[117–119].

Inhibitory metabolites

The metabolic byproducts produced by bacteria have been also demonstrated to have an inhibitory effect on other bacteria. For example, short-chain fatty acids (SCFAs: e.g. acetic, propionic and butyric acid) are now recognized to be a critical factor in the inhibition of *S.* Typhimurium growth in the mouse[120] and are also active against pathogenic *E. coli*[121,122] and *Clostridium difficile (C. difficile)*[123]. These metabolic byproducts are produced mainly by anaerobic symbiotic bacteria *Bacteroides* and *Clostridia*, which are among the the most abundant members of the gut ecosystem. Another example of an inhibitory metabolite is bile acid. Bile acids are molecules that are amphipathic, a derivative of cholesterol that is secreted into the small intestine. A study by Buffie et al[123] found an association between bacterial species with protection from *C. difficile* infection

in antibiotic-treated mice and humans. They were able to identify a single bacterium *Clostridium scindens* as a good predictor of resistance. *C. scindens* is capable of creating secondary bile acids by 7α-dehydroxylation that can inhibit *C. difficile* growth. *C. scindens* was able to protect mice from *C. difficile*, as well as restoring secondary bile acid levels. Apart from the gut, the commensal skin bacterium S*. epidermidis* was shown to inhibit both nare colonization and biofilm formation by *S. aureus*. A subset of *S. epidermidis* expresses the Esp gene, which can synergize with a human-expressed AMP to interfere with *S. aureus* colonization[124].

Competition for availability of nutrients and space

There have been experiments done to support the notion that substrate availibilty is a critical determinant for a bacteria to successfully colonize the gut. One example of this is in *E. coli*, where it has been shown that the capability to utilize one sugar tilts the competitive balance to one strain between otherwise identical strains in the gut[125]. Moreover, using genetic screen, Lee et al. identified a genetic locus linked to host glycan utilization, that governs the intra-species competition among gut *Bacteroides*[126]. One of the bacterial symbionts in the gut, the *Bacteroides*, possess many genes that provides them the ability to digest complex polysaccharides, a trait which the host and other bacteria cannot. Moreover, it has been shown that that sialic acid and fructose, liberated from host glycans by symbionts like *Bacteroides* species, become an important source of sugar for certain pathogens to invade like *C.difficile* and *Citrobacter rodentium*[127]. Another important nutrient is iron, which has been shown to be important competing factor for *E. coli* Nissle's ability to reduce *S. Typhimurium* colonization in mice. Thus the host

microbiota has evolved many different ways to maintain a stable microbial community and provide colonization resistance to invading pathogens and pathobionts for the benefit of the host.

Given the importance of the microbiota in regulating the immune system function and, concomitantly, on succouring the homeostatic equilibrium of the meta-organism, the detailed understanding of the immune-modulatory action exerted by different commensal bacteria might provide new ways to control infectious disease(s) also. Notably, the influence of the microbiota on the severity of malaria, one of the most deadly infectious diseases has only now started to emerge.

Plasmodium infection, Malaria and Microbiota

Plasmodium, the causative agent of malaria, is a rapidly multiplying eukaryotic protozoan unicellular organism undergoing a complex developmental cycle in both the mammalian and the mosquito hosts. *Plasmodium* sporozoites, transmitted by an *Anopheles* mosquito, develop inside hepatocytes, each generating thousands of merozoites, later released into the bloodstream. Once inside red blood cells (RBCs), each merozoite replicates by schizogony into 10-30 new merozoites in every cycle. It is this blood stage that is responsible for the onset of severe disease[128]. While there are 5 *Plasmodium* species infecting humans, *Plasmodium falciparum* is accountable for most of malaria-associated mortality, primarily of young children and pregnant women in sub-Saharan Africa, and much of the morbidity. *P. vivax* also significantly contributes to morbidity and mortality, and *P. knowlesi* is a cause of severe and fatal malaria in South East Asia[129,130]. In numbers, an estimation of 219 million cases in 90 countries and 435 000 related deaths were reported in 2018[131].

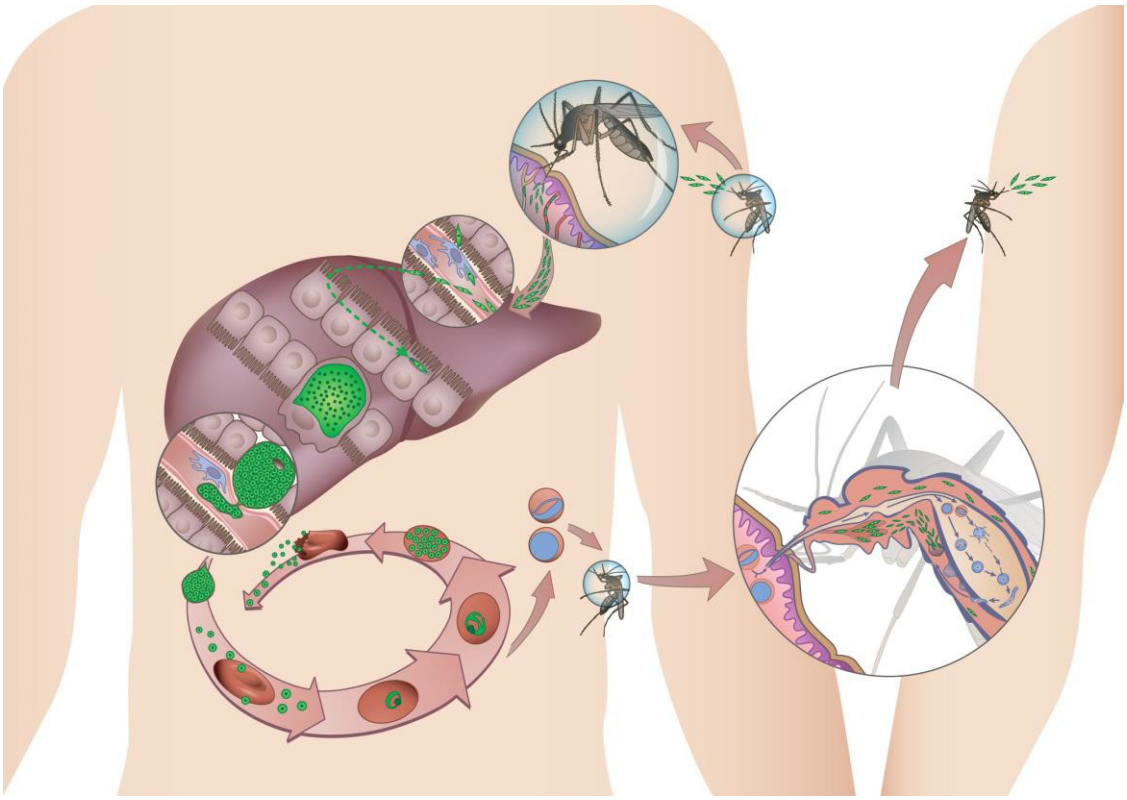

Fig. 1: Life cycle of *Plasmodium falciparum*

Plasmodium sporozoites, transmitted by an *Anopheles* mosquito, develop inside hepatocytes, each generating thousands of merozoites, later released into the bloodstream. Once inside red blood cells (RBCs), each merozoite replicates by schizogony into 10-30 new merozoites in every cycle. These merozoites can re-infect fresh erythrocutes, giving rise to a cyclical blood stage infection. In order to complete the cycle, some merozoites develop into sexual parasite stages, the male and the female

gametocytes, which will be taken up by the mosquitoes during blood meals. Gametocytes undergo fertilization and maturation in the mosquito midgut, forming an infective ookinete form that migrates into the mosquito haemocoel and develops into an oocyst form where sporozoites are developed. When fully matured, oocysts burst and release sporozoites which migrate into the mosquito's salivary glands, ready to be injected into another host.

Despite this unacceptably high health, economic and social burden, the reasons why some individuals develop severe malaria and others do not are only partially understood. Host genetic factors, mostly influencing characteristics of the RBC, have a critical role in affording protection from severe malaria[132,133]. There are also parasite factors associated with a greater likelihood of developing malarial-associated severe pathology. The best documented are the *var* gene polymorphisms in *P. falciparum* which influence sequestration, i.e., the adherence of parasitized RBCs to the vascular endothelium [134,135]. Additionally, we and others have recently shown that environmental cues modulate parasite virulence during malaria infections[136,137]. Still, severe malaria can manifest in very different ways, with a variety of well-recognized clinical phenotypes, which are highly predictive of death, occurring alone or in combination. These include severe anaemia, coma (cerebral malaria), renal failure, and respiratory distress. Interestingly, the reasons why a given individual with malaria develops one or a particular combination of malaria-associated clinical symptoms rather than another remains unknown, although it is clearly not due to chance because these different manifestations have strong associations with factors such as host age and the intensity of malaria transmission in the area they live in.

Notably, it is estimated that malarial infections indirectly contribute to the occurrence of other infectious diseases, predisposing to bacteremia[138,139], and adding to the overall disease burden [138]. Whether these interactions contribute to disease severity, potentially prompting particular severe malaria-associated clinical patterns versus others remains to be tested. Highly relevant is the fact that, after an unprecedented period of success in global malaria control – a reduction of approximately 50% in malaria-associated deaths during the first 15 years of the new millennium - progress has stalled now. World Health Organization reporting on data from 2015–2017 clearly show that no significant progress in reducing global malaria cases was made in this period[131]. While it is consensual that the audacious goal of malaria eradication will not be achieved with the currently available tools [140], we like many others strongly support the novel paradigm in malaria research – to focus on the triad of parasite, hosts (either human or *Anopheles* mosquitoes) and environmental cues to unveil the complex interactions occurring amongst them, rather than on solely the parasite or the host.

Plasmodium Infection and Microbiota: Recent Advances

The intricate relationship established between host and *Plasmodium* parasites during malarial infections manifests itself at several levels. One of the most prominent is, perhaps, the immune response forwarded by the host that, in turn, the parasite attempts to modulate. This ensuing immune response, although limiting parasite burden during both the liver[141] and the blood stages of infection[142], is causally associated to the pathophysiology of severe malaria. Such deviation from immune homeostasis might directly, or indirectly, impact on host microbiota composition during malaria infections. Conversely, and considering its immune-modulatory function, putative changes in

microbiota composition during malaria infections may alter host immunity. It is, therefore, tempting to speculate that a three-way cross-talk between host-*Plasmodium*-microbiota may impact on the clinical outcome of malarial infections. Recent reports suggest that this might be the case.

In a rodent model of malaria infection, mice from different vendors exhibit striking differences in disease severity when infected with *Plasmodium* strains [143]. This differences in disease severity were associated with a particular composition of the gut microbiota, i.e., increased abundances of *Lactobacillus* and *Bifidobacterim* spp. Protection from malarial-associated severe disease could be transferred by fecal-microbiota-transfer (FMT) from mice exhibiting mild disease phenotypes to susceptible ones [143]. Moreover, probiotic administration was sufficient to modulate disease susceptibility [143]. Such observations suggest that differences in the gut microbial community structure may influence malaria disease severity. Conversely, *Plasmodium* infections may impact on the composition of commensal bacteria populations. In fact, in two independent studies, evidence has been provided that infection with 2 distinct rodent *Plasmodium* spp (*P. yoelii* and *P. berghei*) resulted in alterations in the gut microbiota profile[144,145]. The authors propose that such differences in gut microbiota profiles are associated with distinct clinical outcomes of infection, i.e., cerebral and intestinal pathologies.

In humans, the presence of certain bacterial micro-flora in the gut was correlated with protection against *Plasmodium falciparum*[146] as individuals harbouring increased abundance of the bacterial taxa *Bifidobacterium* and *Streptococcus* are at lower risk of *P. falciparum* infection [146]. Interestingly, the suggested protective enterotypes in human

malaria infections are, at least in part, common to those identified by Villarino and colleagues[143].

The influence of host microbiota composition may extend to other aspects of *Plasmodium* infections, beyond malarial disease severity. The complex life cycle of *Plasmodium* parasites is divided between two very distinct hosts, i.e., the vertebrate host and the *Anopheles* mosquito. Evidence has been accumulating which suggests that microbiota strongly influences the mosquito's vectorial ability, mostly by negatively impacting *Plasmodium* development in a bacterial strain-specific manner[147]. While the impact of mosquito microbiota in *Plasmodium* life cycle is not the focus of this thesis, it is important to emphasize a mechanistic study showing that mammalian host microbiota composition influences the interface between mosquito and the vertebrate host, i.e, parasite transmission. Yilmaz et al demonstrated that mice colonized with a human gut pathobiont *E. coli* (O86:B7) expressing α-galactosyl were protected from effective *Plasmodium* liver stage infection[148]. Such inability of the parasite to successfully establish a productive infection was mainly due to cross-reactivity of naturally-occurring α-galactosyl antibodies with *Plasmodium* spp. sporozoites (the mosquito-transmitted and hepato-tropic form of the parasite), thus impairing the establishment of sporozoites within the hepatocyte[148].

The role of the microbiota in pathophysiological mechanisms is, at least in part, attributable to reciprocal immune system-microbial interactions influencing inflammation and immunity, not only locally at the mucosal level but also systemically [149]. Given that *Plasmodium* infections seem to impact significantly on the composition of the host microbiota [150,151], we reasoned in this thesis that *Plasmodium* driven microbiota

alterations may impact inflammatory processes central for the pathophysiology of severe symptoms during malaria.

References

1. Cho, I. & Blaser, M. J. The human microbiome: at the interface of health and disease. *Nat. Rev. Genet.* **13,** 260–70 (2012).
2. Grice, E. A. & Segre, J. A. The skin microbiome. *Nat. Rev. Microbiol.* **9,** 244–253 (2011).
3. Frank, D. N. *et al.* The Human Nasal Microbiota and Staphylococcus aureus Carriage. *PLoS One* **5,** e10598 (2010).
4. Lazarevic, V. *et al.* Metagenomic study of the oral microbiota by Illumina high-throughput sequencing. *J. Microbiol. Methods* **79,** 266–271 (2009).
5. Kim, T. K. *et al.* Heterogeneity of Vaginal Microbial Communities within Individuals. *J. Clin. Microbiol.* **47,** 1181–1189 (2009).
6. Maldonado-Contreras, A. *et al.* Structure of the human gastric bacterial community in relation to Helicobacter pylori status. *ISME J.* **5,** 574–579 (2011).
7. Hilty, M. *et al.* Disordered Microbial Communities in Asthmatic Airways. *PLoS One* **5,** e8578 (2010).
8. Erb-Downward, J. R. *et al.* Analysis of the Lung Microbiome in the 'Healthy' Smoker and in COPD. *PLoS One* **6,** e16384 (2011).
9. Eckburg, P. B. *et al.* Diversity of the Human Intestinal Microbial Flora. *Science*

(80-.). **308,** 1635–1638 (2005).

10. Yatsunenko, T. *et al.* Human gut microbiome viewed across age and geography. *Nature* **486,** 222–227 (2012).
11. Sommer, F., Anderson, J. M., Bharti, R., Raes, J. & Rosenstiel, P. The resilience of the intestinal microbiota influences health and disease. *Nature Reviews Microbiology* **15,** 630–638 (2017).
12. Gilbert, J. A. *et al.* Microbiome-wide association studies link dynamic microbial consortia to disease. *Nature* **535,** 94–103 (2016).
13. Lozupone, C. A., Stombaugh, J. I., Gordon, J. I., Jansson, J. K. & Knight, R. Diversity, stability and resilience of the human gut microbiota. *Nature* **489,** 220–230 (2012).
14. Huttenhower, C. *et al.* Structure, function and diversity of the healthy human microbiome. *Nature* **486,** 207–214 (2012).
15. Wu, G. D. *et al.* Linking long-term dietary patterns with gut microbial enterotypes. *Science (80-.).* **334,** 105–108 (2011).
16. Yatsunenko, T. *et al.* Human gut microbiome viewed across age and geography. *Nature* **486,** 222–227 (2012).
17. David, L. A. *et al.* Host lifestyle affects human microbiota on daily timescales. *Genome Biol.* **15,** R89 (2014).
18. Chow, J. & Mazmanian, S. K. A pathobiont of the microbiota balances host colonization and intestinal inflammation. *Cell Host Microbe* **7,** 265–276 (2010).
19. Stecher, B., Maier, L. & Hardt, W. D. ‘Blooming’ in the gut: How dysbiosis might contribute to pathogen evolution. *Nature Reviews Microbiology* **11,** 277–284

(2013).

20. Frank, D. N. *et al.* Molecular-phylogenetic characterization of microbial community imbalances in human inflammatory bowel diseases. *Proc. Natl. Acad. Sci. U. S. A.* **104,** 13780–13785 (2007).

21. Garrett, W. S. *et al.* Communicable Ulcerative Colitis Induced by T-bet Deficiency in the Innate Immune System. *Cell* **131,** 33–45 (2007).

22. Wang, Z. *et al.* Lung microbiome dynamics in COPD exacerbations. *Eur. Respir. J.* **47,** 1082–1092 (2016).

23. Sze, M. A. *et al.* The Lung Tissue Microbiome in Chronic Obstructive Pulmonary Disease. *Am. J. Respir. Crit. Care Med.* **185,** 1073–1080 (2012).

24. Conti, F. *et al.* Association between Staphylococcus aureus nasal carriage and disease phenotype in patients affected by systemic lupus erythematosus. *Arthritis Res. Ther.* **18,** 177 (2016).

25. Totté, J. E. E. *et al.* A systematic review and meta-analysis on Staphylococcus aureus carriage in psoriasis, acne and rosacea. *Eur. J. Clin. Microbiol. Infect. Dis.* **35,** 1069 (2016).

26. Totté, J. E. E. *et al.* Prevalence and odds of S *taphylococcus aureus* carriage in atopic dermatitis: a systematic review and meta-analysis. *Br. J. Dermatol.* **175,** 687–695 (2016).

27. LJ, Z. *et al.* Innate immunity. Dermal adipocytes protect against invasive Staphylococcus aureus skin infection. *Science* **347,** 67–71 (2015).

28. Korem, T. *et al.* Growth dynamics of gut microbiota in health and disease inferred from single metagenomic samples. *Science (80-.).* **349,** 1101–1106 (2015).

29. Buffington, S. A. *et al.* Microbial Reconstitution Reverses Maternal Diet-Induced Social and Synaptic Deficits in Offspring. *Cell* **165,** 1762–1775 (2016).

30. Hsiao, E. Y. *et al.* Microbiota modulate behavioral and physiological abnormalities associated with neurodevelopmental disorders. *Cell* **155,** 1451–1463 (2013).

31. Buffie, C. G. *et al.* Precision microbiome reconstitution restores bile acid mediated resistance to Clostridium difficile. *Nature* **517,** 205–208 (2015).

32. Cotillard, A. *et al.* Dietary intervention impact on gut microbial gene richness. *Nature* **500,** 585–588 (2013).

33. Le Chatelier, E. *et al.* Richness of human gut microbiome correlates with metabolic markers. *Nature* **500,** 541–546 (2013).

34. Norman, J. M. *et al.* Disease-specific alterations in the enteric virome in inflammatory bowel disease. *Cell* **160,** 447–460 (2015).

35. Monaco, C. L. *et al.* Altered Virome and Bacterial Microbiome in Human Immunodeficiency Virus-Associated Acquired Immunodeficiency Syndrome. *Cell Host Microbe* **19,** 311–322 (2016).

36. Kostic, A. D. *et al.* The dynamics of the human infant gut microbiome in development and in progression toward type 1 diabetes. *Cell Host Microbe* **17,** 260–273 (2015).

37. Mosca, A., Leclerc, M. & Hugot, J. P. Gut microbiota diversity and human diseases: Should we reintroduce key predators in our ecosystem? *Front. Microbiol.* **7,** (2016).

38. Levy, M., Thaiss, C. A. & Elinav, E. Metagenomic cross-talk: The regulatory interplay between immunogenomics and the microbiome. *Genome Medicine* **7,**

(2015).

39. Goodrich, J. K. *et al.* Human genetics shape the gut microbiome. *Cell* **159,** 789–799 (2014).

40. Wang, J. *et al.* Genome-wide association analysis identifies variation in Vitamin D receptor and other host factors influencing the gut microbiota. *Nat. Genet.* **48,** 1396–1406 (2016).

41. Turpin, W. *et al.* Association of host genome with intestinal microbial composition in a large healthy cohort. *Nat. Genet.* **48,** 1413–1417 (2016).

42. Bonder, M. J. *et al.* The effect of host genetics on the gut microbiome. *Nat. Genet.* **48,** 1407–1412 (2016).

43. Benson, A. K. *et al.* Individuality in gut microbiota composition is a complex polygenic trait shaped by multiple environmental and host genetic factors. *Proc. Natl. Acad. Sci. U. S. A.* **107,** 18933–18938 (2010).

44. Koenig, J. E. *et al.* Succession of microbial consortia in the developing infant gut microbiome. *Proc. Natl. Acad. Sci.* **108,** 4578–4585 (2011).

45. Dominguez-Bello, M. G. *et al.* Delivery mode shapes the acquisition and structure of the initial microbiota across multiple body habitats in newborns. *Proc. Natl. Acad. Sci. U. S. A.* **107,** 11971–5 (2010).

46. McCafferty, J. *et al.* Stochastic changes over time and not founder effects drive cage effects in microbial community assembly in a mouse model. *ISME J.* **7,** 2116–2125 (2013).

47. Lax, S. *et al.* Longitudinal analysis of microbial interaction between humans and the indoor environment. *Science (80-.).* **345,** 1048–1052 (2014).

48. Lupp, C. *et al.* Host-Mediated Inflammation Disrupts the Intestinal Microbiota and Promotes the Overgrowth of Enterobacteriaceae. *Cell Host Microbe* **2,** 119–129 (2007).

49. Stecher, B. *et al.* Salmonella enterica serovar typhimurium exploits inflammation to compete with the intestinal microbiota. *PLoS Biol.* **5,** 2177–2189 (2007).

50. Arthur, J. C. *et al.* Intestinal inflammation targets cancer-inducing activity of the microbiota. *Science (80-.).* **338,** 120–123 (2012).

51. Ayres, J. S., Trinidad, N. J. & Vance, R. E. Lethal inflammasome activation by a multidrug-resistant pathobiont upon antibiotic disruption of the microbiota. *Nat. Med.* **18,** 799–806 (2012).

52. David, L. A. *et al.* Diet rapidly and reproducibly alters the human gut microbiome. *Nature* **505,** 559–563 (2014).

53. Sonnenburg, E. D. *et al.* Diet-induced extinctions in the gut microbiota compound over generations. *Nature* **529,** 212–215 (2016).

54. Denou, E., Marcinko, K., Surette, M. G., Steinberg, G. R. & Schertzer, J. D. High-intensity exercise training increases the diversity and metabolic capacity of the mouse distal gut microbiota during diet-induced obesity. *Am. J. Physiol. - Endocrinol. Metab.* **310,** E982–E993 (2016).

55. Abubucker, S. *et al.* Obesity-induced gut microbial metabolite promotes liver cancer through senescence secretome. *Nature* **7,** 1–9 (2015).

56. Zhu, W. *et al.* Gut Microbial Metabolite TMAO Enhances Platelet Hyperreactivity and Thrombosis Risk. *Cell* **165,** 111–124 (2016).

57. Ferreyra, J. A. *et al.* Gut Microbiota-Produced Succinate Promotes C. difficile

Infection after Antibiotic Treatment or Motility Disturbance. *Cell Host Microbe* **16,** 770–777 (2014).

58. Logan, R. F., Logan, R. F. A., Rodrigues, L. C. & Wheeler, J. G. Inflammatory bowel disease incidence: up, down or unchanged? *Gut* **42,** 309–11 (1998).

59. Hufnagl, K., Pali-Schöll, I., Roth-Walter, F. & Jensen-Jarolim, E. Dysbiosis of the gut and lung microbiome has a role in asthma. *Semin. Immunopathol.* **42,** 75–93 (2020).

60. Neish, A. S. Microbes in Gastrointestinal Health and Disease. *Gastroenterology* **136,** 65–80 (2009).

61. Backhed, F. Host-Bacterial Mutualism in the Human Intestine. *Science (80-.).* **307,** 1915–1920 (2005).

62. Sommer, F., Anderson, J. M., Bharti, R., Raes, J. & Rosenstiel, P. The resilience of the intestinal microbiota influences health and disease. *Nat. Rev. Microbiol.* **15,** 630–638 (2017).

63. Ho, J. T. K., Chan, G. C. F. & Li, J. C. B. Systemic effects of gut microbiota and its relationship with disease and modulation. *BMC Immunol.* **16,** 21 (2015).

64. Kostic, A. D., Howitt, M. R. & Garrett, W. S. Exploring host-microbiota interactions in animal models and humans. *Genes Dev.* **27,** 701–18 (2013).

65. Scher, J. U. & Abramson, S. B. The microbiome and rheumatoid arthritis. *Nat. Rev. Rheumatol.* **7,** 569–578 (2011).

66. Tremaroli, V. & Bäckhed, F. Functional interactions between the gut microbiota and host metabolism. *Nature* **489,** 242–249 (2012).

67. Turnbaugh, P. J. *et al.* A core gut microbiome in obese and lean twins. *Nature*

457, 480–484 (2009).

68. Zitvogel, L. *et al.* Cancer and the gut microbiota: an unexpected link. *Sci. Transl. Med.* **7,** 271ps1 (2015).

69. Gevers, D. *et al.* The treatment-naive microbiome in new-onset Crohn's disease. *Cell Host Microbe* **15,** 382–392 (2014).

70. Strauss, J. *et al.* Invasive potential of gut mucosa-derived fusobacterium nucleatum positively correlates with IBD status of the host. *Inflamm. Bowel Dis.* **17,** 1971–1978 (2011).

71. Jabri, B. & Sollid, L. M. Tissue-mediated control of immunopathology in coeliac disease. *Nature Reviews Immunology* **9,** 858–870 (2009).

72. Di Cagno, R. *et al.* Duodenal and faecal microbiota of celiac children: Molecular, phenotype and metabolome characterization. *BMC Microbiol.* **11,** (2011).

73. Wu, H. J. *et al.* Gut-residing segmented filamentous bacteria drive autoimmune arthritis via T helper 17 cells. *Immunity* **32,** 815–827 (2010).

74. Bielski, C. *et al.* Expansion of intestinal Prevotella copri correlates with enhanced susceptibility to arthritis. *Elife* **2,** 1–20 (2013).

75. Zhang, X. *et al.* The oral and gut microbiomes are perturbed in rheumatoid arthritis and partly normalized after treatment. *Nat. Med.* **21,** 895–905 (2015).

76. Achenbach, P., Bonifacio, E., Koczwara, K. & Ziegler, A.-G. Natural history of type 1 diabetes. *Diabetes* **54 Suppl 2,** S25-31 (2005).

77. Wen, L. *et al.* Innate immunity and intestinal microbiota in the development of Type 1 diabetes. *Nature* **455,** 1109–13 (2008).

78. Kostic, A. D. *et al.* The Dynamics of the Human Infant Gut Microbiome in

Development and in Progression toward Type 1 Diabetes. *Cell Host Microbe* **17,** 260–273 (2015).

79. Risnes, K. R., Belanger, K., Murk, W. & Bracken, M. B. Antibiotic Exposure by 6 Months and Asthma and Allergy at 6 Years: Findings in a Cohort of 1,401 US Children. *Am. J. Epidemiol.* **173,** 310–318 (2011).

80. Russell, S. L. *et al.* Early life antibiotic-driven changes in microbiota enhance susceptibility to allergic asthma. *EMBO Rep.* **13,** 440–447 (2012).

81. Cahenzli, J., Köller, Y., Wyss, M., Geuking, M. B. & McCoy, K. D. Intestinal Microbial Diversity during Early-Life Colonization Shapes Long-Term IgE Levels. *Cell Host Microbe* **14,** 559–570 (2013).

82. Hill, D. A. *et al.* Commensal bacteria–derived signals regulate basophil hematopoiesis and allergic inflammation. *Nat. Med.* **18,** 538–546 (2012).

83. Viaud, S. *et al.* The Intestinal Microbiota Modulates the Anticancer Immune Effects of Cyclophosphamide. *Science (80-.).* **342,** 971–976 (2013).

84. Derosa, L., Routy, B., Kroemer, G. & Zitvogel, L. The intestinal microbiota determines the clinical efficacy of immune checkpoint blockers targeting PD-1/PD-L1. *Oncoimmunology* **7,** e1434468 (2018).

85. Daillère, R. *et al.* Enterococcus hirae and Barnesiella intestinihominis Facilitate Cyclophosphamide-Induced Therapeutic Immunomodulatory Effects. *Immunity* **45,** 931–943 (2016).

86. Matson, V. *et al.* The commensal microbiome is associated with anti-PD-1 efficacy in metastatic melanoma patients. *Science* **359,** 104–108 (2018).

87. Routy, B. *et al.* Gut microbiome influences efficacy of PD-1–based

immunotherapy against epithelial tumors. *Science (80-.).* **359,** 91–97 (2018).

88. Nicolaides, N. Skin lipids: their biochemical uniqueness. *Science* **186,** 19–26 (1974).

89. Drake, D. R., Brogden, K. A., Dawson, D. V. & Wertz, P. W. *Thematic Review Series: Skin Lipids* . Antimicrobial lipids at the skin surface. *J. Lipid Res.* **49,** 4–11 (2008).

90. Puhvel, S. M., Reisner, R. M. & Sakamoto, M. Analysis of Lipid Composition of Isolated Human Sebaceous Gland Homogenates After Incubation with Cutaneous Bacteria. Thin-Layer Chromatography. *J. Invest. Dermatol.* **64,** 406–411 (1975).

91. Park, Y. J. & Lee, H. K. The Role of Skin and Orogenital Microbiota in Protective Immunity and Chronic Immune-Mediated Inflammatory Disease. *Front. Immunol.* **8,** 1955 (2018).

92. O'Dwyer, D. N., Dickson, R. P. & Moore, B. B. The Lung Microbiome, Immunity, and the Pathogenesis of Chronic Lung Disease. *J. Immunol.* **196,** 4839–47 (2016).

93. Hilty, M. *et al.* Disordered Microbial Communities in Asthmatic Airways. *PLoS One* **5,** e8578 (2010).

94. Erb-Downward, J. R. *et al.* Analysis of the Lung Microbiome in the 'Healthy' Smoker and in COPD. *PLoS One* **6,** e16384 (2011).

95. O'Dwyer, D. N., Dickson, R. P. & Moore, B. B. The Lung Microbiome, Immunity, and the Pathogenesis of Chronic Lung Disease. *J. Immunol.* **196,** 4839–47 (2016).

96. Salami, O. & Marsland, B. J. Has the airway microbiome been overlooked in

respiratory disease? *Genome Med.* **7,** 62 (2015).

97. Jin, C. *et al.* Commensal Microbiota Promote Lung Cancer Development via γδ T Cells. *Cell* **176,** 998–1013 (2019).

98. Huang, Y. J. *et al.* Airway microbiota and bronchial hyperresponsiveness in patients with suboptimally controlled asthma. *J. Allergy Clin. Immunol.* **127,** 372–381.e3 (2011).

99. Hilty, M. *et al.* Disordered Microbial Communities in Asthmatic Airways. *PLoS One* **5,** e8578 (2010).

100. Vestbo, J. *et al.* Global Strategy for the Diagnosis, Management, and Prevention of Chronic Obstructive Pulmonary Disease. *Am. J. Respir. Crit. Care Med.* **187,** 347–365 (2013).

101. Erb-Downward, J. R. *et al.* Analysis of the Lung Microbiome in the 'Healthy' Smoker and in COPD. *PLoS One* **6,** e16384 (2011).

102. Huang, Y. J. *et al.* Airway Microbiome Dynamics in Exacerbations of Chronic Obstructive Pulmonary Disease. *J. Clin. Microbiol.* **52,** 2813–2823 (2014).

103. Smith, K., McCoy, K. D. & Macpherson, A. J. Use of axenic animals in studying the adaptation of mammals to their commensal intestinal microbiota. *Semin. Immunol.* **19,** 59–69 (2007).

104. Lupp, C. *et al.* Host-Mediated Inflammation Disrupts the Intestinal Microbiota and Promotes the Overgrowth of Enterobacteriaceae. *Cell Host Microbe* **2,** 119–129 (2007).

105. Hammami, R., Fernandez, B., Lacroix, C. & Fliss, I. Anti-infective properties of bacteriocins: an update. *Cell. Mol. Life Sci.* **70,** 2947–2967 (2013).

106. Gillor, O., Giladi, I. & Riley, M. A. Persistence of colicinogenic Escherichia coli in the mouse gastrointestinal tract. *BMC Microbiol.* **9,** 165 (2009).

107. Kommineni, S. *et al.* Bacteriocin production augments niche competition by enterococci in the mammalian gastrointestinal tract. *Nature* **526,** 719–722 (2015).

108. Corr, S. C. *et al.* Bacteriocin production as a mechanism for the antiinfective activity of Lactobacillus salivarius UCC118. *Proc. Natl. Acad. Sci.* **104,** 7617–7621 (2007).

109. Sassone-Corsi, M. *et al.* Microcins mediate competition among Enterobacteriaceae in the inflamed gut. *Nature* **540,** 280–283 (2016).

110. Reyes, A. *et al.* Viruses in the faecal microbiota of monozygotic twins and their mothers. *Nature* **466,** 334–8 (2010).

111. Stern, A., Mick, E., Tirosh, I., Sagy, O. & Sorek, R. CRISPR targeting reveals a reservoir of common phages associated with the human gut microbiome. *Genome Res.* **22,** 1985–1994 (2012).

112. Breitbart, M. *et al.* Metagenomic analyses of an uncultured viral community from human feces. *J. Bacteriol.* **185,** 6220–3 (2003).

113. Minot, S. *et al.* The human gut virome: Inter-individual variation and dynamic response to diet. *Genome Res.* **21,** 1616–1625 (2011).

114. Manrique, P. *et al.* Healthy human gut phageome. *Proc. Natl. Acad. Sci.* **113,** 10400–10405 (2016).

115. Diard, M. *et al.* Inflammation boosts bacteriophage transfer between *Salmonella* spp. *Science (80-.).* **355,** 1211–1215 (2017).

116. Duerkop, B. A., Clements, C. V., Rollins, D., Rodrigues, J. L. M. & Hooper, L. V. A

composite bacteriophage alters colonization by an intestinal commensal bacterium. *Proc. Natl. Acad. Sci.* **109,** 17621–17626 (2012).

117. Russell, A. B. *et al.* A Type VI Secretion-Related Pathway in Bacteroidetes Mediates Interbacterial Antagonism. *Cell Host Microbe* **16,** 227–236 (2014).

118. Wexler, A. G. *et al.* Human symbionts inject and neutralize antibacterial toxins to persist in the gut. *Proc. Natl. Acad. Sci. U. S. A.* **113,** 3639–44 (2016).

119. Hecht, A. L. *et al.* Strain competition restricts colonization of an enteric pathogen and prevents colitis. *EMBO Rep.* **17,** 1281–1291 (2016).

120. Bohnhoff, m., miller, c. P. & martin, w. R. Resistance of the mouse's intestinal tract to experimental salmonella infection. I. Factors which interfere with the initiation of infection by oral inoculation. *J. Exp. Med.* **120,** 805–16 (1964).

121. Cherrington, C. A., Hinton, M., Pearson, G. R. & Chopra, I. Short-chain organic acids at pH 5.0 kill *Escherichia coli* and *Salmonella* spp. without causing membrane perturbation. *J. Appl. Bacteriol.* **70,** 161–165 (1991).

122. SUZUKI, M., MORISHITA, Y. & SHIN, R. Influence of intestinal anaerobes and organic acids on the growth of enterohaemorrhagic Escherichia coli O157:H7. *J. Med. Microbiol.* **51,** 201–206 (2002).

123. Rolfe, R. D. Role of volatile fatty acids in colonization resistance to Clostridium difficile. *Infect. Immun.* **45,** 185–91 (1984).

124. Otto, M. Staphylococcus colonization of the skin and antimicrobial peptides. *Expert Rev. Dermatol.* **5,** 183 (2010).

125. Sweeney, N. J. *et al.* The Escherichia coli K-12 gntP gene allows E. coli F-18 to occupy a distinct nutritional niche in the streptomycin-treated mouse large

intestine. *Infect. Immun.* **64,** 3497–503 (1996).

126. Lee, S. M. *et al.* Bacterial colonization factors control specificity and stability of the gut microbiota. *Nature* **501,** 426–429 (2013).
127. Ng, K. M. *et al.* Microbiota-liberated host sugars facilitate post-antibiotic expansion of enteric pathogens. *Nature* **502,** 96–99 (2013).
128. Phillips, M. A. *et al.* Malaria. *Nat. Rev. Dis. Prim.* **3,** 17050 (2017).
129. Battle, K. E. *et al.* The Global Public Health Significance of Plasmodium vivax. *Adv. Parasitol.* **80,** 1–111 (2012).
130. Baird, J. K. Evidence and implications of mortality associated with acute Plasmodium vivax malaria. *Clin. Microbiol. Rev.* **26,** 36–57 (2013).
131. Health Organization, W. *WORLD MALARIA REPORT 2017*.
132. Hill, A. V. S. *et al.* Common West African HLA antigens are associated with protection from severe malaria. *Nature* **352,** 595–600 (1991).
133. Driss, A. *et al.* Genetic polymorphisms linked to susceptibility to malaria. *Malar. J.* **10,** 271 (2011).
134. Kyriacou, H. M. *et al.* Differential var gene transcription in Plasmodium falciparum isolates from patients with cerebral malaria compared to hyperparasitaemia. *Mol. Biochem. Parasitol.* **150,** 211–8 (2006).
135. Kalmbach, Y. *et al.* Differential *var* Gene Expression in Children with Malaria and Antidromic Effects on Host Gene Expression. *J. Infect. Dis.* **202,** 313–317 (2010).
136. Mancio-Silva, L. *et al.* Nutrient sensing modulates malaria parasite virulence. *Nature* **547,** 213–216 (2017).
137. Lee, H. J. *et al.* Integrated pathogen load and dual transcriptome analysis of

systemic host-pathogen interactions in severe malaria. *Sci. Transl. Med.* **10,** eaar3619 (2018).

138. Scott, J. A. G. *et al.* Relation between falciparum malaria and bacteraemia in Kenyan children: a population-based, case-control study and a longitudinal study. *Lancet (London, England)* **378,** 1316–23 (2011).
139. Were, T. *et al.* Bacteremia in Kenyan children presenting with malaria. *J. Clin. Microbiol.* **49,** 671–6 (2011).
140. malERA Consultative Group on Diagnoses and Diagnostics. A Research Agenda for Malaria Eradication: Diagnoses and Diagnostics. *PLoS Med.* **8,** e1000396 (2011).
141. Liehl, P. *et al.* Host-cell sensors for Plasmodium activate innate immunity against liver-stage infection. *Nat. Med.* **20,** 47–53 (2014).
142. Belnoue, E. *et al.* On the pathogenic role of brain-sequestered alphabeta CD8+ T cells in experimental cerebral malaria. *J. Immunol.* **169,** 6369–75 (2002).
143. Villarino, N. F. *et al.* Composition of the gut microbiota modulates the severity of malaria. *Proc. Natl. Acad. Sci.* **113,** 2235–2240 (2016).
144. Mooney, J. P. *et al.* Inflammation-associated alterations to the intestinal microbiota reduce colonization resistance against non-typhoidal Salmonella during concurrent malaria parasite infection. *Sci. Rep.* **5,** 14603 (2015).
145. Taniguchi, T. *et al.* Plasmodium berghei ANKA causes intestinal malaria associated with dysbiosis. *Sci. Rep.* **5,** 15699 (2015).
146. Yooseph, S. *et al.* Stool microbiota composition is associated with the prospective risk of Plasmodium falciparum infection. *BMC Genomics* **16,** 631 (2015).

147. Romoli, O. & Gendrin, M. The tripartite interactions between the mosquito, its microbiota and Plasmodium. *Parasit. Vectors* **11,** 200 (2018).

148. Yilmaz, B. *et al.* Gut Microbiota Elicits a Protective Immune Response against Malaria Transmission. *Cell* **159,** 1277–1289 (2014).

149. Sharma, A. M. S. K. S. B. Acute lung injury and acute respiratory distress syndrome in malaria. *J Vector Borne Dis* **45,** 179–193

150. Yooseph, S. *et al.* Stool microbiota composition is associated with the prospective risk of Plasmodium falciparum infection. *BMC Genomics* **16,** 631 (2015).

151. Villarino, N. F. *et al.* Composition of the gut microbiota modulates the severity of malaria. *Proc. Natl. Acad. Sci.* **113,** 2235–2240 (2016).

The scientist is not a person who gives the right answers; he is one who asks the right questions - ***Claude Levi-Strauss***

Aims of the thesis

Main aims of the thesis

There is no doubt that human microbiota plays an important role in the well-being of the human host, and participates actively in the development of a wide variety of diseases, ranging from bacterial infections to liver diseases, cancer, metabolic diseases and even psychiatric disorders. Although the studies attempting to understand the possible impact of mammalian host microbiota in the course of a *Plasmodium* infection and the outcome of malaria are still in its budding stage, the main objective of this study is summarized below:

1. To assess mammalian host microbiota changes during *Plasmodium* infection and its impact on disease severity.
2. To unveil the mechanistic factors (both parasite and host) underlying host microbiota dysbiosis during *Plasmodium* infection.
3. To improve the clinical outcome of infection by modulating host microbiota.

“No amount of experimentation can ever prove me right, a single experiment can prove me wrong”. – ***Albert Einstein***

Results

Chapter 1

Phenotype: The impact of the host microbiota on severe malaria

Introduction

The reasons why some individuals develop severe malaria and others do not are only partially understood. Host genetic factors, mostly influencing characteristics of the RBC, have a critical role in affording protection from severe malaria[1,2]. There are also parasite factors associated with a greater likelihood of developing malarial-associated severe pathology. The best documented are the var gene polymorphisms in P. falciparum which influence sequestration, i.e., the adherence of parasitized RBCs to the vascular endothelium[3,4]. However, severe malaria can manifest in very different ways, with a variety of well-recognized clinical phenotypes, which are highly predictive of death, occurring alone or in combination. These include severe anaemia, coma (cerebral malaria), renal failure, and respiratory distress. Even less is known about the reasons why an individual with malaria develops one rather than another, although it is clearly not due to chance because these different manifestations have strong associations with factors such as host age and the intensity of malaria transmission in the area they live in[1,2].

The pathogeneses of severe malaria syndromes, such as MA-ARDS and cerebral malaria (CM), are commonly studied using rodent models of infection. MA-ARDS is recapitulated either by infecting C57BL/6 mice with *P. berghei* K173 (PbK173) (Fig. 1 a-d) or DBA/2 mice with *Pb* ANKA[5,6] (Fig. 1e-g). *P. berghei* strains causing lung injury produce histopathological features very similar to those of human MA-ARDS. It includes expansion of the alveolar septae by parasitized red blood cells (RBCs) and leukocytes, intra-alveolar haemorrhage and pulmonary oedema as measured by increased fluid content in the lung[7]

(Fig. 1c and g). Experimental CM (eCM) can be studied in C57BL/6J mice infected by *P. berghei* ANKA (PbANKA)[8] (Fig. 1 h-k) Importantly, in both the rodent model of MA-ARDS, we see the onset of symptoms around days 6 to 7 post-infection with *Plasmodium* parasites with a significant decrease in oxygen saturation levels (SpO2, <90%, Fig. 1l and m)

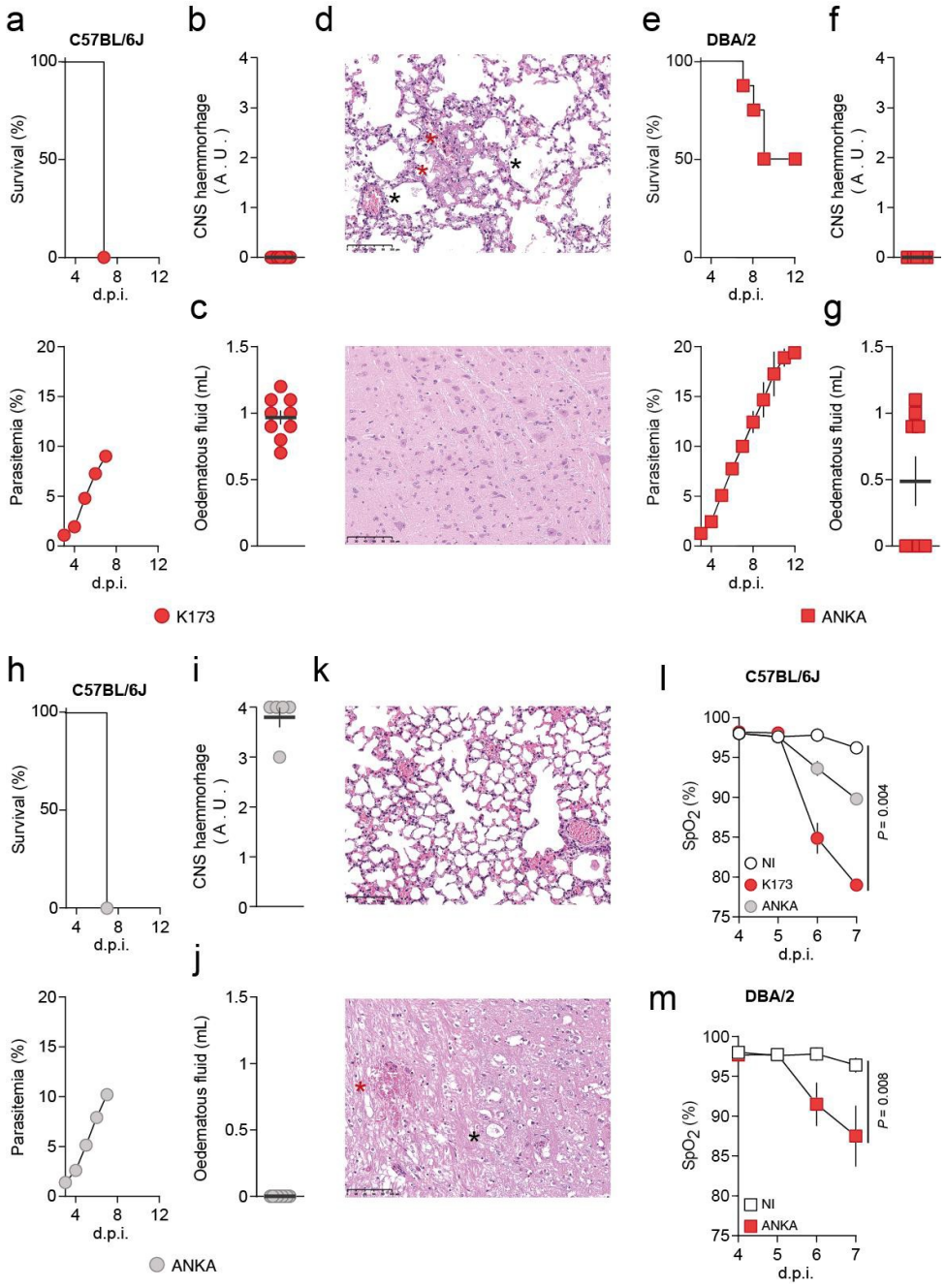

Fig. 1: Rodent models of severe malaria

a, Survival (upper panel; Log-rank Mantel-Cox, n=5;N=1) and parasitaemia (lower panel; linear regression n=5;N=1) of C57BL/6J mice infected with *Pb* K173. **b,** Central Nervous System (CNS) haemorrhage score (n=5;N=1) as measured by mid-brain haemorrhage severity of SPF C57BL/6J mice infected with *Pb* K173. **c,** Pulmonary oedema as measured by increased fluid content in the lungs of SPF C57BL/6J mice infected with *Pb* K173 (n=9;N=2). (Error bars are represented by mean ± s.e.m) **d,** Histological images of lung (upper panel) and CNS (lower panel) of SPF C57BL/6J mice infected with Pb K173. Alveolar oedema in the lung (black asterisk), and hyaline membranes deposition (red asterisk) were observed in the lung. No changes were observed in the brain. Scalebar = 100 µm. **e,** Survival (upper panel; Log-rank Mantel-Cox, n=5;N=1) and parasitemia (lower panel; mean ± s.e.m; linear regression, n=5;N=1) of SPF DBA/2 mice infected with *Pb* ANKA. **f,** CNS haemorrhage score (n=5;N=1) as measured by mid-brain haemorrhage severity of SPF DBA/2 mice infected with *Pb* ANKA. **g,** Pulmonary oedema as measured by increased fluid content in the lungs of SPF DBA/2 mice infected with *Pb* ANKA (n=9;N=2). (Error bars are represented by mean ± s.e.m) **h,** Survival (upper panel; Log-rank Mantel-Cox, n=10;N=1) and parasitemia (lower panel; linear regression, n=10;N=1) SPF C57BL/6J mice infected with *Pb* ANKA. **i,** CNS haemorrhage score (n=5;N=1) as measured by mid-brain haemorrhage severity of SPF C57BL/6J mice infected with *Pb* ANKA. (Error bars are represented by mean ± s.e.m) **j,** Pulmonary oedema as measured by increased fluid content in the lungs of SPF C57BL/6J mice infected with *Pb* ANKA (n=5;N=1) **k,** Histological images of lung (upper panel) and CNS (lower panel) of SPF

C57BL/6J mice infected with *Pb* ANKA. No changes were observed in the lung. There were marked mid-brain hemorrhages (red asterisk) and grey matter vacuolation (black asterisk). Scale bar = 100 μm. **l,** Time course measurement of oxygen saturation levels (SpO_2) as determined by pulse-oximetry (Kruskal-Wallis) of C57BL/6J mice infected either with *Pb* K173 (n=8;N=2), *Pb* ANKA (n=8;N=2) or non-infected (NI) controls (n=8;N=2). **m,** Time course measurement of oxygen saturation levels (SpO_2) as determined by pulse-oximetry (Kruskal-Wallis) of DBA/2 mice infected with *Pb* ANKA (n=5;N=1) or non-infected (NI) controls (n=5;N=1).

In this chapter we wanted to test the hypothesis that the host microbiota can dictate severe malaria pathology. We show that PbK173-infected germ-free mice (GF) had a significant delay in death (the vast majority dying later with hyperparasitaemia, if kept untreated), when compared to specific-pathogen free (SPF) mice. Importantly, GF mice infected with *Pb* ANKA developed eCM and eventually succumbed with the same kinetics as SPF mice. Moreover we show using 2 distinct host-*Plasmodium* combinations that mice that die of MA-ARDS have increased colony-forming-units (CFUs) of bacteria in the lungs and also altered microbiota composition of the lung. Altogether our data support the hypothesis that host microbiota can predispose an individual to one certain pathology over another and that changes in the lung microbiota due to *Plasmodium* infections promote MA-ARDS.

Materials and Methods

Mice. Male C57BL/6J and DBA/2 mice were purchased from Charles River breeding laboratories and housed in the animal facilities at Instituto de Medicina Molecular João Lobo Antunes (iMM-JLA) and Instituto Gulbenkian de Ciência (IGC) in specific pathogen-free (SPF) conditions. Germ-free mice were generated at the Germ Free breeding facility at IGC and housed in gnotobiotic conditions. Animals were housed under the following conditions with 14h Light: 10h Dark cycle, temperature 20-24^{0}C and relative humidity of 55±10%.

Animal experiments were performed according to EU regulations and approved by the Órgão Responsável pelo Bem-estar Animal (ORBEA) of Instituto de Medicina Molecular and by the Direcção-Geral de Alimentação e Veterinária (Portugal),

For gut and lung microbiome analysis, unless otherwise stated, C57BL/6J mice were co-housed under specific pathogen–free conditions with 3 mice per cage in 10 different cages. After 2 weeks of co-housing mice were infected with different *Plasmodium* strains together with non-infected mice in each cage to account for any cage variability. For DBA/2 mice, 4 mice were co-housed together for 2 weeks, with 1 mice kept as sentinel to monitor microbiome variations due to bedding or cage effect.

Parasites and infections. Male C57BL/6J and DBA/2 mice were infected, by intraperitoneal route, with 1 x 10^6 luciferase-expressing *Plasmodium berghei* ANKA (GFP-Luc$_{schiz}$, 1037cl1), *Plasmodium berghei* K173 (GFP-Luc$_{schiz}$, 1006cl1) and *Plasmodium berghei* ANKA *smac*- (1242cl5m1cl1cl2) infected red blood cells (iRBC).

Survival and parasitemia, assessed by Giemsa stained blood smears and expressed as percentage of iRBC, were monitored daily.

Oxygen Saturation measurements. Pulse oximeter (StarLife Sciences) was used to measure blood SpO2 on mice three, five and seven days post-infection. Mice were held by hand and the pulse oximeter clip was placed on the hind leg. Mice were held and covered by the light blocker fabric supplied by the manufacturer and held until calm (several seconds), before placing the probe on the hind leg over the skin near the femur bone. Three minute readings were taken from each mouse the average of 5-10 individual readings were calculated.

Bacterial DNA isolation. Lungs and faecal pellets were harvested under sterile conditions and immediately snap frozen in liquid nitrogen. Samples were stored at −80°C until processing for DNA isolation. Genomic DNA was extracted from lung using a commercial kit (DNeasy tissue kit; Qiagen, Germantown, MD) and from fecal pellets using QIAamp Fast DNA Stool Mini Kit (Qiagen). Lung samples were processed based on a modified protocol previously demonstrated to isolate bacterial DNA from lungs [9,10]. Briefly, lungs were subjected to bead beating for 1min using 1mm diameter silica beads (BioSpec Products, United States, catalog number: 11079110z) in a MiniBeadBeater homogenizer (BioSpec Products) for 2mins. Lung samples were incubated overnight at 60°C with 400µl of Tissue lysis buffer and 50µl of lysozyme included in the kit. Following this, DNA was extracted from both gut and lung samples following instructions from the QIAamp Fast DNA Stool Mini Kit and DNeasy tissue kit. DNA was used directly for 16S rRNA analysis.

16S rRNA analysis. 16S rRNA gene amplification and sequencing was carried out at the Genomics Unit at IGC. The V4 region of the 16S rRNA gene was amplified in triplicate for each sample, using the primer pair F515/R806. PCRs were done under the following conditions: 3 min at 94°C, 35 cycles of 60s at 94°C, 60s at 50°C, and 105s at 72°C, with an extension step of 10 min at 72°C. Samples were then pair-end sequenced on an Illumina MiSeq Benchtop Sequencer (Illumina), following Illumina recommendations [11,12].

Each lung sample was cleaned of *Plasmodium* parasite and host sequences using Kraken2. To do this, we first created a Kraken2 index consisting of the Bacteria and Archaea libraries plus the mouse genome (GRCm39) and the genomes of *Plasmodium berghei* ANKA (GCA_900002375.2) and K173 (GCA_900044334.1), all of which were downloaded from NCBI. The reads of each sample were then mapped against this database with Kraken2 and the script extract_kraken_reads.py (from KrakenTools; https://github.com/jenniferlu717/KrakenTools) was used to filter reads in order to keep only those mapping to Bacteria or Archaea for further analysis (Supplementary Table 3). To ensure the robustness of the conclusions, we sequenced blanks (negative controls that were processed identically for DNA purification, downstream processes and sequencing performed but without lung tissue added) as a negative control.

Illumina-sequenced paired-end fastq files were analyzed using the DADA2 pipeline [13]. Fastq files were filtered and trimmed using the following standard filtering parameters maxN=0, maxEE=c(2,2), truncQ=2. We applied truncLen=c(240,150) for C57BL/6J lung, truncLen=c(230,200) for DBA/2 Lung, truncLen=c(210,160) for C57BL/6J gut, truncLen=c(240,210) for DBA/2 gut datasets.

The data was merged into paired end reads, and used to infer of sample composition and construct an amplicon sequence variants (ASV) table. Then, we removed the chimeras, and assigned to taxonomy using Silva version 138.1 training set[14,15] (released March 7, 2021). We then removed ASVs corresponding to Archea, Chloroplast and Mitochondria. At this point, we were able to identify 2,259 ASVs for C57BL/6J Lung.

Contaminating sequences were identified and removed using decontam v1.12.0[16], based on identities of ASVs from blanks. We used the prevalence test using the parameter threshold=0.5, which identify as contaminants all sequences more prevalent in negative controls than in real samples. We identified and removed 101 sequence features as contaminants in C57BL/6J lung.

All downstream analysis were performed on R (v4.0.2) (R CoreTeam, 2020). For data manipulation, we used the packages dplyr (v 1.0.5)[17] and tidyverse (v1.3.0)[18].

All reads identified as bacteria were kept. Then, we remove C57BL/6J lung samples under 6,000 reads. Consequently, our library size varies between 6,097 and 114,667 for C57BL/6J Lung.

Then we rarefied the data using rrarefy (vegan v2.5.7)[19] (Extended Data Fig. 7c and d). We compared the microbiome between experimental groups with Permutational Multivariate ANalysis Of Variance (PERMANOVA) using the function adonis (vegan v2.5.7) with 999 permutations. Dissimilarity distances (Bray-Curtis) were calculated using vegdist (vegan v2.5.7) then reduced to principal coordinates using betadisper (vegan v2.5.7) and finally plotted using ggplot2 (v3.3.3)[20].

To find the differentially abundant ASVs, we transformed our data into a SummarizedExperiment object using SummarizedExperiment (v1.20.0)[21], then we ran

Linear discriminant analysis Effect Size (LEfSe) algorithm (Kruskal-Wallis test, $p < 0.05$, LDA score > 2.0) using lefser (v1.0.0)[22].

For visualization of the C57BL/6J heatmap we choose to display the bacterial families that have at least 10 reads per mouse in each experimental group (e.g., for a group of 9 mice, the number of reads needed to plot one family is 90.The heatmaps were generated using pheatmap (pheatmap v1.0.12)[23]. Diversity calculations were done at ASV levels using diversity function (vegan v2.5.7) for Shannon index and Chao1 (fossil v 0.4.0)[24].

Determination of bacterial colony-forming-units (CFUs). Whole lung homogenates were prepared as described above, dissolved in 3ml of sterile saline and filtered through a 100-micron filter (Corning, catalogue number: 352360). 100µl from each of the lung homogenates was then plated on blood agar plates (using Columbia blood agar base, Oxoid, catalogue number: CM0331 with 5% sterile defibrinated blood) and incubated at 5% CO_2 at 37°C. CFUs were counted after 24-48 hours.

Histopathology. Mice were euthanized with CO_2 narcosis, necropsy was performed and brains and lungs were collected and fixed in formalin. Heads was decalcified for 3 hours using RDO (Rapid Decalcifying) solution, processed for paraffin-embedding, sectioned at 3 µm and stained with hematoxylin and eosin (H&E) for routine histopathological analysis. Evidence for experimental cerebral malaria, including cerebral oedema and multifocal haemorrhage, were screened (0 – absent, 1 – minimal, 2 – mild, 3 – moderate, 4 – severe) in all animals. Pulmonary oedema was scored as a measure of increased oedematous fluid content in the lungs of mice that succumb to MA-ARDS.

Statistics. Significance was calculated using different tests on the GraphPad (Prism) 5.0 software. Statistical differences between 2 groups were analysed using the non-parametric two-tailed Mann-Whitney test and in case of groups involving more than 2 datasets the data was analysed by Kruskal-Wallis. Survival and parasitaemia curves were analysed using the Log-rank Mantel-Cox Chi-squared test and linear regression curve. Time course measurement of oxygen saturation levels (SpO2) as determined by pulse-oximetry was analysed using Kruskal-Wallis test. Significance was considered for *P* values below 0.05. Biological replicates (n) indicated in figure legends refer to the number of mice. Sample sizes were chosen on the basis of historical data; no statistical methods were used to predetermine sample size. For diversity data, our group comparison were performed using Kruskal–Wallis test with kruskal.test function (R package, stats v4.1.0) followed by two-sided Mann–Whitney post hoc analysis using wilcox.test function (R package, stats v4.1.0). We used Holm correction for multiple comparisons.

Results

Impact of host microbiota on severe malaria pathology

To assess the impact of the host microbiota on the clinical outcome of *Plasmodium* infection, germ-free (GF) and specific-pathogen free (SPF) C57BL/6J mice, infected with either Pb ANKA or *Pb* K173, were compared. As expected, all SPF infected mice died at day 7 after infection. More specifically, SPF mice infected with Pb ANKA died from eCM while those infected with *Pb* K173 died from MA-MARDS (Fig. 2 a-c). GF mice infected with PbANKA also developed eCM and died with a kinetics similar to that of SPF mice (Fig. 2a-c). Even though 60% of the GF animals succumbed to MA-MARDS, this was significantly delayed compared to SPF mice (9.8 days *vs* 7.1, respectively; $P = 0.00001$) (Fig. 2d and f). More important, 40% of the *Pb* K173-infected GF mice did not develop MA-MARDS but died later from hyperparasitaemia (Fig. 2d- f).

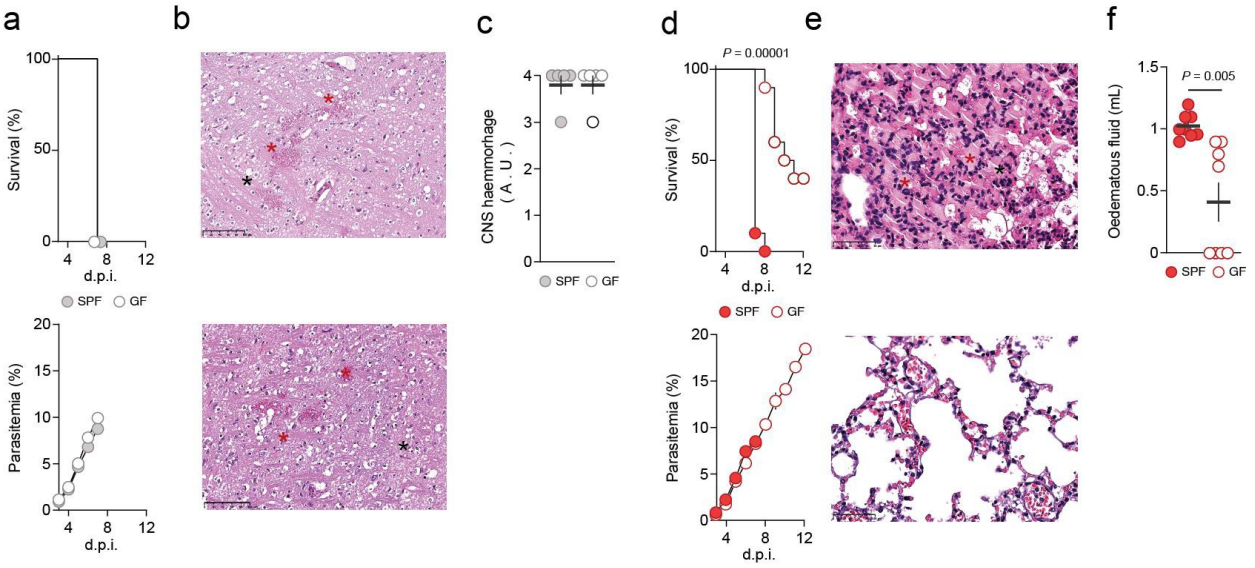

Fig. 2: Host microbiota promote MA-ARDS and not eCM.

a, Survival (upper panel, Log-rank Mantel-Cox) and parasitemia (lower panel, mean ± s.e.m; linear regression) following *Pb* ANKA infection of SPF (n=5;N=1) or GF (n=5;N=1) C57BL/6J mice. **b,** Histological images of brains of SPF (upper panel) and GF (lower panel) C57BL/6J mice following *Pb* ANKA infection. In both groups in the mid-brain, marked hemorrhages (red asterisk) and grey matter vacuolization (black asterisk) were observed. Scale bar = 100 µm. **c,** Cerebral haemorrhage (Mann-Whitney) score as measured by mid-brain haemorrhage severity following *Pb* ANKA infection of GF (n=5;N=1) or SPF (n=5;N=1) C57BL/6J mice. (Error bars are represented by mean ± s.e.m). **d,** Survival (upper panel, Log-rank Mantel-Cox) and parasitemia (lower panel, mean ± s.e.m; linear regression) following *Pb* K173 infection of SPF (n=10;N=2) or GF (n=10;N=2) C57BL/6J mice. **e,** Histological images of lungs of SPF (upper panel) and GF (lower panel) C57BL/6J mice following *Pb* K173 infection. Severe alveolar oedema (red asterisk) in the lung of SPF mice was observed. No changes were observed in the lung

of surviving GF mice (lower panel). Scale bar = 100 μm. In Figure 2e (upper panel) the tissue was collected at day 8 p.i. for SPF mice (time of death) and at day 28 p.i. for GF mice that were protected from MA-ARDS and died of hyperparasitemia **f,** Analysis of pulmonary oedema (Two sided Mann-Whitney test) as measured by increased fluid content in the lungs of GF (n=10;N=2) or SPF (n=10;N=2) C57BL/6J mice following *Pb* K173 infection. (Error bars are represented by mean ± s.e.m)

Increased CFUs of bacteria and altered microbiota composition of the lung promote MA-ARDS

Malaria infections strongly predispose individuals to bacteraemia[25,26], which, in turn increase the risk of death due to malarial severe pathology[27]. Notably, respiratory pathogens account for up to 25% of bacteria isolated in cases of *P. falciparum* malaria with concomitant bacteraemia[28]. This opens the possibility that bacterial species in the lung, either pathogenic or commensal (the lung microbiome), may impact on the clinical outcome of *Plasmodium* infections. Indeed, the role of the lung microbiome in disease is supported by several studies showing that changes in this local microbial community (known as lung microbiota dysbiosis) are associated with the exacerbation of several pulmonary disorders, including chronic obstructive pulmonary disease (COPD), asthma and cystic fibrosis[29,30], and even lung cancer[31]. Thus, we hypothesized that alterations in the lung microbiota composition plays a critical role in the establishment of MA-ARDS. Our initial aim was to understand whether alterations in the microbiota composition in the lung are associated with development of MA-ARDS in mice. We started by quantifying

the number of colony-forming units (CFUs) of bacteria in the lungs of mice that die of MA-ARDS, when compared to those that die of eCM and non-infected (NI) mice. To do this, we plated lung extracts under sterile conditions at days 3 and 5 (prior to onset of MA-ARDS and eCM) as well as 7 (onset of MA-ARDS and eCM) post infection (p.i.) of C57BL/6J mice infected with either *Pb* K173 or *Pb* ANKA parasites. We observed that at day 3 p.i. there is no difference in the number of CFUs of bacteria between any of the groups (Fig. 3a). However, there was a 2-3 fold increment in the number of CFUs of bacteria in the lungs of *Pb* K173 infected mice at day 5 p.i. (Fig. 3a, $P = 0.004$) that further increased by 9-10 fold at day 7 p.i. (Fig. 3a, $P < 0.001$), when compared to *Pb* ANKA-infected mice and non-infected (NI) mice. Notably, C57BL/6J mice infected with *Pb* ANKA, the experimental model of eCM had no increase in CFUs throughout infection, when compared to NI mice (Fig. 3a).

We then investigated the microbial composition in the lungs of *Pb* K173-infected C57BL/6J mice compared to both *Pb* ANKA-infected mice and NI controls at days 5 and 7 p.i. by performing bacterial 16S rRNA gene sequencing. Relative abundance of bacterial families showed that C57BL/6J mice infected with *Pb* K173 exhibited altered lung microbiota composition compared to *Pb* ANKA-infected mice or NI controls both at day 5 (Fig. 3b) and day 7 p.i. (Fig. 3c). Principal coordinate analysis (PCoA) showed that the lung microbiome of *Pb* K173-infected mice was significantly distinct from *Pb* ANKA-infected mice and NI controls both at days 5 (Fig. 3d, Table 1)) and 7 p.i. (Fig. 3e, Table 1).

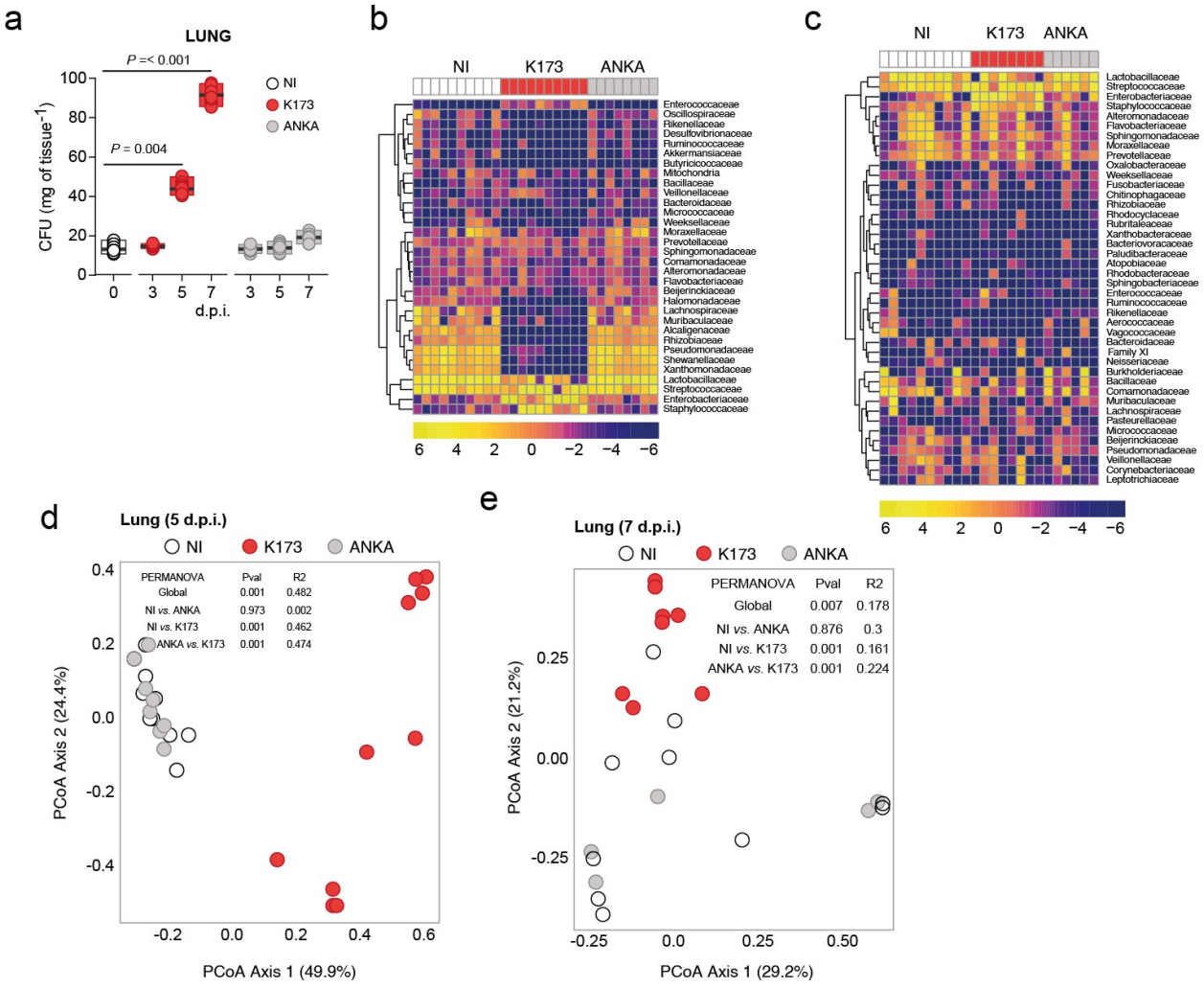

Fig. 3: Altered microbiota composition of the lung promote MA-ARDS

a, Time course measurement of CFUs (Kruskal-Wallis) in the lungs of C57BL/6J mice infected either with *Pb* K173 (n=8;N=2) or *Pb* ANKA (n=8;N=2) at day 3, 5 and 7 post infection (p.i.) and non-infected (NI) controls (n=8;N=2). **b,c** Heatmap of relative abundance of major microbial families in the lungs of C57BL/6J mice 5 days p.i.**(b)** and 7 days p.i.**(c)** with *Pb* K173 (n=10;N=1) or *Pb* ANKA (n=8;N=1) and NI controls (n=10,N=1) is shown using a pseudo-logarithmic scale; each column represents one mouse. Each

row represents a bacterial family. Rows were clustered using hierarchical clustering with Euclidean distance. **d,e** Beta diversity of lung microbial communities of C57BL/6J mice 5 days p.i.**(d)** and 7 days p.i.**(e)** with *Pb* K173 (n=10;N=1) or *Pb* ANKA (n=8;N=1) and NI controls (n=10,N=1). ASVs space was reduced using principal coordinate analysis (PCoA) with Bray-Curtis distance. The first and second principal coordinates were plotted, as well as the variability explained by each principal coordinates (values in brackets).

Reduced bacterial diversity promote MA-ARDS

The *Pb* K173 lung microbiome is also associated with a decrease of microbial ASV (Amplicon Sequence Variant) diversity (Fig. 4 a and b). We then wanted to determine the differentially abundant bacterial ASVs (using Linear discriminant analysis Effect Size) from lungs of C57BL/6J mice. There was an increase in relative abundance of *Escherichia* and *Staphylococcaceae* compared to the controls both at day 5 and day 7 p.i. (Fig. 4c-f) and a relative decrease in relative abundance of many other bacterial families (Fig. 4c-f). The relative increase of bacterial families like *Escherichia* and *Staphylococcaceae* in the lungs has also been recently reported for other pulmonary disorders[32,33], thereby suggesting their potential involvement in the pathogenesis of MA-ARDS. Of additional interest, the gut microbiota is altered in both MA-ARDS and eCM infection models (Fig. 4g, Table 1), which is consistent with previous reports[34,35], although such changes depend on the host's genetic background[36]. Together, our data support the hypothesis that *Plasmodium* infection alters, both qualitatively and quantitatively, the microbial communities in the lung, and that the observed alterations in the lung microbiota composition associates with the development of MA-ARDS.

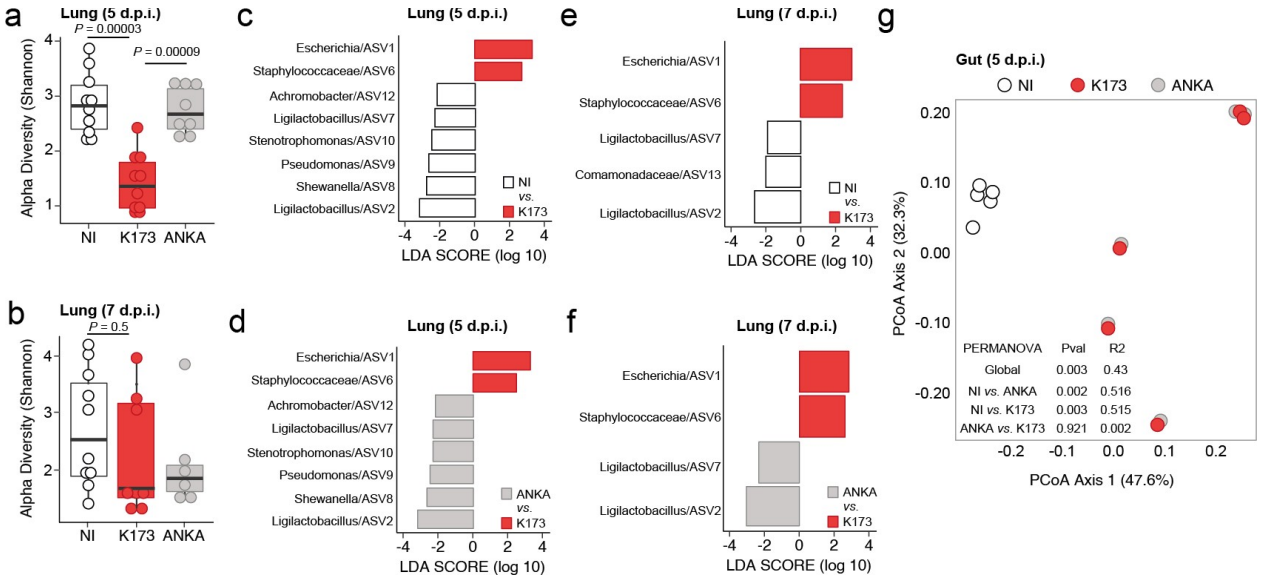

Fig. 4: Reduced bacterial diversity promote MA-ARDS

a, b, Shannon Alpha diversity (Group comparison by Kruskal–Wallis followed by two-sided Mann–Whitney post hoc analysis with Holm correction) of lung microbial composition upon infection of C57BL/6J mice on **(a)** day 5 p.i with *Pb* K173 (n=10;N=1) or *Pb* ANKA (n=8;N=1) and NI controls (n=10,N=1); **(b)** day 7 p.i with *Pb* K173 (n=6;N=1) or *Pb* ANKA (n=7;N=1) and NI controls (n=10,N=1). For group comparison, we used Kruskal–Wallis followed by two-sided Mann–Whitney post hoc analysis with Holm correction. **c-f,** Differentially abundant ASVs (using Linear discriminant analysis Effect Size) from lungs of C57BL/6J mice; **(c)** between NI (n=10;N=1) and *Pb* K173 (n=10;N=1) at day 5 p.i. **(d)** between *Pb* ANKA (n=8;N=1) and *Pb* K173 (n=10;N=1) at day 5 p.i. **(e)** between NI (n=10;N=1) and *Pb* K173 (n=6;N=1) at day 7 p.i. **(f)** between Pb ANKA (n=7;N=1) and *Pb* K173 (n=6;N=1) at day 7 p.i.. **g,** Beta diversity of gut microbial

communities of C57BL/6J mice 5 days p.i. with *Pb* K173 (n=5;N=1) or *Pb* ANKA (n=5;N=1) and NI controls (n=5,N=1).

Table 1

PERMANOVA (C57BL/6J)				
Organ	dpi	**Comparison**	**Pvalue**	**R2**
Lung	5	Global	0.001	0.485
		NI vs ANKA	0.983	0.019
		NI vs K173	0.001	0.466
		ANKA vs K173	0.001	0.474
	7	Global	0.007	0.178
		NI vs ANKA	0.876	0.03
		NI vs K173	0.001	0.161
		ANKA vs K173	0.001	0.224
Gut	5	Global	0.001	0.45
		NI vs ANKA	0.002	0.536
		NI vs K173	0.002	0.535
		ANKA vs K173	0.951	0.45

Discussion

In this chapter we report that the host microbiota can promote the pathogenesis of one severe malaria pathology over the other (MA-ARDS vs eCM). Importantly, we demonstrate that *Plasmodium* infection in the rodent model of MA-ARDS cause an increase in the bacterial load in the lungs. 16s rRNA sequencing revealed alterations in the microbiota of the lungs of mice that die of MA-ARDS compared to eCM.

The concept that the healthy lung is sterile has now been challenged. The lung is an organ that is constantly exposed to the microbiota from the air or through subclinical aspiration[37]. It is well known that the upper respiratory tract and the oropharynx have an abundance of microbes[37]. This is in direct contact with the lungs and studies have demonstrated clearly that subclinical aspiration of oropharyngeal contents occurs universally in humans[38–40]. Thus it is quite rational to believe that the lung is always under constant immigration and elimination of microbes maintained through mucosal defense and mucociliary clearance. Indeed, in the last decade with the advent of culture independent high throughput sequencing techniques, mainly 16s rRNA sequencing, the notion of lung sterility has been debunked. In the last decade we have observed quite a number of studies reporting significantly alterations of the lung microbiota in a number of disease conditions, such as COPD, cystic fibrosis, asthma and lung cancer[41–43]. While such observations suggest that the lung microbiota influences both respiratory health and disease, the gut microbiota can also influence pulmonary immunity through what is commonly referred to as the gut–lung axis[33]. Indeed, gut-associated bacterial families have recently been reported to be over-represented in the lungs of ARDS patients with poorer outcomes [44]. Thus, either remote (gut) or local (lung) microbiota may contribute to

the increase in bacterial burden, which we now report to be present in the lungs of mice before the onset of MA-ARDS. A question that need's to be addressed in the future is the relative contribution of local (lung) and remote (lower gut) bacterial communities to lung inflammation and injury.

Malaria-associated acute respiratory distress syndrome (MA-ARDS), which has been increasingly reported in recent decades[45], is the most severe form of respiratory complications associated with malaria, resulting in high mortality despite adequate therapeutic management[46]. In fact, it has been suggested that as many as 5% of patients with uncomplicated malaria and 20–30% of patients with severe and complicated malaria requiring admission in intensive care units may develop MA-ARDS, which often happens after treatment has been initiated[47]. Additionally, pregnant women with severe *P. falciparum* infection are particularly susceptible to MA-ARDS, which is associated with high mortality[45]. It is, therefore, of the utmost importance that we understand the mechanisms underlying the onset and progression of this syndrome. The data in this chapter provide novel evidence that alterations in the composition of the lung microbiota can be a potential cause for pathogenesis of MA-ARDS. In our mice model of MA-ARDS, we have found the relative increase of bacterial families like *Escherichia* and *Staphylococcaceae* in the lungs. Having established this, we next wanted to understand the mechanisms underlying lung microbiota dysbiosis during MA-ARDS.

References

1. Hill, A. V. S. *et al.* Common West African HLA antigens are associated with protection from severe malaria. *Nature* **352,** 595–600 (1991).
2. Driss, A. *et al.* Genetic polymorphisms linked to susceptibility to malaria. *Malar. J.* **10,** 271 (2011).
3. Kyriacou, H. M. *et al.* Differential var gene transcription in Plasmodium falciparum isolates from patients with cerebral malaria compared to hyperparasitaemia. *Mol. Biochem. Parasitol.* **150,** 211–8 (2006).
4. Kalmbach, Y. *et al.* Differential *var* Gene Expression in Children with Malaria and Antidromic Effects on Host Gene Expression. *J. Infect. Dis.* **202,** 313–317 (2010).
5. Hee, L. *et al.* Reduced activity of the epithelial sodium channel in malaria-induced pulmonary oedema in mice. *Int. J. Parasitol.* **41,** 81–88 (2011).
6. Epiphanio, S. *et al.* VEGF promotes malaria-associated acute lung injury in mice. *PLoS Pathog.* **6,** e1000916 (2010).
7. Van den Steen, P. E. *et al.* Pathogenesis of malaria-associated acute respiratory distress syndrome. *Trends Parasitol.* **29,** 346–58 (2013).
8. BRIAN de SOUZA, J., HAFALLA, J. C. R., RILEY, E. M. & COUPER, K. N. Cerebral malaria: why experimental murine models are required to understand the pathogenesis of disease. *Parasitology* **137,** 755–772 (2010).
9. Ashley, S. L. *et al.* Lung and gut microbiota are altered by hyperoxia and contribute to oxygen-induced lung injury in mice. *Sci. Transl. Med.* **12,** (2020).
10. Mason, K. L. *et al.* Candida albicans and bacterial microbiota interactions in the

cecum during recolonization following broad-spectrum antibiotic therapy. *Infect. Immun.* **80,** 3371–3380 (2012).

11. Caporaso, J. G. *et al.* Global patterns of 16S rRNA diversity at a depth of millions of sequences per sample. *Proc. Natl. Acad. Sci.* **108,** 4516–4522 (2011).
12. Caporaso, J. G. *et al.* Ultra-high-throughput microbial community analysis on the Illumina HiSeq and MiSeq platforms. *ISME J. 2012 68* **6,** 1621–1624 (2012).
13. Callahan, B. *et al.* DADA2: High resolution sample inference from amplicon data. *bioRxiv* 24034 (2015). doi:10.1101/024034
14. Yilmaz, P. *et al.* The SILVA and 'All-species Living Tree Project (LTP)' taxonomic frameworks. *Nucleic Acids Res.* **42,** D643 (2014).
15. Quast, C. *et al.* The SILVA ribosomal RNA gene database project: improved data processing and web-based tools. *Nucleic Acids Res.* **41,** D590 (2013).
16. Davis, N. M., Proctor, D. M., Holmes, S. P., Relman, D. A. & Callahan, B. J. Simple statistical identification and removal of contaminant sequences in marker-gene and metagenomics data. *bioRxiv* 221499 (2018). doi:10.1101/221499
17. Wickham, H. The split-apply-combine strategy for data analysis. *J. Stat. Softw.* **40,** 1–29 (2011).
18. Wickham, H. *et al.* Welcome to the Tidyverse. *J. Open Source Softw.* **4,** 1686 (2019).
19. Oksanen, J. *et al. Package 'vegan' Title Community Ecology Package Version 2.5-7*. (2020).
20. Wickham, H. & Wickham, H. in *ggplot2* 9–26 (Springer New York, 2009). doi:10.1007/978-0-387-98141-3_2

21. Morgan, M., Obenchain, V., Hester, J., Pagès, H. & Bioconductor, M. *Encoding UTF-8*. (2020).

22. Khleborodova, A. lefser: R implementation of the LEfSE method for microbiome biomarker discovery. R package version 1.0.0. (2020).

23. Kolde, R. pheatmap: Pretty Heatmaps. R package version 1.0.12. (2019).

24. Vavrek, M. J. *fossil: Palaeoecological and palaeogeographical analysis tools*. **14,** (2011).

25. Mabey, D. C. W., Brown, A. & Greenwood, B. M. Plasmodium falciparum Malaria and Salmonella Infections in Gambian Children. *J. Infect. Dis.* **155,** 1319–1321 (1987).

26. Scott, J. A. G. *et al.* Relation between falciparum malaria and bacteraemia in Kenyan children: a population-based, case-control study and a longitudinal study. *Lancet (London, England)* **378,** 1316–23 (2011).

27. Taylor, W. R. J., Hanson, J., Turner, G. D. H., White, N. J. & Dondorp, A. M. Respiratory manifestations of malaria. *Chest* **142,** 492–505 (2012).

28. Berkley, J. A. *et al.* HIV Infection, Malnutrition, and Invasive Bacterial Infection among Children with Severe Malaria. *Clin. Infect. Dis.* **49,** 336–343 (2009).

29. O'Dwyer, D. N., Dickson, R. P. & Moore, B. B. The Lung Microbiome, Immunity, and the Pathogenesis of Chronic Lung Disease. *J. Immunol.* **196,** 4839–47 (2016).

30. Salami, O. & Marsland, B. J. Has the airway microbiome been overlooked in respiratory disease? *Genome Med.* **7,** 62 (2015).

31. Jin, C. *et al.* Commensal Microbiota Promote Lung Cancer Development via γδ T

Cells. *Cell* **176,** 998–1013 (2019).

32. Ashley, S. L. *et al.* Lung and gut microbiota are altered by hyperoxia and contribute to oxygen-induced lung injury in mice. *Sci. Transl. Med.* **12,** (2020).
33. Ubags, N. D. J. & Marsland, B. J. Mechanistic insight into the function of the microbiome in lung diseases. *Eur. Respir. J.* **50,** 1602467 (2017).
34. Mooney, J. P. *et al.* Inflammation-associated alterations to the intestinal microbiota reduce colonization resistance against non-typhoidal Salmonella during concurrent malaria parasite infection. *Sci. Rep.* **5,** 14603 (2015).
35. Taniguchi, T. *et al.* Plasmodium berghei ANKA causes intestinal malaria associated with dysbiosis. *Sci. Rep.* **5,** (2015).
36. Taniguchi, T. *et al.* Plasmodium berghei ANKA causes intestinal malaria associated with dysbiosis. *Sci. Rep.* **5,** (2015).
37. Dickson, R. P. & Huffnagle, G. B. The Lung Microbiome: New Principles for Respiratory Bacteriology in Health and Disease. *PLoS Pathog.* **11,** e1004923 (2015).
38. Quinn, l. H. & meyer, o. O. The relationship of sinusitis and bronchiectasis. *Arch. Otolaryngol. - Head Neck Surg.* **10,** 152–165 (1929).
39. Huxley, E. J., Viroslav, J., Gray, W. R. & Pierce, A. K. Pharyngeal aspiration in normal adults and patients with depressed consciousness. *Am. J. Med.* **64,** 564–568 (1978).
40. Gleeson, K., Maxwell, S. L. & Eggli, D. F. Quantitative Aspiration During Sleep in Normal Subjects. *Chest* **111,** 1266–1272 (1997).
41. C, J. *et al.* Commensal Microbiota Promote Lung Cancer Development via γδ T

Cells. *Cell* **176,** (2019).

42. DN, O., RP, D. & BB, M. The Lung Microbiome, Immunity, and the Pathogenesis of Chronic Lung Disease. *J. Immunol.* **196,** (2016).
43. Salami, O. & Marsland, B. J. Has the airway microbiome been overlooked in respiratory disease? *Genome Med.* **7,** (2015).
44. Dickson, R. P. *et al.* Lung Microbiota Predict Clinical Outcomes in Critically Ill Patients. *Am. J. Respir. Crit. Care Med.* **201,** 555–563 (2020).
45. Taylor, W. R. J., Hanson, J., Turner, G. D. H., White, N. J. & Dondorp, A. M. Respiratory Manifestations of Malaria. *Chest* **142,** 492–505 (2012).
46. Mazhar, F. & Haider, N. Respiratory Manifestation of Malaria: An Update. *Int. J. Med. Res. Heal. Sci.* **5,** 59–65 (2016).
47. Mohan, A., Sharma, S. K. & Bollineni, S. Acute lung injury and acute respiratory distress syndrome in malaria. *J. Vector Borne Dis.* **45,** 179–93 (2008).

Chapter 2

Mechanism: The parasite factors underlying altered microbiota composition in the lung

Introduction

Erythrocytes infected with the human malaria parasite *Plasmodium falciparum* have the ability to cytoadhere to endothelial cells lining blood vessels. This critical feature referred to as sequestration – is a crucial event for the onset of malaria pathology[1,2].The *Plasmodium falciparum* parasite transports the protein PfEMP1 to the infected RBC surface to bind to host endothelial receptors such as CD36 and ICAM1[3]. The protein so far shown to be essential for *P. berghei* CD36-mediated sequestration of schizont-infected RBC is a PEXEL-positive exported protein, the schizont membrane-associated cytoadherence protein (SMAC), a molecule restricted to rodent malaria parasites that is found in the cytoplasm of iRBCs but not on their surface[4].

In this chapter, we hypothesized parasite sequestration in the lungs mediate lung microbiota dysbiosis to promote MA-ARDS. Aligned with this, we observed a build-up of iRBCs in the lungs of mice that die of MA-ARDS. Relevantly, infection of mice with parasites that do not sequester to the lung failed to promote lung microbiota dysbiosis and did not develop into MA-ARDS. These data show that iRBCs sequestration is at the basis of host lung microbiota dysbiosis and development of MA-ARDS.

Materials and Methods

Mice

Male C57BL/6J and DBA/2 mice were purchased from Charles River breeding laboratories and housed in the animal facilities at Instituto de Medicina Molecular (iMM) in specific-pathogen-free conditions (SPF conditions). All in vivo experiments were approved by the animal ethics committee of iMM and were performed according to national and European regulations.

Parasites and infections

Male C57BL/6J and DBA/2 mice were infected, by intraperitoneal route, with 1 x 10^6 luciferase-expressing *Plasmodium berghei* ANKA, *Plasmodium berghei* K173 and *Plasmodium berghei smac*- infected red blood cells (iRBC). Parasitaemia, monitored by Giemsa stained blood smears and expressed as percentage of iRBC, and survival were monitored daily.

Bacterial DNA isolation. Lungs and faecal pellets were harvested under sterile conditions and immediately snap frozen in liquid nitrogen. Samples were stored at −80°C until processing for DNA isolation. Genomic DNA was extracted from lung using a commercial kit (DNeasy tissue kit; Qiagen, Germantown, MD) and from fecal pellets using QIAamp Fast DNA Stool Mini Kit (Qiagen). Lung samples were processed based on a modified protocol previously demonstrated to isolate bacterial DNA from lungs [5,6]. Briefly, lungs were subjected to bead beating for 1min using 1mm diameter silica beads (BioSpec Products, United States, catalog number: 11079110z) in a MiniBeadBeater homogenizer (BioSpec Products) for 2mins. Lung samples were incubated overnight at 60°C with 400µl of Tissue lysis buffer and 50µl of lysozyme included in the kit. Following this, DNA was

extracted from gut and lung samples following instructions from the QIAamp Fast DNA Stool Mini Kit (Qiagen) and DNeasy tissue kit. DNA was used directly for 16S rRNA analysis.

16S rRNA analysis. 16S rRNA gene amplification and sequencing was carried out at the Genomics Unit at IGC. The V4 region of the 16S rRNA gene was amplified in triplicate for each sample, using the primer pair F515/R806. PCRs were done under the following conditions: 3 min at 94°C, 35 cycles of 60s at 94°C, 60s at 50°C, and 105s at 72°C, with an extension step of 10 min at 72°C. Samples were then pair-end sequenced on an Illumina MiSeq Benchtop Sequencer (Illumina), following Illumina recommendations[7,8].

Each lung sample was cleaned of *Plasmodium* parasite and host sequences using Kraken2. To do this, we first created a Kraken2 index consisting of the Bacteria and Archaea libraries plus the mouse genome (GRCm39) and the genomes of *Plasmodium berghei* ANKA (GCA_900002375.2) and K173 (GCA_900044334.1), all of which were downloaded from NCBI. The reads of each sample were then mapped against this database with Kraken2 and the script extract_kraken_reads.py (from KrakenTools; https://github.com/jenniferlu717/KrakenTools) was used to filter reads in order to keep only those mapping to Bacteria or Archaea for further analysis (Supplementary Table 3). To ensure the robustness of the conclusions, we sequenced blanks (negative controls that were processed identically for DNA purification, downstream processes and sequencing performed but without lung tissue added) as a negative control.

Illumina-sequenced paired-end fastq files were analyzed using the DADA2 pipeline[9]. Fastq files were filtered and trimmed using the following standard filtering parameters

maxN=0, maxEE=c(2,2), truncQ=2. We applied truncLen=c(240,150) for C57BL/6J lung, truncLen=c(230,200) for DBA/2 Lung, truncLen=c(210,160) for C57BL/6J gut, truncLen=c(240,210) for DBA/2 gut datasets.

The data is merged into paired end reads, and used to infer of sample composition and construct an amplicon sequence variants (ASV) table. Then, we removed the chimeras, and assigned to taxonomy using Silva version 138.1 training set[10,11] (released March 7, 2021). We then removes ASVs corresponding to Archea, Chloroplast and Mitochondria. At this point, we were able to identify 2,109 ASVs for DBA/2 Lung.

Contaminating sequences were identified and removed using decontam v1.12.0[12], based on identities of ASVs from blanks. We used the prevalence test using the parameter threshold=0.5, which identify as contaminants all sequences more prevalent in negative controls than in real samples. We identified and removed 81 sequence features in DBA/2 lung.

All downstream analysis were performed on R (v4.0.2) (R CoreTeam, 2020). For data manipulation, we used the packages dplyr (v 1.0.5)[13] and tidyverse (v1.3.0)[14].

All reads identified as bacteria were kept. Then, we remove DBA/2 Lung samples under 3,000 reads. Consequently, our library size varies between 3,317 to 155,163 for DBA/2 Lung.

Then we rarefied the data using rrarefy (vegan v2.5.7)[15] . We compared the microbiome between experimental groups with Permutational Multivariate ANalysis Of Variance (PERMANOVA) using the function adonis (vegan v2.5.7) with 999 permutations. Dissimilarity distances (Bray-Curtis) were calculated using vegdist (vegan v2.5.7) then

reduced to principal coordinates using betadisper (vegan v2.5.7) and finally plotted using ggplot2 (v3.3.3)[16].

To find the differentially abundant ASVs, we transformed our data into a SummarizedExperiment object using SummarizedExperiment (v1.20.0)[17], then we ran Linear discriminant analysis Effect Size (LEfSe) algorithm (Kruskal-Wallis test, $p < 0.05$, LDA score > 2.0) using lefser (v1.0.0)[18].

For visualization of the DBA/2 heatmap dataset, we removed bacterial families that showed no count (zero) across 22 of the mice. The heatmaps were generated using pheatmap (pheatmap v1.0.12)[19]. Diversity calculations were done at ASV levels using diversity function (vegan v2.5.7) for Shannon index and Chao1 (fossil v 0.4.0)[20].

Determination of bacterial colony-forming-units (CFUs). Whole lung homogenates were prepared as described above, dissolved in 3ml of sterile saline and filtered through a 100-micron filter (Corning, catalogue number: 352360). 100µl from each of the lung homogenates was then plated on blood agar plates (using Columbia blood agar base, Oxoid, catalogue number: CM0331 with 5% sterile defibrinated blood) and incubated at 5% CO_2 at 37°C. CFUs were counted after 24-48 hours.

RNA isolation, cDNA and quantification of gene expression. Lungs were harvested under sterile conditions, placed in 1ml PureZOL (Bio-Rad, catalog number: 732-6890) and mechanically homogenized using 1mm diameter silica beads (BioSpec Products, United States, catalog number: 11079110z) in a MiniBeadBeater homogenizer (BioSpec Products) for 2 mins. Two hundred (200) µl of the lysate was used to isolate total RNA

using the NZY total RNA Isolation kit (NZYTech, catalogue number: MB13402) according to the manufacturer's instructions. DNAse-treated RNA was reverse transcribed with random hexamers using NZY First-Strand cDNA Synthesis Kit (NZYTech, catalogue number: MB12501). Real-time PCR was performed on ABI 7500 or 7900HT systems (Applied Biosystems), using Universal SYBR Green Supermix (Bio-Rad, catalogue number: 172-5121) and the primers listed below. Relative gene expression was normalized to the geometric mean of the housekeeping gene hypoxanthine guanine phosphoribosyltransferase (Hprt) (ΔCt). Gene expression values were then calculated based on the ΔΔCt method, using the mean of the control group as the calibrator to which all other samples were compared.

Primers used were:

mHprt:

CATTATGCCGAGGATTTGGA; AATCCAGCAGGTCAGCAAAG

Pb18S rRNA:

AAGCATTAAATAAAGCGAATACATCCTTAC; GGAGATTGGT TTTGACGTTTATGTG

Histopathology. Mice were euthanized with CO_2 narcosis, necropsy was performed and brains and lungs were collected and fixed in formalin. Heads was decalcified for 3 hours using RDO (Rapid Decalcifying) solution, processed for paraffin-embedding, sectioned at 3 μm and stained with hematoxylin and eosin (H&E) for routine histopathological analysis. Evidence for experimental cerebral malaria, including cerebral oedema and multifocal haemorrhage, were screened (0 – absent, 1 – minimal, 2 – mild, 3 – moderate, 4 – severe) in all animals. Pulmonary oedema was scored as a measure of increased oedematous fluid content in the lungs of mice that succumb to MA-ARDS.

Statistics. Significance was calculated using different tests on the GraphPad (Prism) 5.0 software. Statistical differences between 2 groups were analysed using the non-parametric two-tailed Mann-Whitney test and in case of groups involving more than 2 datasets the data was analysed by Kruskal-Wallis. Survival and parasitaemia curves were analysed using the Log-rank Mantel-Cox Chi-squared test and linear regression curve. Significance was considered for *P* values below 0.05. Biological replicates (n) indicated in figure legends refer to the number of mice. Sample sizes were chosen on the basis of historical data; no statistical methods were used to predetermine sample size. For diversity data, our group comparison were performed using Kruskal–Wallis test with kruskal.test function (R package, stats v4.1.0) followed by two-sided Mann–Whitney post hoc analysis using wilcox.test function (R package, stats v4.1.0). We used Holm correction for multiple comparisons.

Results

Parasite sequestration levels in different host-*Plasmodium* combinations

Adherence of *Plasmodium*-infected red blood cells (iRBCs) to the vascular endothelium, referred to as sequestration, is a crucial event for the onset of malaria pathology[21,22]. We observed that on day 5 p.i. there was increased parasite sequestration in the lungs of *Pb* K173-infected mice, when compared to *Pb* ANKA-infected mice and NI controls (Fig. 2a).

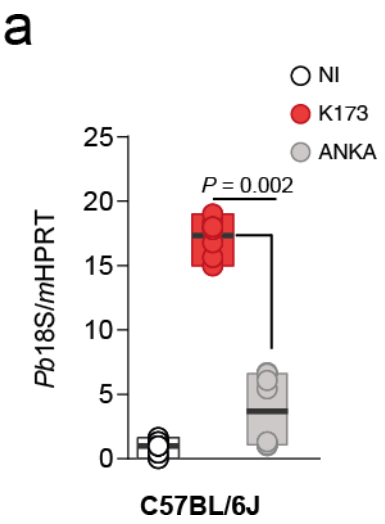

Fig. 2: iRBCs sequestration in the lungs promotes MA-ARDS. a, Parasite sequestration (Kruskal-Wallis) in the lungs of C57BL/6J mice on day 5 p.i. with *Pb* K173 (n=8;N=2) or *Pb* ANKA (n=8;N=2) and non-infected (NI) controls (n=8;N=2).

Infection of DBA/2 mice with *Pb* ANKA is another model of MA-ARDS, leading to lung pathology in ~50% of the mice (Fig. 1 e-g and Fig. 1m in Chapter 1 of this thesis). We observed that there was a correlation between high levels of parasitemia at day 5 p.i. and mice that will succumb to MA-ARDS (Fig. 2a). Accordingly, on day 5 p.i we observed an accumulation of iRBCs in the lungs of DBA/2 mice infected with *Pb* ANKA, which correlated with increased parasitemia and hence, the development of MA-ARDS (Fig.

2b).Next, we also observed an increase in CFUs of bacteria in the lung, seen at day 5 (prior to onset of MA-ARDS) as well as day 7 (onset of MA-ARDS) following infection of DBA/2 mice with *Pb* ANKA parasites but not at day 3 p.i. (Fig. 2c). Importantly, there is a clear segregation in the lung bacterial burden at both days 5 and 7 p.i., with 50% and 60% of DBA/2 mice exhibiting increasing bacterial burden with the progression of the infection, respectively (Fig. 2c). In the remaining mice, the bacterial burden did not increase to the levels observed in those that will succumb to MA-ARDS (Fig. 2c). This is also the case of DBA/2 mice surviving infection with *Pb* ANKA analysed at day 12 p.i. (Fig. 2c), where bacterial burden in the lungs remains roughly at the same levels of those segregating at earlier time points.

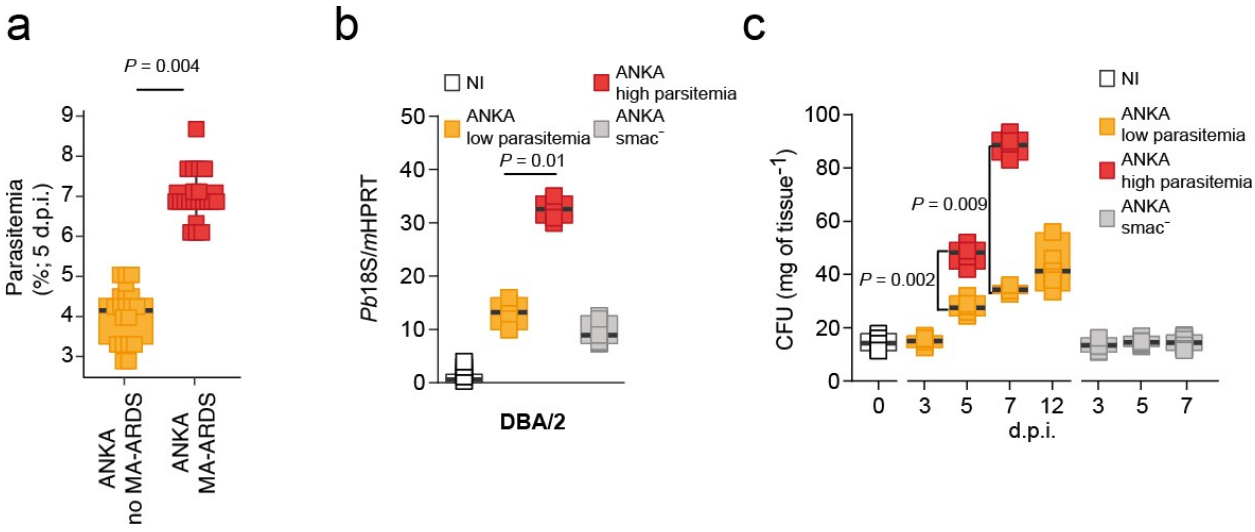

Fig. 2: iRBCs sequestration in the lungs promotes increased bacterial load and MA-ARDS

a, Parasitemia (mean ± s.e.m; linear regression) following *Pb* ANKA infection of DBA/2 mice separating groups of mice that will succumb to MA-ARDS (n=20) and mice that will be protected (n=20). (Two sided Mann-Whitney test). **b,** Parasite sequestration (Kruskal-Wallis) in the lungs of DBA/2 mice on day 5 p.i. with *Pb* ANKA MA-ARDS (n=5;N=2) and *Pb* ANKA no MA-ARDS (n=4;N=2), *Pb* ANKA*smac*- (n=8;N=2) and NI controls (n=8;N=2). **c,** Time course measurement of CFUs (Kruskal-Wallis) in the lungs of DBA/2 mice infected with *Pb* ANKA MA-ARDS (n=6;N=2), *Pb* ANKA no MA-ARDS (n=6;N=2), *Pb* ANKA*smac*- (n=10;N=2) at days 3, 5, 7 and 12 p.i. and non-infected (NI) controls (n=10;N=2).

Parasite sequestration determines lung microbiots dysbiosis and promotes MA-ARDS

Bacterial family abundance analysis showed that DBA/2 mice infected with *Pb* ANKA that will die of MA-ARDS (high parasitemia) have significant changes in the lung microbiome compared to mice that are protected, with the latter being similar to NI mice both at day 5 (Fig. 3a) and day 7 p.i. (Fig. 3b). In addition, principal coordinate analysis (PCoA) showed that the lung microbiome of the mice infected with *Pb* ANKA and suffering MA- ARDS was significantly distinct from that of mice infected with *Pb* ANKA but not showing MA-ARDS, and NI controls both at day 5 (Fig. 3c, Supplementary Table 2) and day 7 p.i. (Fig. 3d, Supplementary Table 2). ASV diversity was decreased in DBA/2 mice infected with *Pb* ANKA and suffering MA-ARDS although this decrease was less pronounced at day 7 p.i.(Fig. 3e and f). There was an increase in relative abundance of *Ligilactobacillus*

compared to the controls at day 5 (Fig. 3g-i) and *Escherichia* at day 7 (Fig. 3j-l). Importantly, infection of DBA/2 mice with *Pb* ANKA parasites lacking the schizont membrane-associated cytoadherence (*smac*) protein (*Pb* ANKA*smac*-), which do not sequester to the lung [23] (Fig. 3b), failed to promote lung dysbiosis (Fig.3a-l) and MA-ARDS (Fig. 3m), but not gut microbiota dysbiosis (Fig. 3n). These data show that iRBCs sequestration is at the basis of alterations in the host lung microbiota and the development of MA-ARDS.

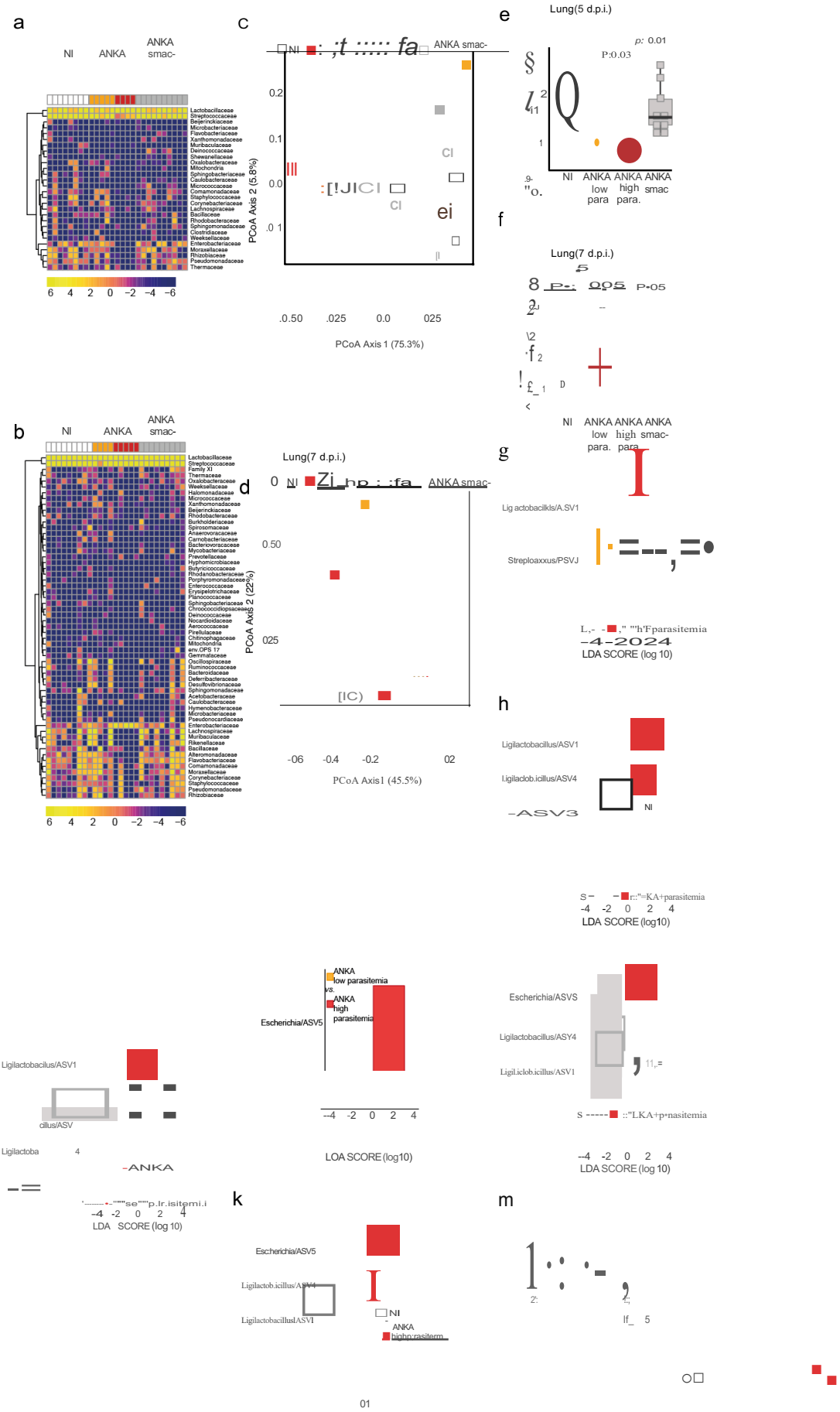
a
NI
ANKA
ANKA smac-
6 4 2 0 −2 −4 −6
b
NI
ANKA
ANKA smac-
6 4 2 0 −2 −4 −6
c
NI
ANKA smac-
PCoA Axis 2 (5.8%)
PCoA Axis 1 (75.3%)
d
Lung(7 d.p.i.)
NI
ANKA smac-
PCoA Axis 2 (22%)
PCoA Axis1 (45.5%)
e
Lung(5 d.p.i.)
p: 0.01
P:0.03
NI
ANKA low para
ANKA high para.
ANKA smac
f
Lung(7 d.p.i.)
NI
ANKA low para.
ANKA high para.
ANKA smac-
g
Lig actobacillkls/A.SV1
Streploaxxus/PSVJ
L,- -■," "'h'Fparasitemia
-4-2024
LDA SCORE (log 10)
h
Ligilactobacillus/ASV1
Ligilaclob.icillus/ASV4
-ASV3
NI
S − −■r:"=KA+parasitemia
-4 -2 0 2 4
LDA SCORE (log10)
Ligilactobacilus/ASV1
cillus/ASV
Ligilactoba 4
-ANKA
-4 -2 0 2 4
LDA SCORE (log 10)
ANKA low parasitemia
vs.
ANKA high parasitemia
Escherichia/ASV5
--4 -2 0 2 4
LOA SCORE (log10)
Escherichia/ASVS
Ligilactobacillus/ASY4
Ligil.iclob.icillus/ASV1
S -----■ ::"LKA+p•nasitemia
--4 -2 0 2 4
LDA SCORE (log 10)
k
Escherichia/ASV5
Ligilactob.icillus/ASV4
LigilactobacillusIASVI
NI
ANKA
highp:rasiterm
m
n
Gut(5 d.p.i.)
0 NI ■ ANKA high parasitemia ■ ANKA smac-

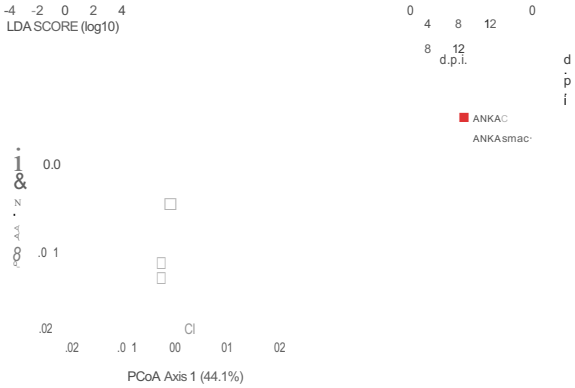
-4 -2 0 2 4
LDA SCORE (log10)
0.0
.0 1
.02
.02 .0 1 00 01 02
PCoA Axis 1 (44.1%)

0 0
4 8 12
8 12
d.p.i.
ANKAC
ANKAsmac

Fig. 3 iRBCs sequestration in the lungs mediates microbiota dysbiosis and promotes MA-ARDS

a, Heatmap of relative abundance of major microbial families in the lungs of DBA/2 mice 5 days p.i. with *Pb* ANKA high parasitemia (n=4;N=1), *Pb* ANKA low parasitemia (n=5;N=1), *Pb* ANKA*smac*- (n=9;N=1) and NI controls (n=7;N=1) and **b,** 7 days p.i. with *Pb* ANKA high parasitemia (n=5;N=1) and *Pb* ANKA low parasitemia (n=4;N=1), *Pb* ANKA*smac*- (n=9;N=1) and NI (n=9;N=1) controls. **c,** Beta diversity analysis of lung microbial communities of DBA/2 mice 5 days p.i. with *Pb* ANKA high parasitemia (n=4;N=1), *Pb* ANKA low parasitemia (n=5;N=1), *Pb* ANKA*smac*- (n=9;N=1) and NI controls (n=7;N=1) (Statistics are provided in supplementary table 2) and **d,** 7 days p.i. infection with *Pb* ANKA high parasitemia (n=5;N=1), *Pb* ANKA low parasitemia (n=4;N=1), *Pb* ANKA*smac*- (n=9;N=1) and NI (n=9;N=1) controls (statistics are provided in supplementary table 2). **e,f,** Alpha diversity (Shannon) of lung microbial composition of DBA/2 mice at **(e)** day 5 p.i. with *Pb* ANKA high parasitemia (n=4;N=1), *Pb* ANKA low parasitemia (n=5;N=1), *Pb* ANKA*smac*- (n=9;N=1) and NI (n=7;N=1) controls; or (**f)** day 7 p.i. with *Pb* ANKA high parasitemia (n=5;N=1), *Pb* ANKA low parasitemia (n=5;N=1), *Pb* ANKA*smac*- (n=9;N=1) and NI controls (n=9;N=1). For diversity statistics, we used two sided Kruskal-Wallis comparison using Kruskal-Wallis test function (stats v4.1.0) followed by two sided Mann Whitney post hoc analysis using holm correction with pairwise Wilcox test function (stats v4.1.0). **g-i** Differentially abundant ASVs (using Linear discriminant analysis Effect Size) from lungs of DBA/2 mice comparing **(g)** *Pb* ANKA high parasitemia (n=4;N=1) and *Pb* ANKA low parasitemia (n=5;N=1) at day 5 p.i.; **(h)** NI (n=7;N=1) and *Pb* ANKA high parasitemia (n=4;N=1) at day 5 p.i.; and **(i)** *Pb* ANKA*smac*-

(n=9;N=1) and *Pb* ANKA high parasitemia (n=4;N=1) at day 5 p.i.. **j-l,** Differentially abundant ASVs (using LEfSe, Linear discriminant analysis Effect Size) from lungs of DBA/2 mice comparing **j,** *Pb* ANKA high parasitemia (n=5;N=1) and *Pb* ANKA low parasitemia (n=4;N=1) at day 7 p.i. **k,** Between NI (n=9;N=1) and *Pb* high parasitemia (n=5;N=1) at day 7 **l,** between *Pb* ANKA-smac (n=9;N=1) and *Pb* ANKA high parasitemia (n=5;N=1) 7 days p.i.. **m,** Survival (left panel, Log-rank Mantel-Cox) and parasitemia (right panel, mean ± s.e.m; linear regression) following infection of DBA/2 mice with either *Pb* ANKA (n=8;N=2) or *Pb* ANKA*smac*- (n=8;N=2) parasites.). **n,** Beta diversity analysis of gut microbial communities of DBA/2 mice 5 days p.i. with *Pb* ANKA high parasitemia (n=4;N=1), *Pb* ANKA*smac*- (n=4;N=1) and NI (n=4;N=1) controls.

Table 2

Permanova (DBA/2)				
Organ	dpi	**Comparison**	**Pvalue**	**R2**
Lung	5	Global	0.006	0.342
		NI vs ANKA low parasitemia	0.859	0.026
		NI vs ANKA high parasitemia	0.008	0.569
		NI vs ANKA smac-	0.673	0.026
		ANKA low parasitemia vs ANKA smac-	0.874	0.019
		ANKA high parasitemia vs ANKA smac-	0.002	0.465
		ANKA low parasitemia vs ANKA high parasitemia	0.015	0.544
	7	Global	0.006	0.342
		NI vs ANKA low parasitemia	0.321	0.091
		NI vs high parasitemia	0.012	0.305
		NI vs ANKA smac-	0.998	0.007
		ANKA low parasitemia vs ANKA smac-	0.41	0.086
		ANKA high parasitemia vs ANKA smac-	0.014	0.308
		ANKA low parasitemia vs ANKA high parasitemia	0.157	0.203
Gut	5	Global	0.001	0.63

		NI vs ANKA high parasitemia	0.03	0.639
		NI vs ANKA smac-	0.031	0.514
		ANKA high parasitemia vs ANKA smac-	0.028	0.499

Discussion

There have been many reports that describe the respiratory symptoms and signs in clinical cases of severe malaria caused by P.f*alciparum*, P.*vivax* or P.*knowlesi*[24]*.* There have been lung function tests done in patients with uncomplicated falciparum and vivax malaria, and the results demonstrate small airways obstruction and reduction in diffusion capacity[25–27]. This reduction in the diffusion capacity has been associated to a reduction in the pulmonary capillary vascular component of gas transfer. The main characteristic that is thought to attribute to all this signs and symptoms are sequestration of parasitized erythrocytes in the pulmonary microcirculation. It has been proposed that the cytoadherence of parasitized RBCs (pRBCs) in the pulmonary microcirculation could potentiate lung damage by direct activation of the lung endothelium and recruitment of host inflammatory mediators. Histology studies from autopsy samples of severe falciparum malaria have indeed shown adherence of pRBCs in the alveoloar septal capillaries. It has been also suggested the sequestration of pRBCs in the lung circulation of *P.vivax* infected patients[27].

In this section we report that indeed, both mouse models of MA-ARDS have increased accumulation of iRBCs in the lungs. Moreover, we show that parasite sequestration is at the basis of the increased bacterial load and dysbiosis observed in the lungs of mice that die of MA-ARDS. Relevantly, lung microbiota dysbiosis is abrogated when we infect mice with a parasite strain that do not sequester to the lungs and are protected from MA-ARDS. So we report here that *Plasmodium* parasite sequestration in the lungs trigger increased bacterial load and alterations of the local microbiota and promote MA-ARDS.

The sequestration of pRBCs in the lungs have been suggested to trigger a local and systemic host inflammatory response that also aid in the pathogenesis of MA-ARDS[24]. In the next chapter, we wanted to determine the host responses that mediate the development of lung microbiota dysbiosis during MA-ARDS.

References

1. Hanson, J. *et al.* Relative Contributions of Macrovascular and Microvascular Dysfunction to Disease Severity in Falciparum Malaria. *J. Infect. Dis.* **206,** 571–579 (2012).
2. Miller, L. H., Ackerman, H. C., Su, X. & Wellems, T. E. Malaria biology and disease pathogenesis: insights for new treatments. *Nat. Med.* **19,** 156–167 (2013).
3. Smith, J. D., Rowe, J. A., Higgins, M. K. & Lavstsen, T. Malaria's deadly grip: Cytoadhesion of Plasmodium falciparum-infected erythrocytes. *Cellular Microbiology* **15,** 1976–1983 (2013).
4. Fonager, J. *et al.* Reduced CD36-dependent tissue sequestration of Plasmodium-infected erythrocytes is detrimental to malaria parasite growth in vivo. *J. Exp. Med.* **209,** 93–107 (2012).
5. Ashley, S. L. *et al.* Lung and gut microbiota are altered by hyperoxia and contribute to oxygen-induced lung injury in mice. *Sci. Transl. Med.* **12,** (2020).
6. Mason, K. L. *et al.* Candida albicans and bacterial microbiota interactions in the cecum during recolonization following broad-spectrum antibiotic therapy. *Infect.*

Immun. **80,** 3371–3380 (2012).

7. Caporaso, J. G. *et al.* Global patterns of 16S rRNA diversity at a depth of millions of sequences per sample. *Proc. Natl. Acad. Sci.* **108,** 4516–4522 (2011).
8. Caporaso, J. G. *et al.* Ultra-high-throughput microbial community analysis on the Illumina HiSeq and MiSeq platforms. *ISME J. 2012 68* **6,** 1621–1624 (2012).
9. Callahan, B. *et al.* DADA2: High resolution sample inference from amplicon data. *bioRxiv* 24034 (2015). doi:10.1101/024034
10. Yilmaz, P. *et al.* The SILVA and 'All-species Living Tree Project (LTP)' taxonomic frameworks. *Nucleic Acids Res.* **42,** D643 (2014).
11. Quast, C. *et al.* The SILVA ribosomal RNA gene database project: improved data processing and web-based tools. *Nucleic Acids Res.* **41,** D590 (2013).
12. Davis, N. M., Proctor, D. M., Holmes, S. P., Relman, D. A. & Callahan, B. J. Simple statistical identification and removal of contaminant sequences in marker-gene and metagenomics data. *bioRxiv* 221499 (2018). doi:10.1101/221499
13. Wickham, H. The split-apply-combine strategy for data analysis. *J. Stat. Softw.* **40,** 1–29 (2011).
14. Wickham, H. *et al.* Welcome to the Tidyverse. *J. Open Source Softw.* **4,** 1686 (2019).
15. Oksanen, J. *et al. Package 'vegan' Title Community Ecology Package Version 2.5-7*. (2020).
16. Wickham, H. & Wickham, H. in *ggplot2* 9–26 (Springer New York, 2009). doi:10.1007/978-0-387-98141-3_2
17. Morgan, M., Obenchain, V., Hester, J., Pagès, H. & Bioconductor, M. *Encoding*

UTF-8. (2020).

18. Khleborodova, A. lefser: R implementation of the LEfSE method for microbiome biomarker discovery. R package version 1.0.0. (2020).
19. Kolde, R. pheatmap: Pretty Heatmaps. R package version 1.0.12. (2019).
20. Vavrek, M. J. *fossil: Palaeoecological and palaeogeographical analysis tools*. **14,** (2011).
21. Miller, L. H., Ackerman, H. C., Su, X. & Wellems, T. E. Malaria biology and disease pathogenesis: insights for new treatments. *Nat. Med.* **19,** 156–167 (2013).
22. Hanson, J. *et al.* Relative Contributions of Macrovascular and Microvascular Dysfunction to Disease Severity in Falciparum Malaria. *J. Infect. Dis.* **206,** 571–579 (2012).
23. Fonager, J. *et al.* Reduced CD36-dependent tissue sequestration of Plasmodium-infected erythrocytes is detrimental to malaria parasite growth in vivo. *J. Exp. Med.* **209,** 93 (2012).
24. Taylor, W. R. J., Hanson, J., Turner, G. D. H., White, N. J. & Dondorp, A. M. Respiratory Manifestations of Malaria. *Chest* **142,** 492–505 (2012).
25. Maguire, G. P. *et al.* Lung Injury in Uncomplicated and Severe Falciparum Malaria: A Longitudinal Study in Papua, Indonesia. *J. Infect. Dis.* **192,** 1966–1974 (2005).
26. Anstey, N. M. *et al.* Pulmonary Manifestations of Uncomplicated Falciparum and Vivax Malaria: Cough, Small Airways Obstruction, Impaired Gas Transfer, and Increased Pulmonary Phagocytic Activity. *J. Infect. Dis.* **185,** 1326–1334 (2002).

27. Anstey, N. M. *et al.* Lung Injury in Vivax Malaria: Pathophysiological Evidence for Pulmonary Vascular Sequestration and Posttreatment Alveolar-Capillary Inflammation. *J. Infect. Dis.* **195,** 589–596 (2007).

Chapter 3

Mechanism: The host factors underlying altered microbiota composition in the lung

Introduction

Malaria is a multi-factorial disease where both parasite and host factors contribute for the establishment of pathology. *Plasmodium* parasite sequestration is known to elicit both systemic and a local inflammatory response[1–3]. In particular raised levels of the inflammatory cytokines tumor necrosis factor (TNF)-*α*, interleukin (IL)-l*β*, and IL-6 have been associated with severe malaria, particularly cerebral malaria in African children[4]. The upregulation of pro-inflammatory cytokines has been implicated also to have an effect of parasite sequestration in the venular endothelium by increasing the expression of adhesion molecules (eg, tumor-necrosis factor which causes an increase in endothelial intracellular adhesion molecule-1 expression)[5]. These pro-inflammatory cytokines is thought to play a role also in the pathogenesis of ARDS. Anti-inflamatory cytokines such as IL-4 and IL-10 are also upregulated, and an imbalance between IL-10 and the pro-inflammatory cytokine IL-6 has prognostic significance for death[5].

In this chapter we questioned if parasite sequestration in the lungs alter the inflammatory mediators locally and promote lung microbiota dysbiosis and death. Indeed, the data demonstrate that a specific inflammatory signature, mostly supported by local production of the anti-inflammatory cytokine IL-10 by αβ T cells, promotes alterations in the lung microbiota composition that ultimately leads to MA-ARDS.

Materials and methods

Determination of bacterial burden

Whole lung homogenates were prepared as described above, dissolved in 3 ml of sterile saline and filtered through a 100-micron filter (Corning, catalog number: 352360). 100 µl from each of the lung homogenates was then plated on blood agar plates (using Columbia blood agar base, Oxoid, catalog number: CM0331 with 5% sterile defibrinated blood) and incubated at 5%CO_2 at 37°C. Colony forming units (CFUs) were counted after 24-48 hours.

RNA isolation, cDNA and quantification of gene expression

Lungs were harvested under sterile conditions and dissolved in 1 ml PureZOL (Bio-Rad, catalog number: 732-6890) and then mechanically homogenized using 1 mm diameter silica beads (BioSpec Products, United States, catalog number: 11079110z) in a MiniBeadBeater homogenizer (BioSpec Products) for 2min. 200µl of the lysate was used to isolate total RNA using the NZY total RNA Isolation kit (NZYTech, catalog number: MB13402) according to the manufacturer's instructions. DNAse-treated RNA was reverse transcribed with random hexamers using NZY First-Strand cDNA Synthesis Kit (NZYTech, catalog number: MB12501). Real-time PCR was performed on ABI 7500 or 7900HT systems (Applied Biosystems), using Universal SYBR Green Supermix (Bio-Rad, catalog number: 172-5121) and the primers listed below. Relative gene expression was normalized to the geometric mean of hypoxanthine guanine phosphoribosyltransferase (Hprt) housekeeping gene (Δ Ct). Gene expression values

were then calculated based on the ΔΔ Ct method, using the mean of the control group as the calibrator to which all other samples were compared.

mHprt- CATTATGCCGAGGATTTGGA; AATCCAGCAGGTCAGCAAAG

Pb18S rRNA- AAGCATTAAATAAAGCGAATACATCCTTAC; GGAGATTGGT TTTGACGTTTATGTG

IL-10- CAGCCGGGAAGACAATAACT; GTTGTCCAGCTGGTCCTTTG

Broncho Alveolar Lavage (BAL) collection

The trachea was exposed through a midline incision and cannulated with a sterile 21-gauge T catheter (Venofix, catalog number: 4056337). BAL was performed by instillation of two 0.5-ml aliquots of sterile saline into the right lung. The retrieved BAL fluid (~0.8 ml) was spun at 260 × *g* for 10 min at 4°C, and the pellet was resuspended in 0.5 ml of sterile PBS.

Measurement of cytokines and chemokines

BAL fluid was harvested on day 5 post infection from different rodent-parasite combinations and assayed for IL-10 levels by sandwich enzyme-linked immunosorbent assay (ELISA) method using a commercially available murine IL-10 capture kit (PeproTech, catalog number: 900-K53) according to the manufacturer's instructions.

Circulating cytokine and chemokine levels were quantified in serum using Mouse cytokine 32-plex discovery assay by Eve Technologies (Canada).

Mononuclear cell isolation from lungs

Lungs were harvested from C57BL/6 Vert-X IL-10^{GFP} reporter mice and washed with sterile 1x PBS and placed in Petri dishes with RPMI 1640 medium (3 ml) (Sigma-Aldrich, catalog number: C5138). Whole lung was minced with forceps and scissors to 1mm sized

pieces and incubated with 3ml of digestion medium and Type IV DNase I (final concentration: 25 units/ml, Sigma-Aldrich, catalog number: C5138) at 37 °C under agitation (200 rpm) conditions for 45 min. Following that, tissue digestion was stopped by adding 1 ml of heat-inactivated FBS (Life Technologies, catalog number: 10437-028). The cells were then dispersed with a 10-ml syringe (BD Biosciences, catalog number: 301604) fitted with an 18-gauge needle (10-times) (BD Biosciences, catalog number: 305180) and filtered using a cell strainer (100 µm, Corning, catalog number: 352360). The cells were then centrifuged (Centrifuge 5810 Eppendorf) at 10 °C and 300 *x g* for 5 min. The supernatant was discarded and 1 ml of Red cells lysis buffer (0.144M NH_4Cl, 0.0169 M TRIS base,pH 7.4) was added and incubated at room temperature for 1 min. The reaction was stopped by adding 10 ml of 1x PBS with 10% FBS heat inactivated. Finally the cells were centrifuge at 10 °C and 300 *x g* for 5 min and the pellet was resuspended in FACS buffer (PBS + 2%FCS) for further stainings.

Flow cytometry stainings and antibodies

For direct multi-color flow cytometry (LRS Fortessa X-20; BD Bioscience), cells were incubated for 30 min at 4 °C with the following antibodies mentioned below. Live/dead cell discrimination was performed by staining with the Zombie Aqua Fixable Viability Kit (BioLegend, catalog number: 423101). To block Fc receptors, a purified anti-mouse CD16/CD32 (eBioscience, catalog number: 14-0161-86) was used.

CD19 APCCy7 (clone 6D5, Biolegend, catalog number: 115530), Ly6G PerCPCy5.5 (clone 1A8, Biolegend, catalog number: 127616, CD45 PEDazzle (clone 30-F11, Biolegend, catalog number: 103146), F4/80PECy7 (clone BM8, eBioscience, catalog number:254801-82), CD3 APC (clone 145-2c11, Biolegend, catalog number: 100312),

Cd11B Alexa700 (clone M170, Biolegend, catalog number: 101222), BV421 (clone GL3, Biolegend, catalog number: 118120),CD4 BV605 (clone RM4-5, Biolegend, catalog number: 100548), CD8 BV711 (clone 53-6.7, Biolegend, catalog number: 100748) NK1.1 PE (clone PK136, Biolegend, catalog number: 557391).

Antibody treatments

α-IL-10R monoclonal antibody (clone 1B1.2), αCD4 (clone YTA 3.1) and α-CD8 (clone YTS 156/169) were kindly provided by Dr. Luis Graça[6]. IL-10 signaling was blocked by injecting i.p 100µg of an anti-IL-10R monoclonal antibody at day0, day2 and day4 post infection. Control groups were injected with rat immunoglobulin in parallel. For in vivo CD4+ and CD8+T cell depletion experiments, mice were intraperitoneally (i.p) injected with 100µg of corresponding antibody individually and their IgG control (rat IgG2b Biocell, catalog number: BE0117) at day0 and day3 post *Plasmodium* infection.

T cell transfer

Lymphocytes were isolated from spleens and lymph-nodes of WT and IL10$^{-/-}$ mice. T cells were separated using magnetic-activated cell sorting (MACS). Briefly, lymphocytes were incubated in MACS buffer with anti-Thy1.2 (CD90.2) (clone 53-2.1, Biolegend, catalog number: 140312) -APC antibody for 10 min, washed and subsequently incubated with anti-APC microbeads (Milteny Biotec, catalog number: 130-090-855) for 20 min at 4°C. The cell suspension was filtered and APC/Thy1.2 positive cells (CD4$^+$ and CD8$^+$) were collected using an autoMACS separator (Milteny Biotec). Live cells obtained from the positive fraction were counted in trypan blue solution (Sigma-Aldrich, catalog number: T8154) using a hemocytometer (Marienfeld, catalog number: 0640010) . An aliquot of the cells was analysed by flow cytometry in a Fortessa X20 to determine the distribution of

$CD4^+$ and $CD8^+$ cells, using α-CD4 PeCy7 (clone RM4-5, BioLegend, catalog number: 100528) and α-CD8 FITC (clone 53-6.7, catalog number: 100706) antibodies. 50-60% and 40-50% of the cells were $CD4^+$ and $CD8^+$, respectively. 2.5 x 10^7 live cells in 200µL PBS were injected intravenous in $TCR\alpha^{-/-}$ recipient mice.

MACS buffer: 1x PBS (Sigma-Aldrich, catalog number: F9665) with 0.5% FBS (Sigma-Aldrich, catalog number: F9665) and 2mM EDTA (Sigma-Aldrich, catalog number: 03690).

Histopathology. Mice were euthanized with CO_2 narcosis, necropsy was performed and brains and lungs were collected and fixed in formalin. Heads was decalcified for 3 hours using RDO (Rapid Decalcifying) solution, processed for paraffin-embedding, sectioned at 3 µm and stained with hematoxylin and eosin (H&E) for routine histopathological analysis. Evidence for experimental cerebral malaria, including cerebral oedema and multifocal haemorrhage, were screened (0 – absent, 1 – minimal, 2 – mild, 3 – moderate, 4 – severe) in all animals. Pulmonary oedema was scored as a measure of increased oedematous fluid content in the lungs of mice that succumb to MA-ARDS.

Statistics. Significance was calculated using different tests on the GraphPad (Prism) 5.0 software. Statistical differences between 2 groups were analysed using the non-parametric two-tailed Mann-Whitney test and in case of groups involving more than 2 datasets the data was analysed by Kruskal-Wallis. Survival and parasitaemia curves were analysed using the Log-rank Mantel-Cox Chi-squared test and linear regression curve. Significance was considered for *P* values below 0.05.Biological replicates (n) indicated in

figure legends refer to the number of mice. Sample sizes were chosen on the basis of historical data; no statistical methods were used to predetermine sample size.

Results

Increased level of IL-10 mediates lung microbiota dysbiosis and MA-ARDS

In order to determine specific inflammatory signature molecule(s) that play a role in lung microbiota dysbiosis associated death due to MA-ARDS, we performed an unbiased screening of different cytokines in the serum using 32plex cytokine array between PbK173 infected C57BL/6J mice (MA-ARDS) and PbANKA infected C57BL/6 mice (eCM). In addition to VEGF, which is critical for the development of MA-ARDS[7], we observed significant differences in the levels of IFN-γ and of the IFN-γ-induced molecules MCP-1 and IP-10, TNF, IL-6, and the anti-inflammatory cytokines LIF and IL-10 in the serum of PbK173 infected C57BL/6J mice when compared to PbANKA-infected C57BL/6 mice (eCM) (Fig. 1a).

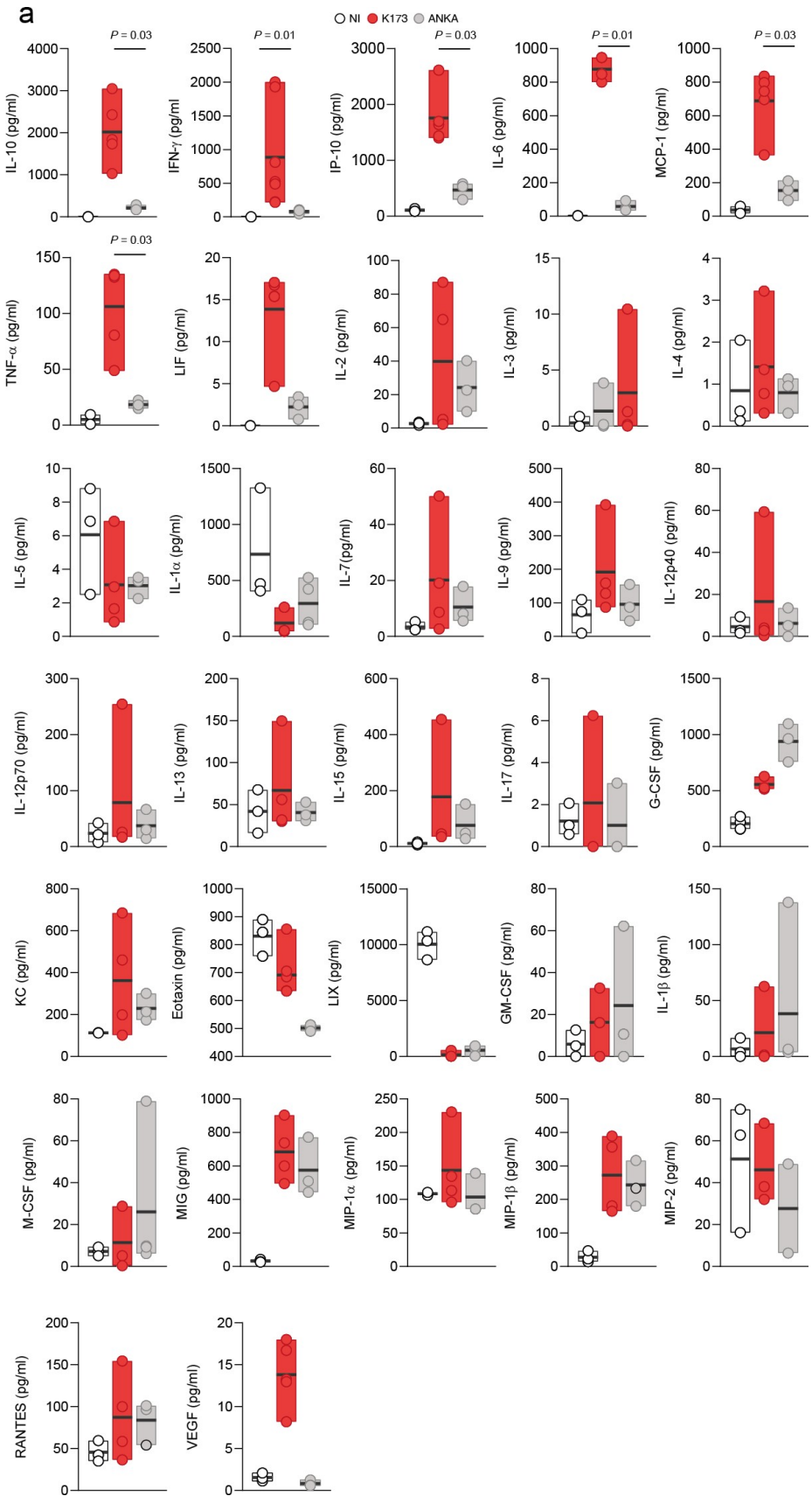
a
NI
K173
ANKA
P = 0.03
P = 0.01
IL-10 (pg/ml)
IFN-γ (pg/ml)
IP-10 (pg/ml)
IL-6 (pg/ml)
MCP-1 (pg/ml)
TNF-α (pg/ml)
LIF (pg/ml)
IL-2 (pg/ml)
IL-3 (pg/ml)
IL-4 (pg/ml)
IL-5 (pg/ml)
IL-1α (pg/ml)
IL-7(pg/ml)
IL-9 (pg/ml)
IL-12p40 (pg/ml)
IL-12p70 (pg/ml)
IL-13 (pg/ml)
IL-15 (pg/ml)
IL-17 (pg/ml)
G-CSF (pg/ml)
KC (pg/ml)
Eotaxin (pg/ml)
LIX (pg/ml)
GM-CSF (pg/ml)
IL-1β (pg/ml)
M-CSF (pg/ml)
MIG (pg/ml)
MIP-1α (pg/ml)
MIP-1β (pg/ml)
MIP-2 (pg/ml)
RANTES (pg/ml)
VEGF (pg/ml)

Fig. 1: Unbiased cytokine array of serum in different *Plasmodium* infected mice

a, 32-plex cytokine array analysis of serum of *Pb* K173 (n=5) and *Pb* ANKA (n=3) infected C57BL/6J mice compared to NI controls (n=3) 5 days p.i. (Kruskal-Wallis).

One of the most differentially expressed cytokines observed was IL-10, which has been implicated in increased susceptibility to bacterial infections[8,9]. Thus, we hypothesized that the IL-10 levels observed in PbK173 infection lead to bacterial expansion in the lung, ultimately leading to death by MA-ARDS. Indeed, we observed increased IL-10 production in the lungs of C57BL/6J mice infected with PbK173, both at the mRNA and protein levels (Fig. 2a and b, $P = 0.0003$ and $P = 0.005$, respectively).

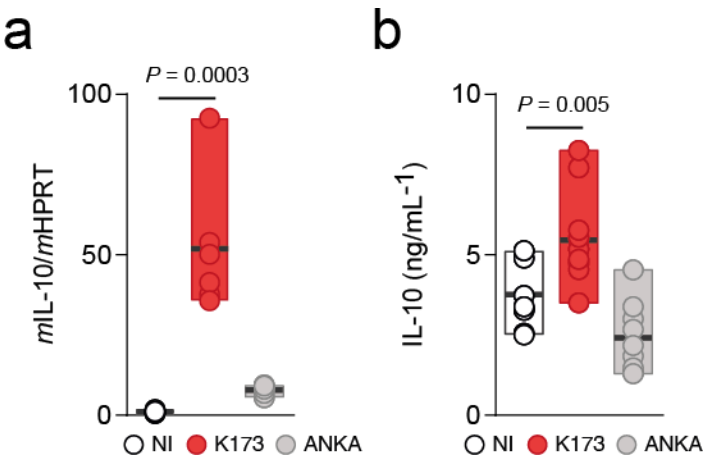

Fig. 2: IL-10 levels in the lungs of different *Plasmodium* infected mice

a, Total mRNA (Kruskal-Wallis) and **b,** protein levels (Kruskal-Wallis) of IL-10 in the lungs of C57BL/6J mice 5 days p.i. with *Pb* K173 (n=6;N=2) or *Pb* ANKA (n=6;N=2) compared to NI controls (n=6;N=2)**.**

Next we treated mice with an anti-IL-10R neutralizing antibody to determine if blocking IL-10-mediated signalling had any impact on severe malaria pathology. Indeed, while blocking IL-10-mediated signalling had no impact on eCM development (Fig. 3a-b)

treatment of PbK173-infected C57BL/6J mice with anti-IL-10R neutralizing antibody conferred complete protection, compared to isotype-treated mice that died due to MA-ARDS (Fig. 3c-d).

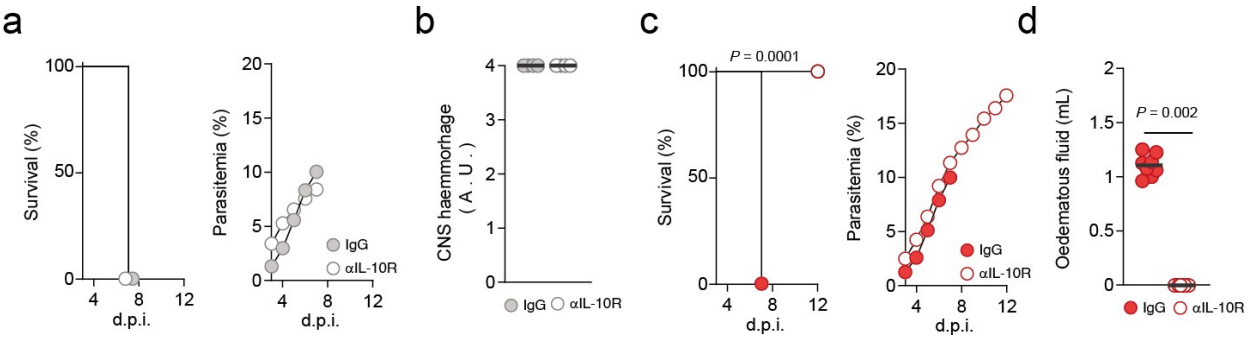

Fig. 3: Blocking of IL-10 mediated signalling in different *Plasmodium* infected mice

a, Survival (left panel, Log-rank Mantel-Cox) and parasitemia (right panel, mean ± s.e.m; linear regression) following *Pb* ANKA infection of IgG (n=10;N=2) or αIL-10R neutralizing antibody (n=10;N=2) treated C57BL/6J mice **b,** Cerebral malaria score as measured by haemorrhage in the brain following PbANKA infection of isotype treated (n=10) or IL-10R neutralizing antibody (n=10) treated C57BL/6J mice. **c,** Survival (left panel, Log-rank Mantel-Cox) and parasitemia (right panel, mean ± s.e.m; linear regression) following *Pb* K173 infection of IgG (n=10;N=2) or αIL-10R neutralizing antibody (n=10;N=2) treated C57BL/6J mice **d,** Pulmonary oedema as measured by increased fluid content in the lungs following PbK173 infection of isotype treated (n=10) or IL-10R neutralizing antibody (n=10) treated C57BL/6J mice.

We then determined the bacterial load in the lungs and parasite sequestration of PbK173 infected C57BL/6J mice after anti-IL-10R neutralizing antibody treatment compared to

isotype controls. This protection from MA-ARDS after blocking IL-10-mediated signalling was associated with decreased bacterial load (Fig. 4a, $P = 0.002$), without any impact on parasite iRBC sequestration in the lungs (Fig. 4b).

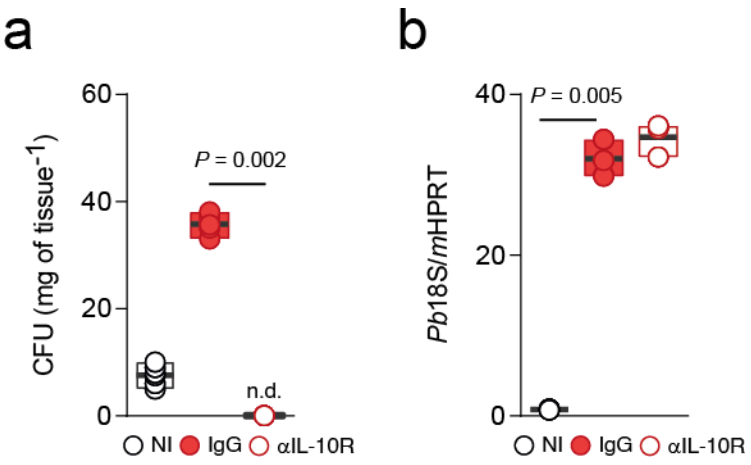

Fig. 4: Bacterial load and parasite sequestration in the lungs

a, Total CFUs (Kruskal-Wallis) in the lungs of C57BL/6J mice 5 days p.i. with *Pb* K173 (n=6;N=2) treated with αIL-10R neutralizing antibody and compared to IgG treated (n=6;N=2) and NI (n=6;N=2) controls (n.d=not detected). **b,** Parasite sequestration (Kruskal-Wallis) in the lungs of C57BL/6J mice 5 days p.i. with *Pb* K173 (n=6;N=2) treated with αIL-10R neutralizing antibody and compared to IgG treated (n=6;N=2) and NI (n=6;N=2) controls.

αβ T cells producing IL-10 that promotes MA-ARDS via lung microbiota dysbiosis. Next, we sought to identify the source of IL-10. To this end, we used the C57BL/6 Vert-X IL-10^{GFP} reporter mice. Infection with PbK173 resulted in a build-up of IL-10-producing leucocytes, specifically in the lung when compared to NI mice (Fig. 5a). Leucocytes producing of IL-10 were barely detectable in the spleen (Fig. 5b). Importantly, we

observed mostly CD4⁺ and CD8⁺ αβ T cells to be the source of IL-10 in the lungs of PbK173 infected C57BL/6J mice (Fig. 5c-e).

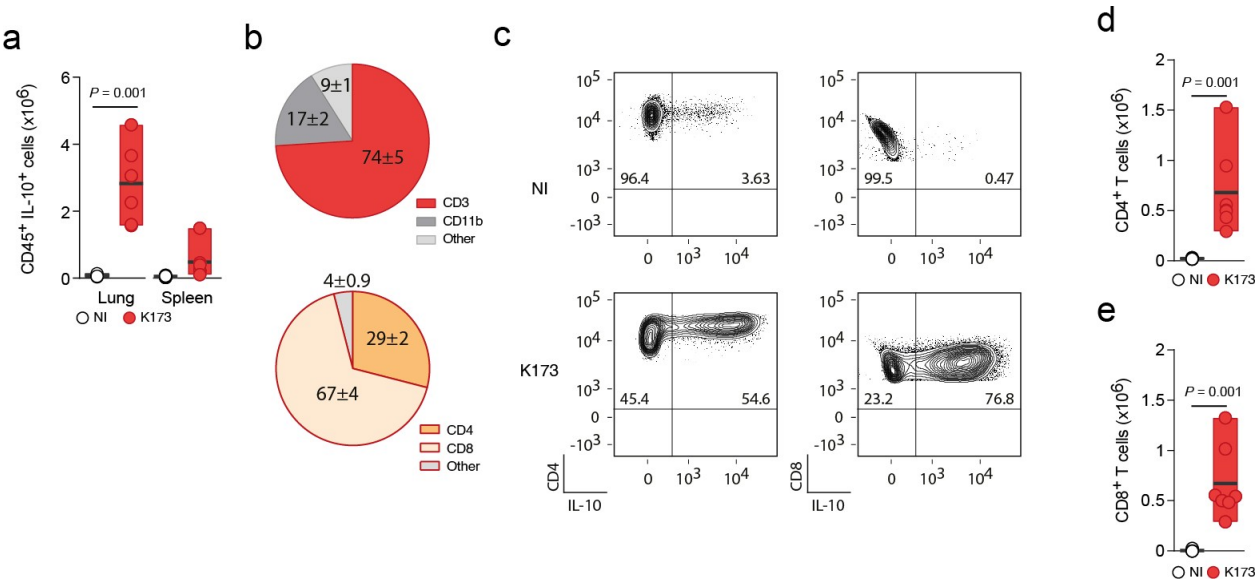

Fig. 5: IL-10 production by CD4⁺ and CD8⁺ T cells in the lungs of PbK173 infected mice

a, Total IL-10⁺ CD45⁺ leukocytes in the lungs and spleen (Mann-Whitney) of C57BL/6J mice 5 days p.i. with *Pb* K173 (n=6;N=2) compared to NI (n=6;N=2) controls. The gating was done on live CD45⁺ cells. **b,** Average percentage of different immune cells (upper pie chart, the gating was done on live CD45⁺ cells) and T cells (lower pie chart, the gating was done on live CD45⁺CD3⁺ cells) producing IL-10 in the lungs of C57BL/6J Vert-X IL-10^{GFP} reporter mice 5 days p.i. with *Pb* K173 (n=6;N=2). **c,** Representative FACS plots of CD4⁺ (left panel) and CD8⁺ (right panel) T cells producing IL-10 in the lung of C57BL/6J Vert-X IL-10^{GFP} reporter mice 5 days p.i. with *Pb* K173 compared to NI controls. The gating was done on live CD45⁺CD3⁺ cells **d,** Total CD4⁺ (n=6;N=2) and **e**, CD8⁺ T (n=6;N=2) cells producing IL-10 in the lungs of C57BL/6J Vert-X IL-10^{GFP} reporter mice 5

days p.i. with *Pb* K173 compared to NI controls (n=6;N=2) (Two sided Mann-Whitney test).

Finally, we hypothesized that it is $CD4^+$ and $CD8^+$ αβ T cells producing IL-10 that promotes MA-ARDS via lung microbiota dysbiosis. Consistent with the hypothesis, depletion of both $CD4^+$ and $CD8^+$ T cells by depleting antibodies resulted in a significant decrease in IL-10 levels (Fig. 6a, $P < 0.001$ and $P = 0.002$)

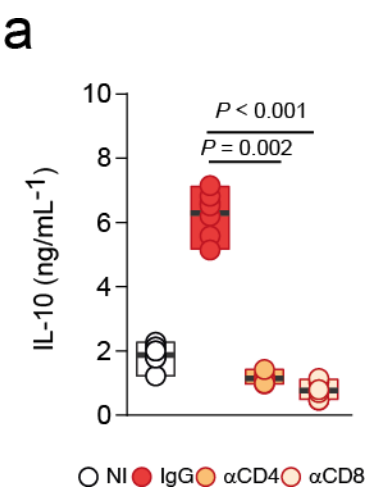

Fig. 6: Total IL-10 levels in the BAL

a, IL-10 protein levels in the BAL of IgG, anti-CD4 or anti-CD8 depleting antibody treated C57BL/6J mice infected with PbK173 5 days p.i. compared to NI mice. (n=8 mice/group, Kruskal-Wallis).

Notably, depletion of both $CD4^+$ and $CD8^+$ T cells conferred full protection from MA-ARDS compared to isotype treated controls without affecting parasite load (Fig. 7a-c).

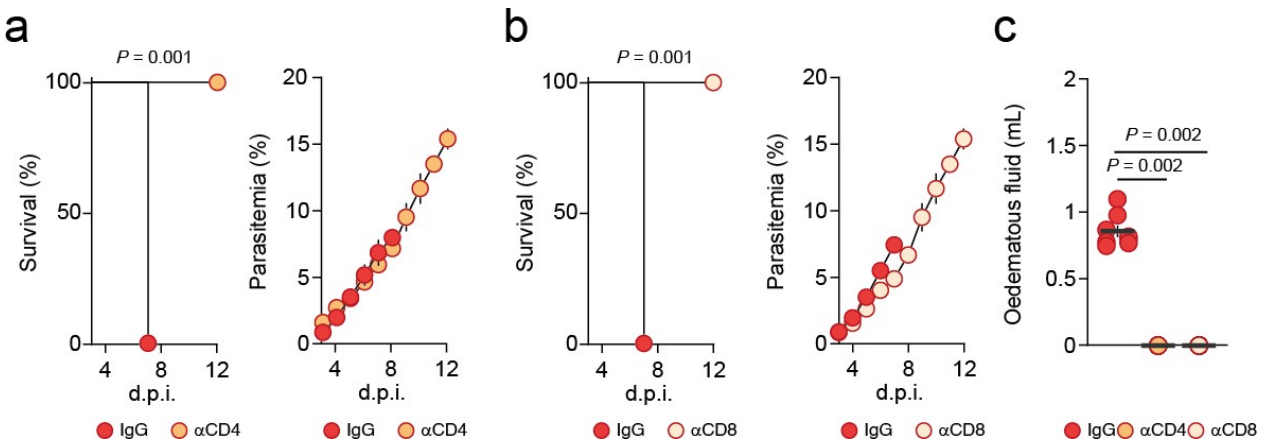

Fig. 7: Depletion of CD4⁺ and CD8⁺ T cells protect from MA-ARDS

a, Survival (left panel, Log-rank Mantel-Cox) and parasitemia (right panel, mean ± s.e.m; linear regression) following *Pb* K173 infection of IgG (n=10;N=2) or αCD4 depleting antibody (n=10;N=2) treated C57BL/6J mice, starting at day 3 p.i. **b,** Survival (left panel, Log-rank Mantel-Cox) and parasitemia (right panel, mean ± s.e.m; linear regression) following *Pb* K173 infection of IgG (n=10;N=2) or αCD8 depleting antibody (n=10;N=2) treated C57BL/6J mice, starting at day 3 p.i.

Having established that depletion of both CD4⁺ and CD8⁺ T cells conferred full protection from MA-ARDS, we then assessed the bacterial load in the lungs of these mice and also *Plasmodium* parasite sequestration. We observed that CD4⁺ or CD8⁺ T cell depletion decreased the bacterial load in the lung, with no significant changes in *Plasmodium* iRBC sequestration (Fig. 8a and b).

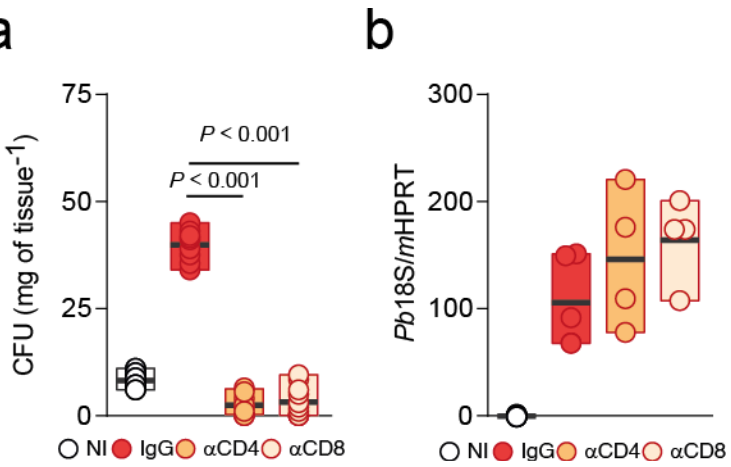

Fig. 8: Bacterial load and parasite sequestration in the lungs

a, Total CFUs (Kruskal-Wallis) in the lungs of C57BL/6J mice 5 days p.i. with *Pb* K173 treated with either αCD4 (n=8;N=2) or αCD8 (n=8;N=2) depleting antibody compared to IgG treated (n=8;N=2) and NI (n=8;N=2) controls. **b,** Parasite sequestration (Kruskal-Wallis) in the lungs of C57BL/6J mice 5 days p.i. with *Pb* K173 treated with either αCD4 (n=4;N=1) or αCD8 (n=4;N=1) depleting antibody compared to IgG treated (n=4;N=1) and NI (n=4;N=1) controls.

Finally, to show a causal relationship between αβ T cells producing IL-10 and death due to MA-ARDS, we performed cell adoptive transfer experiments. Importantly, transfer of wild type, but not IL-10-deficient αβ T cells, resulted in MA-ARDS in otherwise protected TCRα-deficient mice, which are only deficient in TCRαβ T cells (Fig. 9a and b). Altogether, these data demonstrate that a specific inflammatory signature, mostly supported by local production of the anti-inflammatory cytokine IL-10 by αβ T cells, promotes lung microbiota dysbiosis that ultimately leads to MA-ARDS.

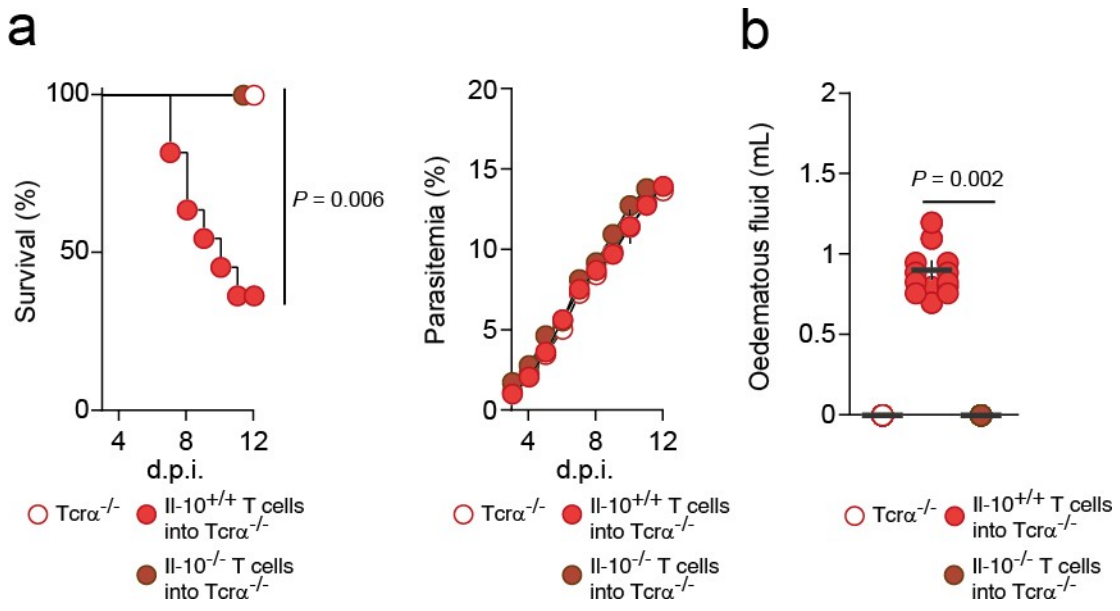

Fig. 9: IL-10 production by CD4$^+$ and CD8$^+$ T cells mediate lung microbiota dysbiosis and promotes MA-ARDS

a, Survival (left panel, Log-rank Mantel-Cox) and parasitemia (right panel, mean ± s.e.m; linear regression) of control TCRα$^{-/-}$ mice, or upon adoptive transfer of wild-type or IL-10$^{-/-}$ T cells, infected with *Pb* K173 (n=12;N=2). **b.** Pulmonary oedema as measured by increased water content in the lungs of control TCRαKO mice, or upon adoptive transfer of control or IL-10KO T cells, infected with PbK173 (n=12 mice per group, Kruskal-Wallis).

4. Discussion

The role of IL-10 during malaria infections remains quite dubious. *IL10* gene polymorphisms associated with high IL-10 production have been found to increase the risk of developing clinical malaria in young children[10]. Moreover, increased levels of circulating IL-10 have been also reported in patients with mild, severe and cerebral malaria[11,12]. Similar to studies in pre-clinical models, African children with severe anemia had lower plasma IL-10 levels than patients with moderate anemia or cerebral malaria, suggesting that IL-10 plays an important role in preventing severe anemia[13]. On the contrary a case control study in an African population with mild or severe malaria observevd that both IL-10 and TNF-α were elevated in severe malaria and positively correlated with parasitemia[14]. In another study in children from Western Kenya, higher ratios of plasma IL-10 to TNF levels were strongly associated with protection against severe malaria anemia, providing evidence that IL-10 may be protective by inhibiting TNF activity[15]. This observation was corroborated by data from pre-clinical malaria models that have shown over-expression of TNF can suppress haematopoiesis in the bone marrow and promote RBC destruction[16]. It has been reported that on the contrary to TNF, IL-10 may enhance hematopoietic activity[17]. High levels of plasma TNF have also been associated with anemia and high-density *P. falciparum* infection in Zairian children[18]. This has been also correlated to the development of severe malaria complications such as renal failure[19]. Thus, IL-10 appears to play a critical role in regulating the pathogenic effects of TNF during malaria, but in performing this important role, IL-10 may promote high-density infections that can result in other complications of malaria, including

accumulation of pRBC in tissue that can cause hypoxia and direct damage to the vasculature.

In our mice model of MA-ARDS we show that it is predominantly αβ T cells that are the major producers of IL-10 in the lung. Mechanistically, we demonstrate that is the local production of IL-10 by αβ T cells that promote lung microbiota dysbiosis and ultimately lead to MA-ARDS. The seemingly surprising disease-promoting role of IL-10 in MA-ARDS may represent an imbalance between its cardinal role in preventing immunopathology during infection, and its concomitant inhibition of microbial control resulting in bacterial outgrowth and dissemination[20,21]. IL-10 is a cytokine with potent anti-inflammatory properties that plays a central and non-redundant role in limiting host immune responses to distinct danger signals, thereby preventing damage to the host and restoring tissue homeostasis. Indeed, dysregulation of IL-10 is frequently associated with enhanced immunopathology, as many of the severe complications observed in a wide range of infections (including malaria) result from excessive immune activation. However, our data show that blockage of IL-10 signaling fully protects mice from the onset of MA-ARDS, which is characterized by inflammatory injury to the alveolar capillary barrier both in mice and humans. We propose that this unexpected result is due to the fact that IL-10 may prevent appropriate bacterial control[22], which ultimately causes an increase in the relative abundance of certain bacterial species. Indeed, we now show that MA-ARDS prevention by IL-10 signaling blockage is accompanied by a strong and significant decrease in bacterial load. A previous study highlighted the critical role of CD8+ T cells in mediating MA-ARDS[23]. Indeed, we see that $CD8^+$ T cell depletion protects mice from MA-ARDS. However, here we provide novel evidence that IL-10 production by either $CD4^+$ or $CD8^+$

T cells is responsible for alterations in the microbiota composition of the lungs and development of MA-ARDS. Most importantly, and in line with our data, elevated IL-10 levels in adults with *P. falciparum* malaria has prognostic significance for death in severe malaria cases without cerebral involvement[24] and early measurement of IL-10 predicts a worse outcome of patients with non-malaria ARDS receiving extracorporeal membrane oxygenation[25]. The latter implies that our observations may extend to ARDS originating from various etiologies.

References

1. Amante, F. H. *et al.* Immune-mediated mechanisms of parasite tissue sequestration during experimental cerebral malaria. *J. Immunol.* **185,** 3632–42 (2010).
2. Anstey, N. M. *et al.* Lung Injury in Vivax Malaria: Pathophysiological Evidence for Pulmonary Vascular Sequestration and Posttreatment Alveolar-Capillary Inflammation. *J. Infect. Dis.* **195,** 589–596 (2007).
3. Lovegrove, F. E. *et al.* Parasite Burden and CD36-Mediated Sequestration Are Determinants of Acute Lung Injury in an Experimental Malaria Model. *PLoS Pathog.* **4,** e1000068 (2008).
4. Fonager, J. *et al.* Reduced CD36-dependent tissue sequestration of Plasmodium-infected erythrocytes is detrimental to malaria parasite growth in vivo. *J. Exp. Med.* **209,** 93–107 (2012).
5. Taylor, W. R. J., Hanson, J., Turner, G. D. H., White, N. J. & Dondorp, A. M. Respiratory Manifestations of Malaria. *Chest* **142,** 492–505 (2012).
6. Agua-Doce, A. *et al.* Route of Antigen Presentation Can Determine the Selection of Foxp3-Dependent or Foxp3-Independent Dominant Immune Tolerance. *J. Immunol.* **200,** 101–109 (2018).
7. Epiphanio, S. *et al.* VEGF promotes malaria-associated acute lung injury in mice. *PLoS Pathog.* **6,** e1000916 (2010).
8. Lokken, K. L. *et al.* Malaria Parasite Infection Compromises Control of Concurrent Systemic Non-typhoidal Salmonella Infection via IL-10-Mediated Alteration of

Myeloid Cell Function. *PLoS Pathog.* **10,** e1004049 (2014).

9. Metzger, D. W. & Sun, K. Immune dysfunction and bacterial coinfections following influenza. *J. Immunol.* **191,** 2047–52 (2013).
10. Zhang, G. *et al.* Interleukin-10 (IL-10) polymorphisms are associated with IL-10: Production and clinical malaria in young children. *Infect. Immun.* **80,** 2316–2322 (2012).
11. Lyke, K. E. *et al.* Serum levels of the proinflammatory cytokines interleukin-1 beta (IL-1β), IL-6, IL-8, IL-10, tumor necrosis factor alpha, and IL-12(p70) in Malian children with severe Plasmodium falciparum malaria and matched uncomplicated malaria or healthy controls. *Infect. Immun.* **72,** 5630–5637 (2004).
12. PEYRON, F. *et al.* High levels of circulating IL-10 in human malaria. *Clin. Exp. Immunol.* **95,** 300–303 (2008).
13. Kurtzhals, J. A. L. *et al.* Low plasma concentrations of interleukin-10 in severe malarial anaemia compared with cerebral and uncomplicated malaria. *Lancet* **351,** 1768–1772 (1998).
14. Luty, A. J. *et al.* Low interleukin-12 activity in severe Plasmodium falciparum malaria. *Infect. Immun.* **68,** 3909–15 (2000).
15. Othoro, C. *et al.* A Low Interleukin-10 Tumor Necrosis Factor-α Ratio Is Associated with Malaria Anemia in Children Residing in a Holoendemic Malaria Region in Western Kenya. *J. Infect. Dis.* **179,** 279–282 (1999).
16. Taverne, J. *et al.* Anaemia and resistance to malaria in transgenic mice expressing human tumour necrosis factor. *Immunology* **82,** 397–403 (1994).
17. Van Vlasselaer, P., Falla, N., Van Den Heuvel, R., Dasch, J. & de Waal Malefijt,

R. Interleukin-10 stimulates hematopoiesis in murine osteogenic stroma. *Clin. Orthop. Relat. Res.* 103–14 (1995).

18. Shaffer, N. *et al.* Tumor necrosis factor and severe malaria. *J. Infect. Dis.* **163,** 96–101 (1991).

19. Day, N. P. J. *et al.* The Prognostic and Pathophysiologic Role of Pro- and Antiinflammatory Cytokines in Severe Malaria. *J. Infect. Dis.* **180,** 1288–1297 (1999).

20. Peñaloza, H. F. *et al.* Opposing roles of IL-10 in acute bacterial infection. *Cytokine Growth Factor Rev.* **32,** 17–30 (2016).

21. Ouyang, W. & O'Garra, A. IL-10 Family Cytokines IL-10 and IL-22: from Basic Science to Clinical Translation. *Immunity* **50,** 871–891 (2019).

22. Peñaloza, H. F. *et al.* Opposing roles of IL-10 in acute bacterial infection. *Cytokine Growth Factor Rev.* **32,** 17–30 (2016).

23. Claser, C. *et al.* Lung endothelial cell antigen cross-presentation to CD8+T cells drives malaria-associated lung injury. *Nat. Commun.* **10,** 1–16 (2019).

24. Taylor, W. R. J., Hanson, J., Turner, G. D. H., White, N. J. & Dondorp, A. M. Respiratory manifestations of malaria. *Chest* **142,** 492–505 (2012).

25. Liu, C.-H. *et al.* Early measurement of IL-10 predicts the outcomes of patients with acute respiratory distress syndrome receiving extracorporeal membrane oxygenation. *Sci. Rep.* **7,** 1021 (2017).

Chapter 4

Relevance: The clinical outcome of *Plasmodium* infection can be improved by manipulating alterations in the microbial composition of the lung

Introduction

In malaria, ARDS can develop either at initial presentation or after initiation of treatment when the parasitaemia is falling and the patient is improving[1]. Patients present with acute onset dysnoea that can rapidly progress to respiratory failure. Bacterial sepsis is an important contributor to the genesis of ALI/ARDS in severe falciparum malaria[1]. In patients with severe falciparum malaria, the prevalence of bacteraemia in published studies has varied from 6%–15%[2,3]. Although enteric bacteria predominate, respiratory pathogens, including *Streptococcus pneumoniae* and *Haemophilus influenzae* , account for up to 25% of bacteria isolated from African children with severe falciparum malaria and concomitant bacteremia[4].The administration of broad-spectrum parenteral antibiotics (eg, third-generation cephalosporins), is increasingly advocated as a standard concomitant treatment of children with severe falciparum malaria. Having established that *Plasmodium*-driven lung microbiota dysbiosis is at the basis of MA-ARDS development, we assessed whether the clinical outcome of infection could be modulated by controlling bacterial expansion.

In this chapter we report that administration of a broad spectrum antibiotic commonly used to treat lung-associated bacterial infections, had a significant impact on the pathogenesis of MA-ARDS and prevented the development of MA-ARDS but not eCM. Importantly, antibiotic elicited protection was associated with lower bacterial load in the as well as with significantly lower IL-10. Altogether these data provide evidence of *Plasmodium*-triggered IL-10 promotes severe malaria via lung microbiota dysbiosis.

Materials and Methods

Mice

Male C57BL/6J mice were purchased from Charles River breeding laboratories and housed in the animal facilities at Instituto de Medicina Molecular (iMM) specific-pathogen-free conditions (SPF conditions). All in vivo experiments were approved by the animal ethics committee of iMM and were performed according to national and European regulations.

Parasites and infections

Male C57BL/6J mice were infected, by intraperitoneal route, with 1 x 10^6 luciferase-expressing *Plasmodium berghei* ANKA, *Plasmodium berghei* K173. Parasitaemia, monitored by Giemsa stained blood smears and expressed as percentage of iRBC, and survival were monitored daily.

Determination of bacterial burden

Whole lung homogenates were prepared as described above, dissolved in 3 ml of sterile saline and filtered through a 100-micron filter (Corning, catalog number: 352360). 100 µl from each of the lung homogenates was then plated on blood agar plates (using Columbia blood agar base, Oxoid, catalog number: CM0331 with 5% sterile defibrinated blood) and incubated at 5%CO_2 at 37°C. Colony forming units (CFUs) were counted after 24-48 hours.

RNA isolation, cDNA and quantification of gene expression

Lungs were harvested under sterile conditions and dissolved in 1 ml PureZOL (Bio-Rad, catalog number: 732-6890) and then mechanically homogenized using 1 mm diameter silica beads (BioSpec Products, United States, catalog number: 11079110z) in a

MiniBeadBeater homogenizer (BioSpec Products) for 2min. 200µl of the lysate was used to isolate total RNA using the NZY total RNA Isolation kit (NZYTech, catalog number: MB13402) according to the manufacturer's instructions. DNAse-treated RNA was reverse transcribed with random hexamers using NZY First-Strand cDNA Synthesis Kit (NZYTech, catalog number: MB12501). Real-time PCR was performed on ABI 7500 or 7900HT systems (Applied Biosystems), using Universal SYBR Green Supermix (Bio-Rad, catalog number: 172-5121) and the primers listed below. Relative gene expression was normalized to the geometric mean of hypoxanthine guanine phosphoribosyltransferase (Hprt) housekeeping gene (Δ Ct). Gene expression values were then calculated based on the ΔΔ Ct method, using the mean of the control group as the calibrator to which all other samples were compared.

mHprt- CATTATGCCGAGGATTTGGA; AATCCAGCAGGTCAGCAAAG

Pb18S rRNA- AAGCATTAAATAAAGCGAATACATCCTTAC; GGAGATTGGT TTTGACGTTTATGTG

IL-10- CAGCCGGGAAGACAATAACT; GTTGTCCAGCTGGTCCTTTG

Broncho Alveolar Lavage (BAL) collection

The trachea was exposed through a midline incision and cannulated with a sterile 21-gauge T catheter (Venofix, catalog number: 4056337). BAL was performed by instillation of two 0.5-ml aliquots of sterile saline into the right lung. The retrieved BAL fluid (~0.8 ml) was spun at 260 × *g* for 10 min at 4°C, and the pellet was resuspended in 0.5 ml of sterile PBS.

Measurement of cytokines and chemokines

BAL fluid was harvested on day 5 post infection from different rodent-parasite combinations and assayed for IL-10 levels by sandwich enzyme-linked immunosorbent assay (ELISA) method using a commercially available murine IL-10 capture kit (PeproTech, catalog number: 900-K53) according to the manufacturer's instructions.

Histopathology

Mice were euthanized with CO_2 narcosis, necropsy was performed and brain and lung were collected and fixed in formalin. Head was decalcified for 3 hours using RDO solution, processed for paraffin-embedding, sectioned at 3 µm and stained with hematoxylin and eosin (H&E), for routine histopathological analysis. Evidence for experimental cerebral malaria, including cerebral edema and multifocal hemorrhage, were screened (0=absent,1=minimal, 2=mild, 3=moderate, 4=severe) in all animals. Pulmonary oedema was scored as a measure of increased water content in the lungs of mice that succumb to MA-ARDS.

Statistics

Significance was calculated using different tests on the GraphPad (Prism) 5.0 software. Statistical differences between two groups were analysed using the non-parametric two-tailed Mann-Whitney test. Survival and parasitaemia curves were analysed using the Log-rank Mantel-Cox Chi-squared test and mean± two way anova. Significance was considered for *P* values below 0.05.Biological replicates (n) indicated in figure legends refer to the number of mice. Sample sizes were chosen on the basis of historical data; no statistical methods were used to predetermine sample size.

Results

Antibiotic treatment prevents MA-ARDS

To assess whether the clinical outcome of infection could be modulated by controlling bacterial expansion we treated C57BL/6 mice infected with either PbANKA or PbK173 with a broad-spectrum antibiotic, linezolid at different time points during infection (day 3 and day 5 post-infection). We observed that administration of linezolid, an antibiotic commonly used to treat lung-associated bacterial infections, prevented the development of MA-ARDS in vast majority of PbK173 infected mice, although the treatment had no impact on eCM (Fig.1a and b). Relevantly, administration of linezolid had an impact on establishment of MA-ARDS only when administered at day 3 post-infection, since the effect seems to be abrogated once lung microbiota dysbiosis is established (starting at day 5 post-infection) (Fig.1c).

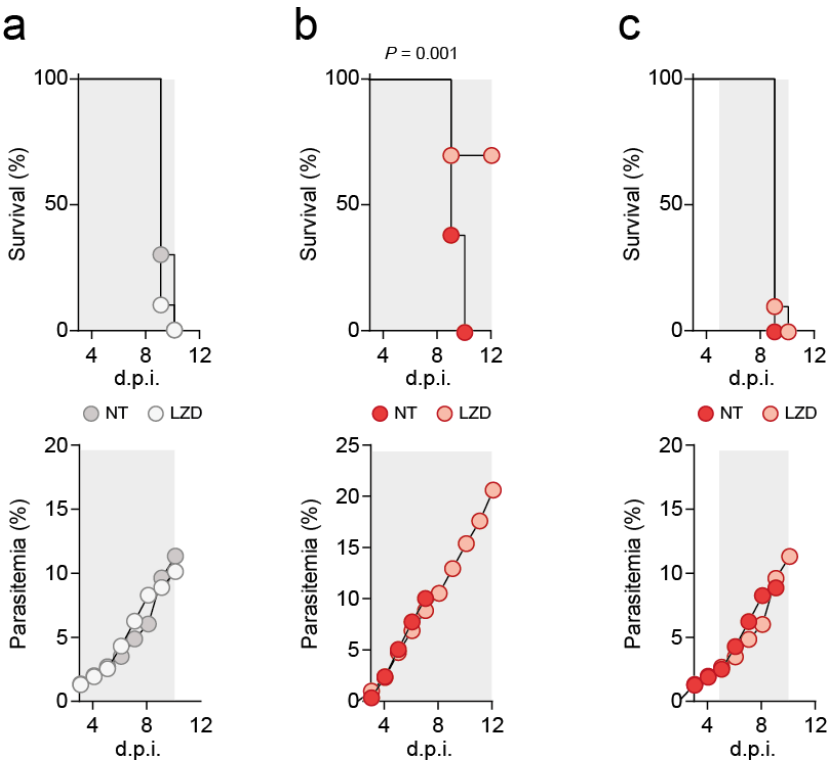

Fig.1: Antibiotic treatment prevents MA-ARDS.

a, Survival (upper panel, Log-rank Mantel-Cox) and parasitemia (lower panel, mean ± s.e.m; linear regression) following *Pb* ANKA infection of linezolid treated C57BL/6J mice (n=10;N=2) compared to non-treated, infected

controls (n=10;N=2). **b,** Survival (upper panel, Log-rank Mantel-Cox) and parasitemia (lower panel, mean ± s.e.m; linear regression) following *Pb* K173 infection of linezolid treated C57BL/6J mice (n=10;N=2) compared to non-treated, infected controls (n=10;N=2). Shaded area represents duration of antibiotic treatment starting at day 3 p.i. **c,** Survival (upper panel, Log-rank Mantel-Cox) and parasitemia (lower panel, mean ± s.e.m; linear regression) following *Pb* K173 infection of linezolid treated C57BL/6J mice (n=10;N=2) compared to non-treated, infected controls (n=10;N=2). Shaded area represents duration of antibiotic treatment starting at 5 days p.i **g,** Survival (upper panel, Log-rank Mantel-Cox) and parasitemia (lower panel, mean ± s.e.m; linear regression) following *Pb* ANKA infection of linezolid treated C57BL/6J mice (n=10;N=2) compared to non-treated, infected controls (n=10;N=2).

Antibiotic mediated protection is due to lower bacterial load and IL-10 levels in the lung

Next we determined the bacterial load and levels of IL-10 in the lungs of linezolid treated PbK173 infected compared to non-treated infected mice. We observed that the antibiotic associated delay in death as well as protection was associated with lower bacterial load in the lung (Fig. 2a, $P < 0.001$) as well as with significantly lower IL-10 levels (Fig. 2b $P = 0.002$) without any impact on parasite sequestration (Fig. 2c).

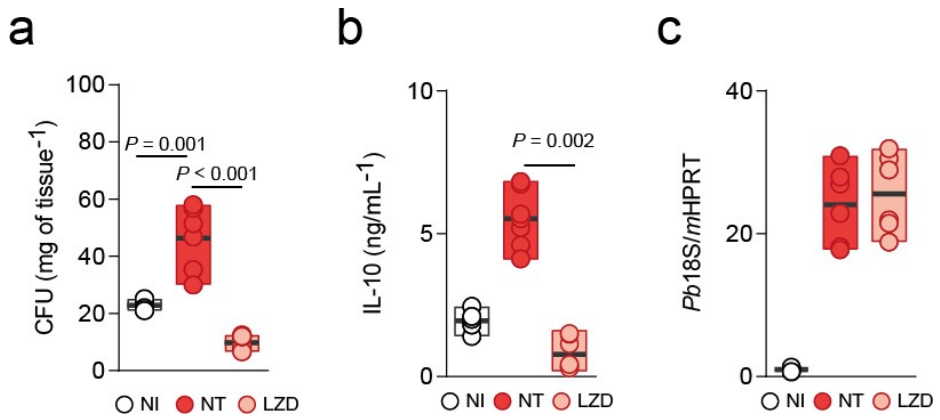

Fig. 2: Antibiotic mediated protection is due to lower bacterial load and IL-10 levels in the lung

a, Total CFU's (Kruskal-Wallis) in the lungs of C57BL/6J mice 5 days p.i. with *Pb* K173 and treated with linezolid starting at 3 days p.i. (n=6;N=2) compared to non-treated, *Pb* K173 infected (n=6;N=2) and NI (n=6;N=2) controls. **b,** IL-10 protein levels (Kruskal-Wallis) in the lungs of C57BL/6J mice 5 days p.i. with *Pb* K173 treated with linezolid starting 3 days p.i. (n=4;N=1) compared to NI (n=4;N=1) and non-treated, *Pb* K173 (n=4;N=1) infected controls. **c,** Parasite sequestration in the lungs of C57BL/6J mice 5 days p.i. with *Pb* K173 and treated with linezolid starting at 3 days p.i. (n=6;N=2) compared to non-treated *Pb* K173 (n=6;N=2) infected and NI (n=6;N=2) controls.

Discussion:

Respiratory complications are a major feature in severe malaria. In African children, respiratory distress is an important risk factor for fatal outcome. Metabolic acidosis is a critical cause of respiratory distress in these children[5–8]. However, pneumonitis from the sequestered parasitized red blood cells and inflammatory cells seen in postmortem pulmonary microvasculature[9] has been also attributed to respiratory distress. In adults, noncardiogenic pulmonary edema and acute respiratory distress syndrome (ARDS) with normal pulmonary artery occlusion pressure are grave complications of falciparum malaria, with a high mortality rate. They are also a major cause of death in those adults who present with other manifestations of severe malaria[10–13]. In some patients, ARDS is present at admission and is associated with high parasitemia[12]; however, in many instances, ARDS commences 1–5 days after treatment has begun, when peripheral parasitemia has decreased or disappeared[14-15].

The findings from this chapter may potentially highlight the importance of administering antibiotics specifically when patients have pulmonary complications during severe malaria. This also suggests that administering antibiotics might give a critical window for the administration of an effective anti-malarial treatment that may save the lives of thousands of individuals. In the future more elaborate experiments need to be performed where we can screen many other broad-spectrum antibiotics in combination with anti-malarial compounds to see if we can improve the clinical outcome of MA-ARDS. In conclusion, the data in this thesis provides novel evidence that lung microbiota dysbiosis promotes MA-ARDS and relevantly use of linezolid, an antibiotic used to treat lung bacterial infection significantly prevented the development of MA-ARDS, thus highlighting

the potential of broad-spectrum antibiotics as interventional strategies against this life-threatening syndrome.

References

1. Mohan, A., Sharma, S. K. & Bollineni, S. Acute lung injury and acute respiratory distress syndrome in malaria. *J. Vector Borne Dis.* **45,** 179–93 (2008).
2. Taylor, W. R. J., Ca??on, V. & White, N. J. Pulmonary Manifestations of Malaria. *Treat. Respir. Med.* **5,** 419–428 (2006).
3. Taylor, W. R. J. & White, N. J. Malaria and the lung. *Clin. Chest Med.* **23,** 457–68 (2002).
4. Berkley, J. A. *et al.* HIV infection, malnutrition, and invasive bacterial infection among children with severe malaria. *Clin. Infect. Dis.* **49,** 336–43 (2009).
5. Taylor, T. E., Borgstein, A. & Molyneux, M. E. Acid-base status in paediatric Plasmodium falciparum malaria. *Q. J. Med.* **86,** 99–109 (1993).
6. Marsh, K. *et al.* Indicators of Life-Threatening Malaria in African Children. *N. Engl. J. Med.* **332,** 1399–1404 (1995).
7. Amukoye, E. *et al.* Deep Breathing in Children with Severe Malaria: Indicator of Metabolic Acidosis and Poor Outcome. *Am. J. Trop. Med. Hyg.* **55,** 521–524 (1996).
8. Bassat, Q. *et al.* Distinguishing malaria from severe pneumonia among hospitalized children who fulfilled integrated management of childhood illness criteria for both diseases: a hospital-based study in Mozambique. *Am. J. Trop. Med. Hyg.* **85,** 626–34 (2011).
9. Anstey, N. M. *et al.* Pulmonary Manifestations of Uncomplicated Falciparum and Vivax Malaria: Cough, Small Airways Obstruction, Impaired Gas Transfer, and Increased Pulmonary Phagocytic Activity. *J. Infect. Dis.* **185,** 1326–1334 (2002).

10. Patel, V. & Khan, F. Pulmonary Complications of Malaria. *Semin. Respir. Crit. Care Med.* **12,** 8–17 (1991).

11. James, M. F. M. Pulmonary damage associated with falciparum malaria; a report of ten cases. *Ann. Trop. Med. Parasitol.* **79,** 123–138 (1985).

12. Charoenpan, P., Indraprasit, S., Kiatboonsri, S., Suvachittanont, O. & Tanomsup, S. Pulmonary Edema in Severe Falciparum Malaria. *Chest* **97,** 1190–1197 (1990).

13. Brooks, M. H., Kiel, F. W., Sheehy, T. W. & Barry, K. G. Acute Pulmonary Edema in falciparum Malaria. *N. Engl. J. Med.* **279,** 732–737 (1968).

14. Severe falciparum malaria. World Health Organization, Communicable Diseases Cluster. *Trans. R. Soc. Trop. Med. Hyg.* **94 Suppl 1,** S1-90 (2000).

15. Martell, R. W., Kallenbach, J. & Zwi, S. Pulmonary oedema in the falciparum malaria. *Br. Med. J.* **1,** 1763–4 (1979).

“When you reach the end of what you should know, you will be at the beginning of what you should sense.”

— Kahlil Gibrán

Conclusion and Future perspectives

Conclusion

In conclusion, although several correlations between gut microbiota and *Plasmodium* infections have been shown[1–3], the data reported in this thesis provides novel evidence of a three-way axis between *Plasmodium*, the host and its microbiota that dictates the onset of one severe malaria pathology over the other (MA-ARDS *versus* eCM), and explain the peculiar features of MA-ARDS development. The data presented here support the notion in which a pathological cycle triggered by the infectious agent (sequestration of *Plasmodium* iRBCs) is self-amplified by the cross-talk between the host response (increased IL-10 levels) and its local microbiota (establishment of lung microbiota dysbiosis) (Fig. 1).

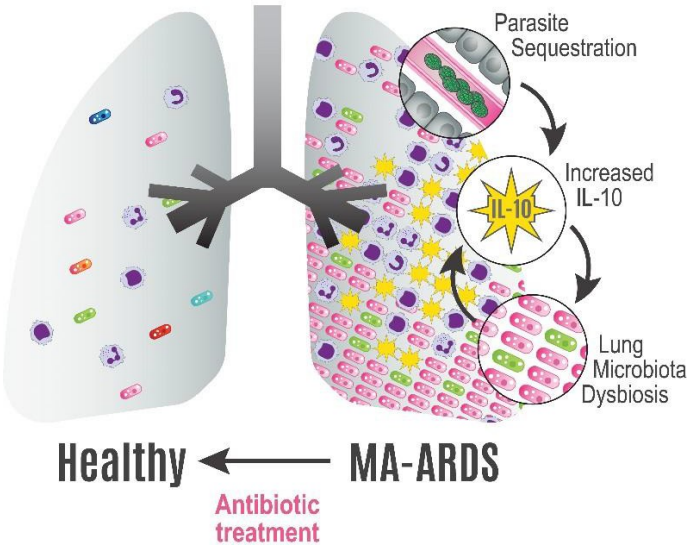

Fig.1: *Plasmodium*-triggered IL-10 promotes severe malaria via lung microbiota dysbiosis. Figure depicting the sequence of events leading to MA-ARDS, where a pathological cycle is triggered by the infectious agent (sequestration of *Plasmodium*

iRBCs) and self-amplified by the cross-talk between the host response (increased IL-10 levels) and its local microbiota (establishment of lung microbiota dysbiosis). Harnessing bacterial expansion by antibiotic treatment during a malaria infection results in protection from MA-ARDS.

In humans, MA-ARDS development is associated with a poor prognosis, with death rates ranging from 40 to 100%, depending on the availability of mechanical ventilation (reviewed in[4]). While this syndrome is proportionally most common in *P. vivax* and *P. knowlesi* infections[4], its frequency is becoming increasingly evident in *P. falciparum* infection clinical series[5]. It has been proposed that iRBCs sequestration in the lungs and concomitant local inflammatory changes, are the main cause of MA-ARDS in humans[4]. Our data, using distinct rodent models of infection, shows unequivocally that this is the case (Chapter 3). Moreover, and in agreement with our data, increased levels of seric IL-10 in adults with *P. falciparum* malaria has prognostic significance for death in severe malaria cases without cerebral involvement[5]. Lastly, bacteraemia and pneumonia may contribute to death in patients with MA-ARDS[6]. Due to the clinical overlap between bacteraemia, pneumonia and severe malaria, the World Health Organization recommends the use of broad-spectrum antibiotics to be included in the treatment regiments of such malaria cases[7]. Our findings provide the explanation for this empirical clinical intervention. Indeed, antibiotic treatment controlling lung microbiota dysbiosis is sufficient to prevent MA-ARDS and may provide a critical time window for the administration of an effective anti-malarial treatment that may save the lives of thousands of individuals.

Below the tip of the iceberg-Future Perspectives

Although this study reveals that *Plasmodium* triggered IL-10 production in the lungs promote lung microbiota dysbiosis and the onset of MA-ARDS, there are still relevant questions that remain unanswered. Firstly, even though we show an association between lung microbiota dysbiosis and development of MA-ARDS we still don't know which bacterial species (or a minimalistic consortium of bacterial species) are responsible for this severe malaria pathology. To do this we can perform temporal culturomics techniques and identify the bacterial species that bloom in the lungs of this mice over time. As it has been discussed before, the concept of dysbiosis is related to the bloom of pathobionts and depletion of beneficial symbionts. So one can envision, in our mice model of MA-ARDS the dysbiosis we observe in the lungs could be related to both the phenomenon. So it is of utmost importance that we do culturomic techniques in different medium (aerobic and anaerobic) over time to identify which bacteria expands and which bacteria are depleted. Then we can identify these bacteria by either 16S sequencing or by Maldi TOF Mass spectrometry analsysis.

After the identification the potential bacterial species that expand the lungs of the mice the die of MA-ARDS we can do causation experiments by transferring these individual bacterial species or groups of minimalistic bacterial species intranasaly into Germ-Free mice and reveal which ones are relevant for the onset of MA-ARDS.

It is, however, important to keep in mind that there are significant differences in microbiota composition between mice and humans (both qualitative and quantitative)[8] and caution should be taken when extrapolating knowledge gathered in mouse models into humans. Additionally, it has been demonstrated that microbiota composition varies between different mouse strains and even in the same mouse strain from distinct providers or housed in different conditions[9,10]. In the future, and to increase the robustness of the conclusions gathered from rodent models of malaria infection, studies should focus on reproducing microbial differences and its impact on malaria infections in different locations. Moreover, experiments where GF mice are colonized with human microbiotas, which have significantly improved our knowledge on the critical contribution of microbiota for other pathologies[11], should be also applied in the field of malaria research. One can envision, as is the case with gut microbiota research, to perform 16S rRNA and metagenomic sequencing analysis from the BAL of humans that are diagnosed with MA-ARDS in malaria endemic regions. This can allow us to do humanized mice lung microbiota research where we can intranasally inoculate mice with human lung bacteria by culturomics techniques. This will definitely help us to extrapolate the data from mice to humans and also help us to do causation experiments to identify bacterial species in humans responsible for the onset of MA-ARDS. This will also broaden the field of lung microbiota research where we can do more definitive experiments to understand the role of lung microbiota not only underlying the onset of MA-ARDS but also other pulmonary disorders.

Does increased IL-10 altered microbiota composition promote ARDS in other diseases also?

Malaria occupies a unique place in human History since its prehistoric origin. Although *Plasmodium*, the protozoan parasite that causes malaria, has been discovered more than a century ago, this devastating disease claimed (in the 20th century alone) between 150 million and 300 million lives, accounting for 2 to 5 percent of all deaths[12]. Moreover, and in spite of two worldwide eradication campaigns in the past 70 years, malaria still kills a child every minute[12]. COVID-19, on the other hand, is quickly claiming a place in History. Caused by the coronavirus SARS-CoV-2, it is already responsible for taking more than 5 million lives since its discovery in late 2019.

Despite the many differences in their etiology and natural history, malaria and COVID-19 share some clinical features. Besides similarities in the mild symptoms (e.g. fever and fatigue among others), life-threatening complications like acute respiratory distress syndrome (ARDS) frequently occur in severe forms of either malaria or COVID-19. Thus one can hypothesize that pathogen-triggered inflammatory/immune/tissue responses results in local loss of control of commensal bacterial communities, which together strongly impact the clinical outcome of malaria or COVID-19, and possibly other respiratory life-threatening complications.

SARS-CoV-2-infected K18hACE2 mice showed more than 20% body weight loss 4 days after infection and were euthanised on day 5 (Fig. 2a). Preliminary data shows a similar pattern in microbiota abundance is observed in the lungs of SARS-CoV-2-infected mice (Fig. 2b). In agreement with our data, direct sampling of lung alveoli of critically-ill human

patients infected with SARS-CoV-2 shows that both lung microbiota and an impaired alveolar immune response correlate with poor clinical outcomes, while patients treated with piperacillin/tazobactam show a high survival rate.[13]

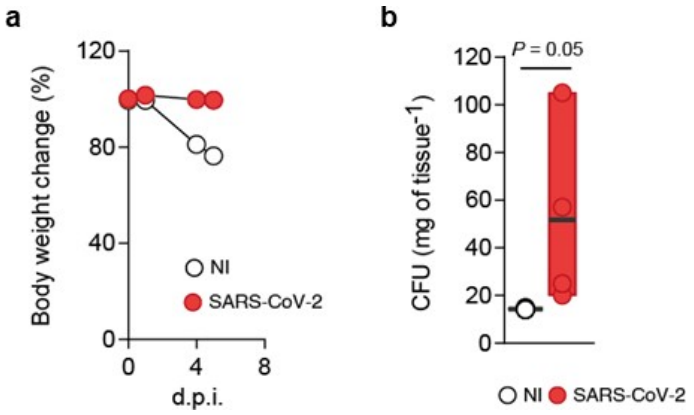

Fig. 2: Increased CFUs in the lungs of SARS-CoV-2 infected mice

a,Time course measurement of body weight of SARS-CoV-2-infected mice**. b,** Total CFUs (n=4 mice per group; Mann-Whitney) at day 5 p.i. in the lungs of of SARS-CoV-2 infected mice when compared to non-infected (NI) mice.

Additionally, like in our mice model of MA-ARDS we observed altered levels of local IL-10 in our COVID-19 animal model also (Fig. 3a). Notably, data in the clinical setting also show high IL-10 levels at disease peak and their decrease is associated with recovery in COVID-19 patients at the ICU of Centro Hospitalar Universitário Lisboa Norte (Fig.3b,median 17 at peak versus 4 in recovery, p=0.0012). Normal levels in control subjects is 0.3 (0.1 - 0.6).

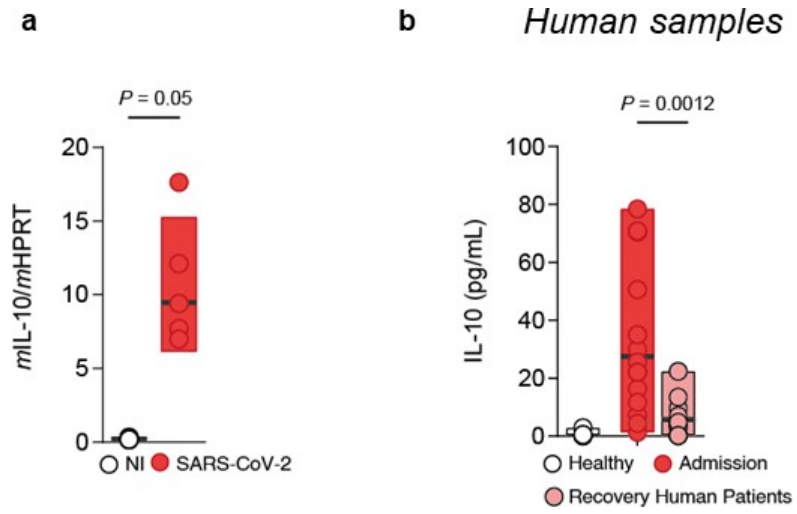

Fig. 3: Levels of IL-10 in SARS-CoV-2 infected mice and Human serum samples

a, Total mRNA (Mann-Whitney) levels of IL-10 in the lungs of SARS-CoV-2 infected mice (n=5;N=1) compared to NI controls (n=5;N=1)**. b,** Total IL-10 levels from the serum of human patients.

The findings of this thesis that infection-triggered, host-dependent alterations in lung commensal communities promote ARDS, makes malaria and COVID-19 an excellent paradigm for investigation of this novel concept. Ultimately, in the future more experiments are needed to reveal the causal link between the host's inflammatory/immune/tissue responses and bacterial outgrowth in the outcome of lung disease, thus opening the possibility for tailormade therapies to prevent severe forms of malaria, COVID-19 or other ARDS-promoting diseases.

Below the tip of the iceberg-Future Perspectives beyond the thesis

There is no doubt that human microbiota plays an important role in the well-being of the human host, albeit participating actively in the development of a wide variety of diseases, ranging from bacterial infections to liver diseases, cancer, metabolic diseases and even psychiatric disorders[14]. The findings of this study reveal a critical role of the host microbiota (specifically the lung microbiota) in dictating the onset of one severe malaria pathology over another. However, these finding also open more questions that remain unanswered but have the potential to expose distinct aspects of *Plasmodium* parasites biology and interaction with their hosts and the host's microbiota discussed below.

Role of skin microbiota on sporozoite migration

Another line of research arises from numerous evidences indicating that sporozoites are first deposited into the skin before they find their way into the bloodstream and, ultimately, reach the liver[15,16]. As previously mentioned, it is now clearly demonstrated that different body sites harbor a unique core microbiota, with the skin being no exception. This raises the question whether the skin microbiota of the host can have an effect on sporozoite migration in the skin thus hampering (or facilitating) its establishment in the liver. In particular, recent evidences have shown that resident skin commensals can influence the expression of different innate factors, including inflammatory cytokines, different arms of the complement system and production of anti-microbial peptides (AMP´s)[17]. These studies have shown that the skin microbiota can balance the innate environment within the tissue and aid protection against cutaneous infections by pathogens like *Leishmania major* and *Candida albicans* independently of gut microbes[18]. Thus, it remains to be

explored if the host's skin microbiota can have an impact on *Plasmodium* sporozoite migration within the dermal compartment.

Gut-Liver axis during Plasmodium infection

Within seconds or minutes of transmission, productive sporozoites must travel to the liver and establish into hepatocytes where they replicate into thousands of new RBC-infecting merozoites. Importantly, the liver has a unique vascular system within the gastrointestinal tract, as the majority of the liver's blood supply comes from the intestine through the portal vein. Liver products are known to influence the gut microbiota composition and gut barrier integrity, whereas intestinal factors regulate bile acid synthesis, glucose and lipid metabolism in the liver[19], all of which may directly or indirectly impact *Plasmodium* liver stage infection[20,21]. Moreover, this gut-liver axis strongly influences several liver diseases and certain liver viral infections[22], though the underlying mechanisms are still to be fully uncovered. Still, the impact of such gut-liver cross-talk on the innate immune response seems to be evident[23]. We and others have shown that the liver has sensor mechanisms that are able to recognize *Plasmodium* and mediate a functional anti-parasitic response driven by type I IFN[24,25]. Whether this response is influenced by the host microbiota remains to be established.

Role of bacterial metabolites on Plasmodium infection

Moreover, one can also envision manipulating the production of metabolites by specific bacterial species in the gut that have a protective role against the establishment of infection or disease severity. Indeed, the human gut microbiota produces numerous **metabolites** that accumulate in the bloodstream, where they can exert systemic effects on the host[26]. It has been shown that short-chain fatty acids (SCFAs), which are bacterial

fermentation products of dietary fibres, can confer protection for a variety of inflammatory disorders including colitis and asthma[27,28]. It is, therefore, a compelling idea to test if specific bacterial metabolites can influence immune responses in distant tissues like the CNS, the liver and the lungs and have a significant impact on *Plasmodium* infection. Whether there are any different transcriptomic and metabolic signatures between enteric commensals in individuals that develop severe malaria compared to those that do not remains to be tested. In a preliminary study done in mice, Stough and colleagues identified differentially-expressed metabolic pathways between resistant and susceptible mice infected with *P. yoelii*[29]. Mechanistic studies are now needed to better understand the cross-talk between microbial metabolites, the host immune system and malaria-associated disease severity.

Ultimately, knowledge produced by experiments as those proposed here may lead to the use of **pre- or pro-biotics** to manipulate microbiota composition in malaria endemic regions to prevent disease incidence and/or severity.

Concluding Remarks

While the current state-of-art is to consider malaria infections as a bidirectional cross-talk between *Plasmodium* parasites and the host, this thesis highlights the potential complexity of the system – we, like many others, envisage a three-way axis where host-*Plasmodium*-microbiota becomes central to better understand and fight malaria in the future. In the future, more definitive experiments are required to identify the 'dysbiotic' bacterial signatures between symptomatic and asymptomatic patients in malaria endemic regions. Moreover, and apart from the gut, we need to dig deeper and understand if

tissue-specific microbiota changes such as of liver, lung or skin can have an impact on *Plasmodium* parasite establishment in the host and disease severity.

References

1. Villarino, N. F. *et al.* Composition of the gut microbiota modulates the severity of malaria. *Proc. Natl. Acad. Sci. U. S. A.* **113,** 2235–40 (2016).
2. Yooseph, S. *et al.* Stool microbiota composition is associated with the prospective risk of Plasmodium falciparum infection. *BMC Genomics* **16,** 631 (2015).
3. Yilmaz, B. *et al.* Gut Microbiota Elicits a Protective Immune Response against Malaria Transmission. *Cell* **159,** 1277–1289 (2014).
4. Taylor, W. R. J., Hanson, J., Turner, G. D. H., White, N. J. & Dondorp, A. M. Respiratory manifestations of malaria. *Chest* **142,** 492–505 (2012).
5. Milner, D. *et al.* Pulmonary pathology in pediatric cerebral malaria. *Hum. Pathol.* **44,** 2719–2726 (2013).
6. Bruneel, F. *et al.* The clinical spectrum of severe imported falciparum malaria in the intensive care unit: Report of 188 cases in adults. *Am. J. Respir. Crit. Care Med.* **167,** 684–689 (2003).
7. World Malaria Report, World Health Organization, W. H.O (2021).
8. Hugenholtz, F. & de Vos, W. M. Mouse models for human intestinal microbiota research: a critical evaluation. *Cellular and Molecular Life Sciences* **75,** 149–160 (2018).
9. Spor, A., Koren, O. & Ley, R. Unravelling the effects of the environment and host genotype on the gut microbiome. *Nat. Rev. Microbiol.* **9,** 279–290 (2011).

10. Xiao, L. *et al.* A catalog of the mouse gut metagenome. *Nat. Biotechnol.* **33,** 1103–8 (2015).

11. Zitvogel, L., Ma, Y., Raoult, D., Kroemer, G. & Gajewski, T. F. The microbiome in cancer immunotherapy: Diagnostic tools and therapeutic strategies. *Science* **359,** 1366–1370 (2018).

12. World Malaria Report", "World Health Organization. (2021).

13. Sulaiman, I. *et al.* Microbial signatures in the lower airways of mechanically ventilated COVID-19 patients associated with poor clinical outcome. *Nat. Microbiol. 2021 610* **6,** 1245–1258 (2021).

14. Durack, J. & Lynch, S. V. The gut microbiome: Relationships with disease and opportunities for therapy. *J. Exp. Med.* **216,** 20–40 (2019).

15. Hopp, C. S. *et al.* Longitudinal analysis of Plasmodium sporozoite motility in the dermis reveals component of blood vessel recognition. *Elife* **4,** (2015).

16. Sinnis, P. & Coppi, A. A long and winding road: the Plasmodium sporozoite's journey in the mammalian host. *Parasitol. Int.* **56,** 171–8 (2007).

17. Belkaid, Y. & Segre, J. A. Dialogue between skin microbiota and immunity. *Science* **346,** 954–9 (2014).

18. Naik, S. *et al.* Compartmentalized Control of Skin Immunity by Resident Commensals. *Science (80-.).* **337,** 1115–1119 (2012).

19. Tripathi, A. *et al.* The gut-liver axis and the intersection with the microbiome. *Nat. Rev. Gastroenterol. Hepatol.* **15,** 397–411 (2018).

20. Mancio-Silva, L. *et al.* Nutrient sensing modulates malaria parasite virulence. *Nature* **547,** 213–216 (2017).

21. Zuzarte-Luís, V. *et al.* Dietary alterations modulate susceptibility to Plasmodium infection. *Nat. Microbiol.* **2,** 1600–1607 (2017).

22. Tripathi, A. *et al.* The gut–liver axis and the intersection with the microbiome. *Nat. Rev. Gastroenterol. Hepatol.* **15,** 397–411 (2018).

23. Seki, E. & Schnabl, B. Role of innate immunity and the microbiota in liver fibrosis: crosstalk between the liver and gut. *J. Physiol.* **590,** 447–458 (2012).

24. Liehl, P. *et al.* Host-cell sensors for Plasmodium activate innate immunity against liver-stage infection. *Nat. Med.* **20,** 47–53 (2014).

25. Miller, J. L., Sack, B. K., Baldwin, M., Vaughan, A. M. & Kappe, S. H. I. Interferon-Mediated Innate Immune Responses against Malaria Parasite Liver Stages. *Cell Rep.* **7,** 436–447 (2014).

26. Dodd, D. *et al.* A gut bacterial pathway metabolizes aromatic amino acids into nine circulating metabolites. *Nature* **551,** 648–652 (2017).

27. Maslowski, K. M. *et al.* Regulation of inflammatory responses by gut microbiota and chemoattractant receptor GPR43. *Nature* **461,** 1282–6 (2009).

28. Sun, M., Wu, W., Liu, Z. & Cong, Y. Microbiota metabolite short chain fatty acids, GPCR, and inflammatory bowel diseases. *J. Gastroenterol.* **52,** 1–8 (2017).

29. Stough, J. M. A. *et al.* Functional Characteristics of the Gut Microbiome in C57BL/6 Mice Differentially Susceptible to Plasmodium yoelii. *Front. Microbiol.* **7,** 1520 (2016).